Miscellaneous Paper CHL-97-1
January 1997

US Army Corps of Engineers
Waterways Experiment Station

Coast of Delaware Hurricane Stage-Frequency Analysis

by David J. Mark, Norman W. Scheffner

Prepared for U.S. Army Engineer District, Philadelphia

The contents of this report are not to be used for advertising, publication, or promotional purposes. Citation of trade names does not constitute an official endorsement or approval of the use of such commercial products.

PRINTED ON RECYCLED PAPER

Miscellaneous Paper CHL-97-1
January 1997

Coast of Delaware
Hurricane Stage-Frequency Analysis

by David J. Mark, Norman W. Scheffner

U.S. Army Corps of Engineers
Waterways Experiment Station
3909 Halls Ferry Road
Vicksburg, MS 39180-6199

Final report

Prepared for U.S. Army Engineer District, Philadelphia
Philadelphia, PA 19106-2991

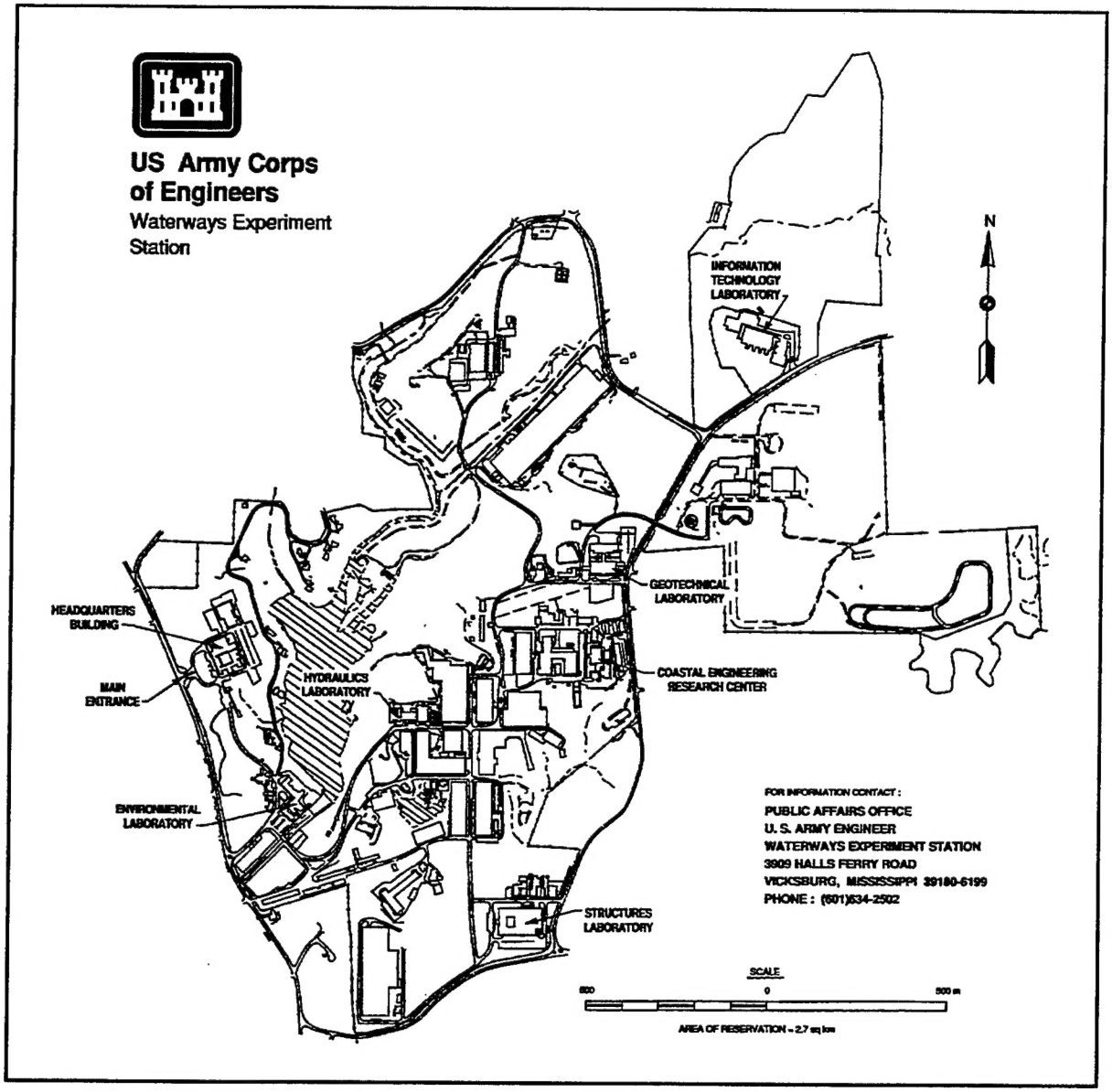

Waterways Experiment Station Cataloging-in-Publication Data

Mark, David J.

Coast of Delaware hurricane stage-frequency analysis / by David J. Mark, Norman W. Scheffner ; prepared for U.S. Army Engineer District, Philadelphia.

112 p. : ill. ; 28 cm. — (Miscellaneous paper ; CHL-97-1)

Includes bibliographic references.

1. Coasts — Delaware. 2. Storm surges — Evaluation — Delaware. 3. Hurricanes —Tracks — Mathematical models. I. Scheffner, Norman W. II. United States. Army. Corps of Engineers. Philadelphia District. III. U.S. Army Engineer Waterways Experiment Station. IV. Coastal and Hydraulics Laboratory (U.S. Army Engineer Waterways Experiment Station) V. Title. VI. Series: Miscellaneous paper (U.S. Army Engineer Waterways Experiment Station) ; CHL-97-1.

TA7 W34m no.CHL-97-1

Contents

Preface

This report describes the procedures and results of a hurricane stage-frequency analysis for the open coast of Delaware. This analysis represents one component of the Delaware Coast Feasibility Study, which is being conducted to develop a regional plan for storm damage reduction and shoreline protection for the open coast of Delaware. This study was performed by the U.S. Army Engineer Waterways Experiment Station (WES) for the U.S. Army Engineer District, Philadelphia (CENAP). Appreciation is extended to Mr. Keith D. Watson, Engineering Division, CENAP, for his assistance during this study.

The investigation reported herein was conducted by Mr. David J. Mark and Dr. Norman W. Scheffner, Coastal Oceanography Branch (COB), Research Division (RD), Coastal and Hydraulics Laboratory (CHL), WES. The CHL was formed in October 1996 with the merger of the WES Coastal Engineering Research Center and Hydraulics Laboratory. Dr. James R. Houston is the Director of the CHL and Messrs. Richard A. Sager and Charles C. Calhoun, Jr., are Assistant Directors.

Direct supervision of this project was provided by Mr. H. Lee Butler, Chief, RD, and by Dr. Martin Miller, Chief, COB, RD, CHL. The final report was prepared by Mr. Mark.

At the time of publication of this report, Director of WES was Dr. Robert W. Whalin. Commander was COL Bruce K. Howard, EN.

Conversion Factors, Non-SI to SI Units of Measurement

Non-SI units of measurement used in this report can be converted to SI units as follows:

Multiply	By	To Obtain
feet	0.3048	meters
knots (international)	0.5144444	meters per second
miles (U.S. nautical)	1.852	kilometers
miles (U.S. statute)	1.609347	kilometers

1 Introduction

The U.S. Army Engineer District, Philadelphia, is presently developing a storm damage reduction and shoreline protection program for the open coast of Delaware. Because of existing and possible future development in coastal areas, this program is being undertaken to prevent loss of life and to minimize property damage resulting from storm events. Development of effective protective measures includes investigating short-term beach and dune erosion patterns together with long-term shoreline evolution trends. In order to estimate these phenomena, a hurricane stage-frequency analysis is required.

This report describes the procedure and results of a hurricane stage-frequency analysis for the open coast of Delaware. This analysis consisted of three interrelated tasks, each employing a numerical model. In the first task, historical hurricanes impacting the study area were analyzed to determine storm statistics and correlations. From these data, a reduced set of hurricanes, representative of all storms impacting the area, were chosen and subsequently simulated with a tropical wind field model to generate wind and atmospheric pressure fields.

In the second task, storm surge events developed with the wind model output were simulated using a long-wave, finite-element-based hydrodynamic model to obtain peak storm surge elevations. With the hurricane parameters serving as input to the wind field model, together with the corresponding storm surge elevations predicted by the storm surge model, statistical techniques are used for developing frequency-of-occurrence relationships in the third task.

An empirical simulation technique (EST) procedure was used for determining frequency-of-occurrence relationships. The EST is a statistical resampling procedure which uses historical data to develop joint probability relationships among the various measured storm parameters (e.g., maximum wind speed). The resampling scheme generates large populations of data which are statistically similar to a much smaller database of historical events. Using this expanded data set, the EST generates a database of peak storm surge elevations by simulating multiple-year periods (e.g., 200-year periods) of storm activity a multiple number of times. Stage-frequency relationships are then generated using the database of peak storm surge elevations.

This report is divided into six chapters, with Chapter 1 being the introduction. Chapter 2 describes the EST, whereas Chapter 3 describes the meteorological and hydrodynamic models applied in this study. Model calibration and validation to the coast of Delaware are presented in Chapter 4 and development of the stage-frequency relationships is discussed in Chapter 5. Chapter 6 summarizes the procedures and results of this study. Appendix A contains stage-frequency relationship tables, and stage-frequency relationship figures are presented in Appendix B. Appendix C is a collection of hurricane track figures. Appendix D is a notation of mathematical symbols used in the report.

2 Empirical Simulation

Technique

Storm damage reduction programs and design of coastal structures typically require a storm surge analysis to obtain a peak water surface elevation for design water levels. Because hurricanes occur infrequently at a given site, and therefore a lack of peak storm surge stages, standard ranking methods cannot be used in a stage-frequency analysis. Thus, numerical models are often applied for simulating a larger population of storm surge events. Traditionally, modeled hurricanes are synthesized via a joint probability method (JPM) to describe storm attributes, such as maximum wind speeds and pressure deficits. First employing a statistical analysis of historical storms, a range of values is chosen for each parameter. A series of hypothetical hurricanes are then synthesized by combining the various parameter values.

One shortcoming of this approach, however, is that the JPM usually assumes that all parameters are independent, ignoring the interdependence of storm parameters. Consequently, unrealistic hurricanes are synthesized by arbitrarily combining parameter values. For example, one parameter can be assigned a value typical of a weak storm, whereas a second is assigned a value representative of an intense storm. Thus, a level of uncertainty is incorporated into the stage-frequency computations. An alternative approach to the JPM is the EST or extended "bootstrap" approach, which preserves the interdependence of hurricane parameters. Details of the EST are given in Scheffner and Borgman (1993) and Borgman et al. (1992).

Description of Technique

EST is a statistical resampling technique that uses historical data to develop joint probability relationships among the various measured storm parameters. In contrast to the JPM discussed above, there are no simplifying assumptions concerning the development of probability density functions describing historical events. Thus, the interdependence of parameters is maintained. In this manner, parameter probabilities are site-specific, do not depend on fixed parametric relationships, and do not assume parameter independence. Thus, the EST is distribution-free and nonparametric.

For this study, the EST was developed to generate numerous multi-year intervals of possible future hurricane events for a specific location. The ensemble of modeled or simulated events is consistent with the statistics and correlations of past storm activity at a site. Furthermore, the EST permits random deviations in storm behavior (when compared to historic events) that could occur in the future. For example, simulated hurricanes are permitted to make landfall at locations other than those made by the historical storms. These random deviations can also result in more intense storms than the historical events themselves, allowing for the possibility of a future hurricane being the storm of record.

The simulation approach requires specifying a set of parameters which describe the dynamics of some physical system, such as hurricanes. These parameters, which must be descriptive of both the process being modeled and the effects of that process, are defined as an N-dimensional vector space. The parameters which describe only the physical attributes of the process are referred to as input vectors. For example,[1]

$$\underline{v} = (v_1 , v_2 , v_3 , \ldots\ldots , v_N) \qquad (1)$$

In the case of hurricanes, pertinent input vectors include: the central pressure deficit; the radius to maximum winds; maximum winds; minimum distance from the eye of the storm to the location of interest; forward speed of the eye; and the tidal phase during the event. These values, as they will later be described, can be defined for each specific location corresponding to each particular historical or hypothetical event of the total set of storm events used in the study.

The second class of vectors involve some selected response resulting from the N-dimensional parameterized storm, i.e.,

$$\underline{r} = (r_1 , r_2 , r_3 , \ldots\ldots , r_M) \qquad (2)$$

For hurricanes, response vectors can include maximum storm surge, shoreline erosion, dune recession, wind-generated wave (short) height and period, bottom erosion, or any response which can be attributed to the passage of the storm. For this study, the maximum total water surface elevation, reflecting the combined tide plus storm surge, is the response vector of interest.

Although response vectors are related to input vectors

$$v \Rightarrow r \qquad (3)$$

[1] For convenience, mathematical symbols are listed in the notation (Appendix D).

the interrelationship is highly nonlinear and involves correlation relationships which cannot be directly defined, i.e., a nonparametric relationship. For example, in addition to the storm input parameters, storm surge is a function of local bathymetry, shoreline slope and exposure, ocean currents, temperature, etc., as well as their spatial and temporal gradients. It is assumed, however, that these combined effects are reflected in the response vector. For the case of storm surge along the coast of Delaware, atmospheric and hydrodynamic models are used to compute response vectors as a function of the input vectors and local bathymetry together with shoreline configuration. Other response vectors such as sediment transport, shoreline response, and dune recession require application of additional models.

Historical data for storms can thus be characterized as

$$[\boldsymbol{v}_i \; ; \; i = 1, \; \ldots \; , \; I] \tag{4}$$

where I is the number of historical storm events. For example, let v_i have d_v-components

$$\boldsymbol{v}_i = \Re^{d_v} \tag{5}$$

where $\Re^{d_v}$ denotes a d_v-dimensional space.

From this historical data set, a subset of storm events is selected

$$[\; \boldsymbol{v}_j^* \; , j = 1, \; \ldots \; , \; J \;] \tag{6}$$

which is representative of the entire set of historical storms. This subset is referred to as the "training set." Furthermore, those storms comprising the training set are subsequently used as input to appropriate numerical models for computing the desired response vectors. The set of v^*_j usually includes historical events but may include historical storms with a deviation or perturbation, such as a hurricane with a slightly altered path. Some historical events may also be deleted from the training set if two events are nearly identical such that both would produce the same response. Because the purpose is to fill parameter space $\Re$, two similar events are redundant.

The training set of storms can be augmented with additional storms contained in the historical data set. Storm events augmenting the training set are referred to as the "statistical set" of storms. Whereas numerical models are used for generating response vectors for those events in the training set, response vectors for the statistical set of storms are interpolated using the training set response vectors. Thus, stage-frequency relationships can be generated using the entire historical data set without need of simulating all storms in that data set.

With the augmented storm data set (i.e., training and statistical storm sets), the EST produces N simulations of a T-year sequence of events (hurricanes), each with their associated input vectors and response vectors. Because there are N-repetitions of a T-year sequence of events, an error analysis of the results can be performed with respect to median, worst, least, standard deviations, etc. The following describes the procedures by which the input and response data are used to produce multiple simulations of multiple years of events.

Empirical Simulation

Two criteria are required of the T-year sequence of events. The first criteria is that the individual events must be similar in behavior to historical events in order that the interrelationships among the input and response vectors remain realistic. For example, a hurricane with a high central pressure deficit and low maximum winds is not a reasonable event - the two parameters are not independent although their precise dependency is unknown.

Simulation of realistic events is accounted for in the nearest-neighbor interpolation resampling technique developed by Borgman et al. (1992). The basic technique can be described in two dimensions as follows. Let $X_1, X_2, X_3, ..., X_n$ be n independent, identically distributed random vectors (storm events), each having two components $[X_i = \{\underline{x}_i(1), \underline{x}_i(2)\};\ i = 1, n]$. The two-dimensional vector space can be plotted as shown in Figure 1.

Each event X_i has a probability p_i as $1/n$; therefore, a cumulative probability relationship can be developed in which each storm event is assigned a segment of the total probability of 0.0 to 1.0. If each event has an equal probability, then each event is assigned a segment s_j such that $s_j \rightarrow X_j$.

$$
\begin{aligned}
&\left[\ 0 < s_1 \leq \frac{1}{n}\ \right] \\
&\left[\ \frac{1}{n} < s_2 \leq \frac{2}{n}\right] \\
&\left[\ \frac{2}{n} < s_3 \leq \frac{3}{n}\right] \\
&\qquad\vdots \\
&\left[\ \frac{n-1}{n} < s_n \leq .\ 1\right]
\end{aligned}
\tag{7}
$$

A random number from 0 to 1 is selected to identify a storm event from the total storm population. The procedure is equivalent to drawing and replacing random samples from the full storm event population.

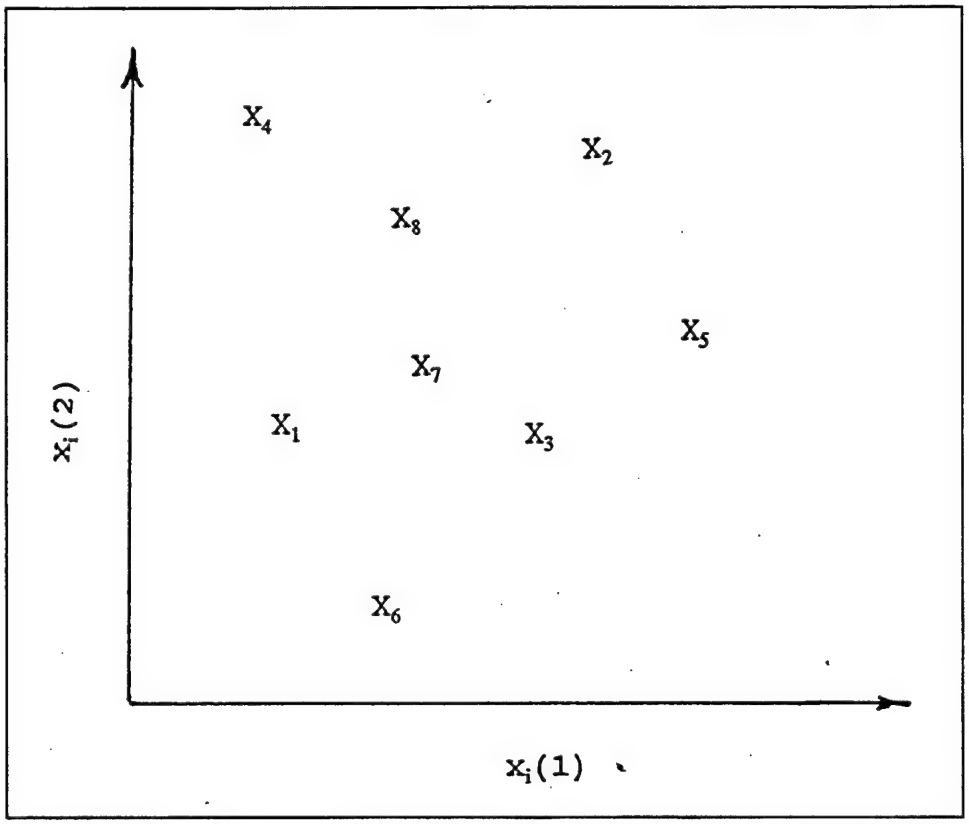

Figure 1. Two-dimensional vector space

The EST is not simply a resampling of historical events technique, but rather an approach intended to simulate the vector distribution contained in the training set population. The EST approach is to select a sample storm based on a random number selection from 0 to 1 and then perform a random walk from the event X_i with x_1 and x_2 response vectors to the nearest neighbor vectors. The walk is based on independent uniform random numbers with the range of (-1,1) and has the effect of simulating responses which are not identical to the historical events but are similar to events which have historically occurred.

Because the simulated events correspond to a specific location, the second criteria to be satisfied is that the total number of storm events selected in the T-years must be statistically representative of the number of historical events which have occurred at the area of concern. For this study, 33 hurricane events were identified which impacted the coast of Delaware during the 104-year period extending from 1886 through 1989 (Jarvinen, Neumann, and Davis 1988). Given the mean frequency of storm events for a particular region, a Poisson distribution is used to determine the average number of expected events in a given year. For example, the Poisson distribution can be written in the following form:

$$Pr\ (s;\lambda) = \frac{\lambda^s e^{-\lambda}}{s!} \tag{8}$$

for s=0,1,2,3,... The probability Pr(s;λ) defines the probability of having s events per year where λ is a measure of the historically based number of events per year. For this study, λ is computed as 0.32 (33/104).

A 10,000-element array is initialized to the above Poisson distribution. The number corresponding to s=0 storms per year is 0.7261; thus, if a random number selection is less than or equal to 0.7261 on an interval of 0.0 to 1.0, no hurricanes would occur during that year of simulation. If the random number is between 0.7261 and 0.7261 + $P[N$=1] = 0.7261 + 0.2324 = 0.9585, one event is selected. Two events for 0.9585 + 0.0372 = 0.9957, etc. When one or more storms are indicated for a given year, they are randomly selected from the nearest neighbor interpolation technique described above.

Output of the EST program is N repetitions of T-years of simulated storm event responses. It is from these responses that frequency-of-occurrence relationships are computed. The computational procedure followed is based on the generation of a probability distribution function corresponding to each of the T-year sequence of simulated data.

Recurrence Relationships

Estimates of frequency-of-occurrence begin with the calculation of a probability distribution function (pdf) for the response vector of interest. Let X_1, X_2, X_3, ..., X_n be n-independent, identically distributed, random response variables with a cumulative pdf

$$F_X\ (x) = Pr[X \leq x] \tag{9}$$

where $Pr[\ ]$ represents the probability that the random variable X is less than or equal to some value x and $F_X(x)$ is the cumulative probability density function ranging from 0.0 to 1.0. The problem is to estimate the value of F_X without introducing some parametric relationship for probability. The following procedure is adopted because it makes use of the probability laws defined by the data and does not incorporate any prior assumptions concerning the probability relationship.

Assume a set of n observations of data. The n values of x are first ranked in order of increasing size. In the following analysis, the parentheses surrounding the subscript indicate that the data have been rank-ordered. The value $x_{(1)}$ is the smallest in the series and $x_{(n)}$ represents the largest value. Let r denote the rank of the value $x_{(r)}$ such that rank 1 is the smallest and rank $r = n$ is the largest.

An empirical estimate of $F_X(x_{(r)})$, denoted by $\hat{F}_X(x_{(r)})$, is given by Gumbel (1954) (see also Borgman and Scheffner (1991) or Scheffner and Borgman (1992)).

$$\hat{F}_x(x_{(r)}) = \frac{r}{(n+1)} \tag{10}$$

for $\{x_{(r)}, r = 1, 2, 3,....., n\}$. This form of estimate allows for future values of x to be less than the smallest observation $x_{(1)}$ with probability of $1/(n+1)$, and to be larger than the largest value $x_{(n)}$ also with probability $m/(n+1)$.

An example set of 10 years of observed elevations, the rank ordered set of observations, the rank, and the cumulative pdf are shown in Table 1. As can be seen in the table, this form of the cumulative distribution function allows for values of x to be greater than the maximum or less than the minimum observed values in the historical database. A plot of the cumulative distribution function versus $x_{(r)}$ as computed by Equation 10 is shown in Figure 2. In the implementation of the EST, tail functions (Borgman and Scheffner 1991) are used to define the pdf for events larger than the largest or smaller than the smallest observed event so that there is no discontinuity in the pdf.

Table 1
Sample Distribution Function Calculation

Year	$x_{1,2,...n}$	$X_{(r)}$	Rank r	$\hat{F}_x(X_{(r)})$
1	3.2	10.5	10	0.91
2	3.5	8.6	9	0.82
3	8.0	8.0	8	0.73
4	1.0	7.5	7	0.64
5	10.5	5.9	6	0.55
6	5.9	4.1	5	0.45
7	8.6	3.5	4	0.36
8	4.1	3.2	3	0.27
9	2.3	2.3	2	0.18
10	7.5	1.0	1	0.10

The cumulative pdf as defined by Equation 11 and shown in Figure 2 is used to develop stage-frequency relationships in the following manner. Consider that the cumulative probability for an n-year return period storm can be written as:

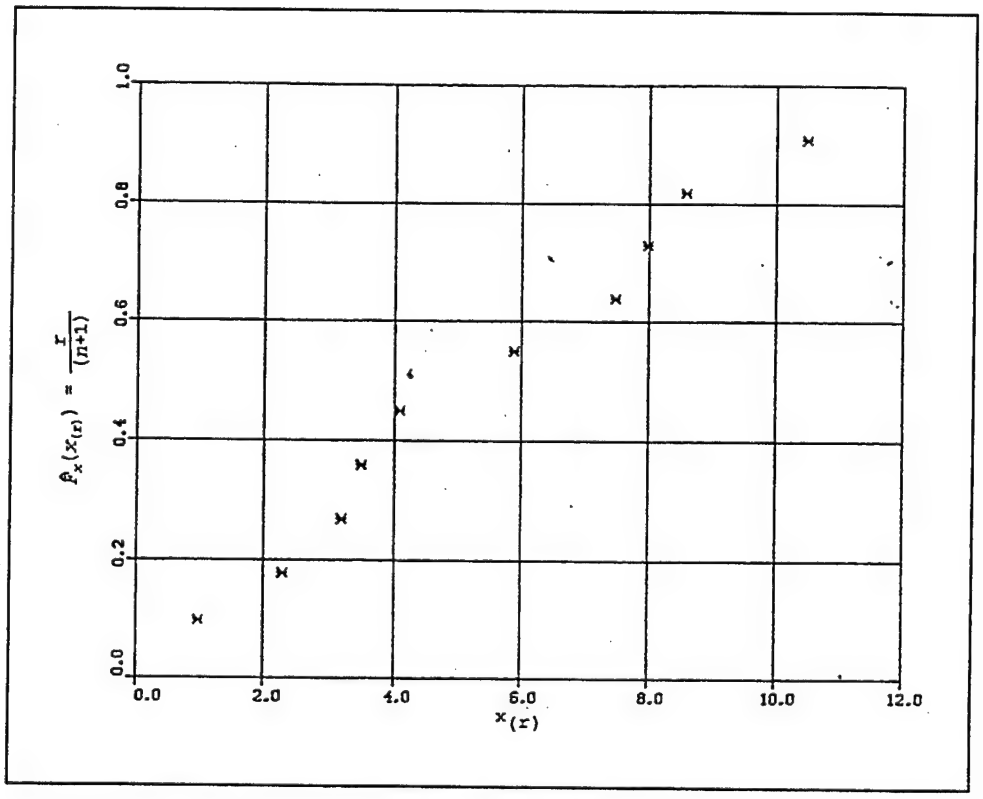

Figure 2. Example of cumulative probability distribution plot

$$F(n) = 1 - \frac{1}{n} \tag{11}$$

where $F(n)$ is the simulated cumulative probability of occurrence for an event with a return period of n years. Frequency-of-occurrence relationships are obtained by linearly interpolating a stage from Equation 10 corresponding to the pfd associated with the return period specified in Equation 11.

3 Description of Numerical Models

Generation of hurricane stage-frequency relationships for the coast of Delaware can be divided into three interrelated tasks, each using a numerical model. In the first task, hurricane-induced wind and atmospheric pressure fields are generated to replicate those hurricanes which have impacted the study area. Using these wind and pressure fields, storm surge events are simulated in the second task using a long-wave hydrodynamic model to obtain peak water surface levels. With the information obtained in the above tasks, the EST is employed, which utilizes the inter-relationships of historic storm events and the computed surge. Application of the EST provides the desired stage-frequency relationships for the study area. Descriptions of the wind and atmospheric pressure model and the hydrodynamic model are presented below.

Wind and Atmospheric Pressure Field Model

The Planetary Boundary Layer (PBL) wind field numerical model was selected for simulating hurricane-generated wind and atmospheric pressure fields. The model employs the vertically averaged primitive equations of motion for predicting wind velocities experienced within a hurricane. The model includes parameterization of the momentum, heat, and moisture fluxes together with the surface drag and roughness formulations. Through hindcast applications, Cardone, Greenwood, and Greenwood (1992) found that their model yields accurate surface wind speeds and directions when compared to measured data collected while the hurricane was in open water. An additional feature incorporated within the model is a surface friction drag formulation for simulating the passage of hurricanes over various terrains, including lakes, marshes, plains, woods, and cities.

The authors found that the surface drag formulation resulted in wind speeds which were greater in the hurricane's left-rear quadrant for cases where a hurricane is situated above land-water terrain, such as at landfall, than for cases where a hurricane resides in open seas. Physically, however, these winds should be lower. Given that hurricane winds blow in a counterclockwise manner in the Northern Hemisphere, winds entering the left-rear quadrant have

previously blown across land which reduces wind speeds for various reasons. First, higher surface drag effects imposed by land reduce wind speeds. Second, heat and moisture fluxes needed to sustain winds are lower for land than water.

The PBL hurricane wind model requires a series of "snapshots" for input consisting of a set of meteorological storm parameters defining the storm at various stages in its development or at particular times during its life. These parameters include: latitude and longitude of the storm's eye; track direction and forward speed measured at the eye; radius to maximum winds; central and peripheral atmospheric pressures; and an estimate of the geostrophic wind speed and direction. Also, the direction and speed of steering currents can be provided for representing asymmetric hurricanes.

Some meteorological storm parameters were obtained from the hurricane database developed by the National Oceanic and Atmospheric Administration's (NOAA) National Hurricane Center (NHC) (Jarvinen, Neumann, and Davis 1988). This database summarizes all hurricanes and tropical storms which occurred in the North Atlantic Ocean over the 104-year period from 1886 through 1989. Information contained in this database is provided at 0000, 0600, 1200, and 1800 hr Greenwich Mean Time (GMT), and includes: latitude and longitude of the storm, central pressure, and maximum wind speed.

Radius to maximum winds is approximated using a function that incorporates the maximum wind speed and the atmospheric pressure anomaly (Jelesnianski and Taylor 1973). Track directions and forward speeds required by the PBL model are approximated hourly, using cubic spline interpolation technique, from the storm's 6-hr latitudinal and longitudinal positions provided in the database. Peripheral atmospheric pressures were assumed equal to 1013 mb, and geostrophic wind speeds were specified as 6 knots and have the same direction as the storm track.

The spatial area over which a hurricane resides is defined in the model via a numerical grid or a lattice network of nodes. Wind velocities and atmospheric pressures are computed at each node in the grid. Whereas some models employ a fixed grid system to simulate a hurricane (i.e., stationary grid with a moving storm), the PBL model simulates the hurricane as a stationary storm with a moving grid. A hurricane's translational or forward motion is incorporated into model calculations by adding the forward and rotational velocity vector components.

The model uses a nested gridding technique, composed of five layers or subgrids, for computing the wind fields. Each subgrid measures 21 by 21 nodes in the x- and y-directions, respectively, and the centers of all subgrids, node (11,11), are defined at the eye of the hurricane. Whereas the number of nodes composing each subgrid is the same, the area of coverage and spatial resolution differs for each grid. For this study, the subgrid with the finest resolution had an incremental distance of 5 km between nodes and covered an area of 10,000 sq km. Incremental distances for the remaining

subgrids were 10, 20, 40, and 80 km and their areas of coverage were 40,000, 160,000, 640,000, and 2,560,000 sq km, respectively.

For each snapshot, the equations of motion are first solved using the grid covering the greatest area, which in this study is the grid having an incremental distance of 80 km between nodes. Computed wind velocities are then used as boundary conditions on the second-largest grid, and the equations of motion are solved again. This same procedure is followed for the remaining grids where wind fields are computed using sequentially smaller grids together with wind velocities computed with the next larger grid serving as boundary conditions. Thus, the nested gridding technique provides wind field information over a wide spatial area while sufficient grid resolution is provided to accurately compute winds within the eye of the hurricane.

After all snapshots have been processed, hourly wind and atmospheric pressure fields are interpolated using a nonlinear blending algorithm which produces a smooth transition from one snapshot to the next. Hourly wind and pressure fields are then interpolated from the PBL grid onto the hydrodynamic grid and subsequently stored for use by the hydrodynamic model.

Storm Surge Model

The ADvanced CIRCulation (ADCIRC) numerical model was chosen for simulating the long-wave hydrodynamic processes in the study area. This program employs a two-dimensional, depth-integrated finite-element solution of the generalized Wave-Continuity equation (GWCE). The fundamental components of the GWCE equation are the depth-integrated continuity and Navier-Stokes equations for conservation of mass and momentum. The time-differentiated form of the conservation of mass is combined with a space-differentiated form of the conservation of momentum equation to develop the GWCE equation (Westerink et al. 1992).

The GWCE-based solution scheme eliminates several problems associated with finite element programs which solve the primitive forms of the continuity and momentum equations (i.e. Navier-Stokes equations), including spurious modes of oscillation and artificial damping of the tidal signal. Forcing functions include time-varying water surface elevations, wind shear stresses, atmospheric pressure gradients and the Coriolis effect. Also, the study area can be described in ADCIRC using either a Cartesian (flat earth) or spherical coordinate system.

The storm surge model was adapted from the east and gulf coasts hydrodynamic model developed in the U.S. Army Engineer Dredging Research Program (DRP). On a "continental" scale, the DRP model has been calibrated and validated. (Continental scale refers to the larger-domain circulation patterns in deeper waters and open coast locations; however, model testing in shallow waters, such as in inlets and estuaries, must still be performed.) Thus, adapting this model to the present study minimizes the effort needed to define

boundary conditions, generate a completely new grid, and conduct model testing.

Using a grid which incorporates the entire eastern seaboard provides several benefits. First, extending the seaward boundary beyond the continental shelf enables a linear tidal signal to be specified at the mid-Atlantic open water boundary. Historically, a time-series of water surface elevations measured at the coastline would be specified at the seaward boundary to drive the model. Through a trial-and-error procedure, the time-series specified at the boundary would be adjusted in phase and amplitude until the model-generated time-series (computed at the gaging station on shore) matched the measured data. Although minimized, the tidal signal contains phase and amplitude errors induced by the nonlinear tidal effects generated in shallow water. Thus, by placing the seaward boundary in the abyssal plain, errors in the water surface elevation time-series specified at the seaward boundary are minimized.

Second, the nonlinear effects described above must also be addressed for the lateral open-water boundaries, which extend from shore to the ocean's abyssal plain. Typically, lateral boundaries are placed sufficiently far from the study area so that errors in the time-series do not corrupt model-generated results within the area of interest. With the grid extending from Nova Scotia, Canada, to Venezuela, this problem is effectively eliminated.

Third, the majority of hurricanes affecting the coast of Delaware approach the mainland from the southeast, then veer away to the northeast before making landfall. As the hurricane enters the model area, the tidal signal along the lateral open-water boundary can be significantly altered by the storm's atmospheric pressure anomaly. Thus, the flow field can be corrupted in much the same manner as described above. As before, this problem can be alleviated by modeling the entire eastern seaboard.

The numerical grid, specified in spherical coordinates, was developed by increasing the resolution of the DRP east coast gird in the study and surrounding areas. The grid consists of 11,829 nodes and 21,917 elements. Figure 3 presents the numerical grid used in this study and the bathymetry contours are presented in Figure 4. Figures 5 and 6 provide a "zoomed-in" picture of the grid and bathymetry, respectively, in the study area. Note, however, the grid was plotted using a uniform longitudinal spacing (with respect to latitude); thus the spherical projection of the grid was not maintained.

Bathymetry was obtained from the National Center for Atmospheric Research ETOPO5 database. Bathymetry is stored at a resolution of 5 min latitude by 5 min longitude and depths have units of meters. While this resolution is adequate for open ocean waters, it is inadequate to resolve estuarine and nearshore areas. Bathymetry in these areas was updated using depths supplied from NOAA nautical charts 12214, 12211, and 12304.

Time-series of astronomical tidal elevations specified at the open water boundary were synthesized from tidal amplitudes and phases obtained from

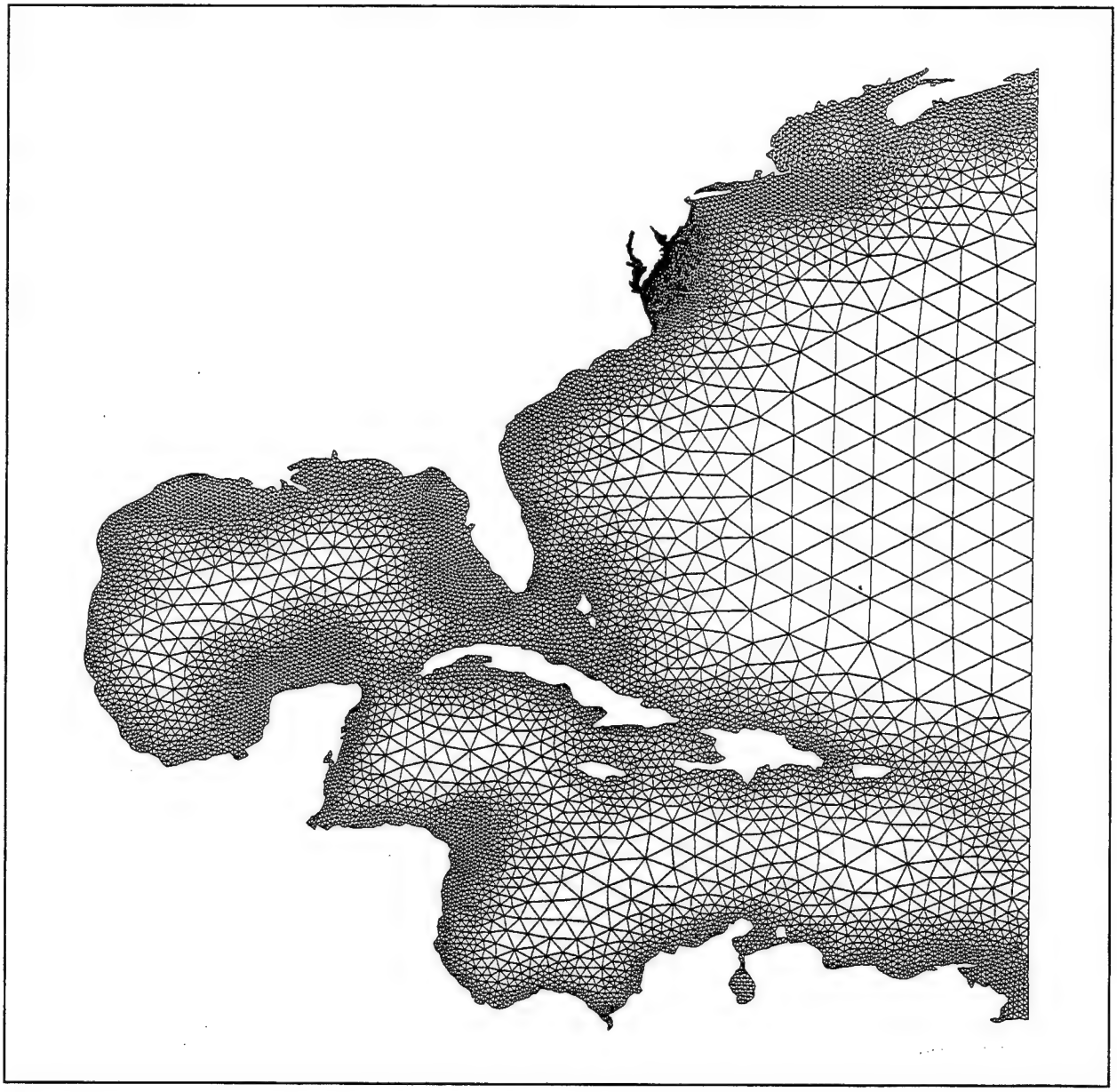

Figure 3. Numerical grid of U.S. east and gulf coasts

Schwiderski and Szeto (1981). Modeled constituents include M_2, S_2, N_2, O_1, P_1, K_2, K_1, and Q_1. Constituent data are provided at 1-deg increments in latitude and longitude. A bilinear interpolation algorithm was used for estimating tidal amplitudes and phases at the 61 grid nodes composing the open water boundary, which is located at approximately latitude 60.4° W.

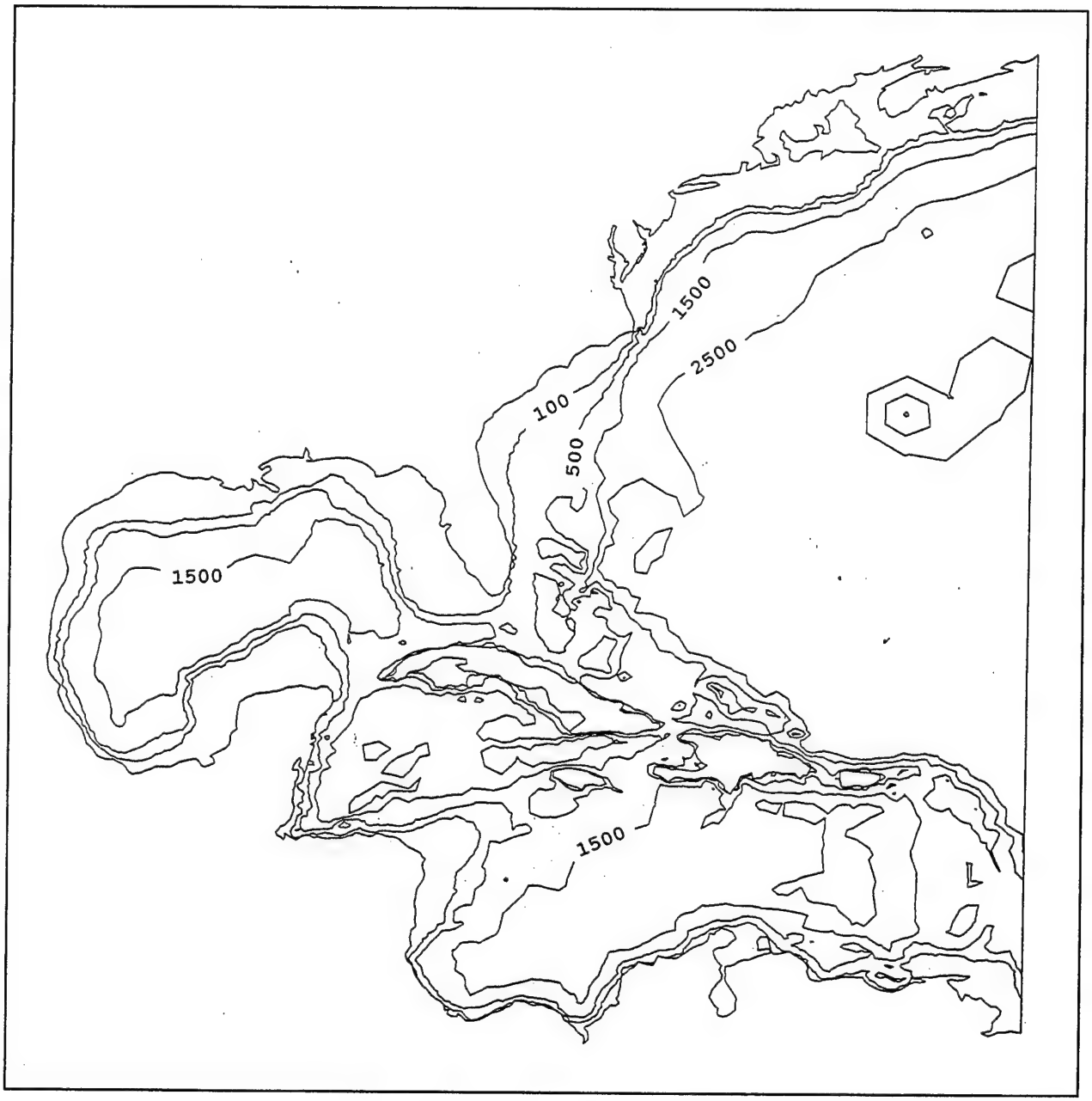

Figure 4. Bathymetric contours (in fathoms) in modeling domain

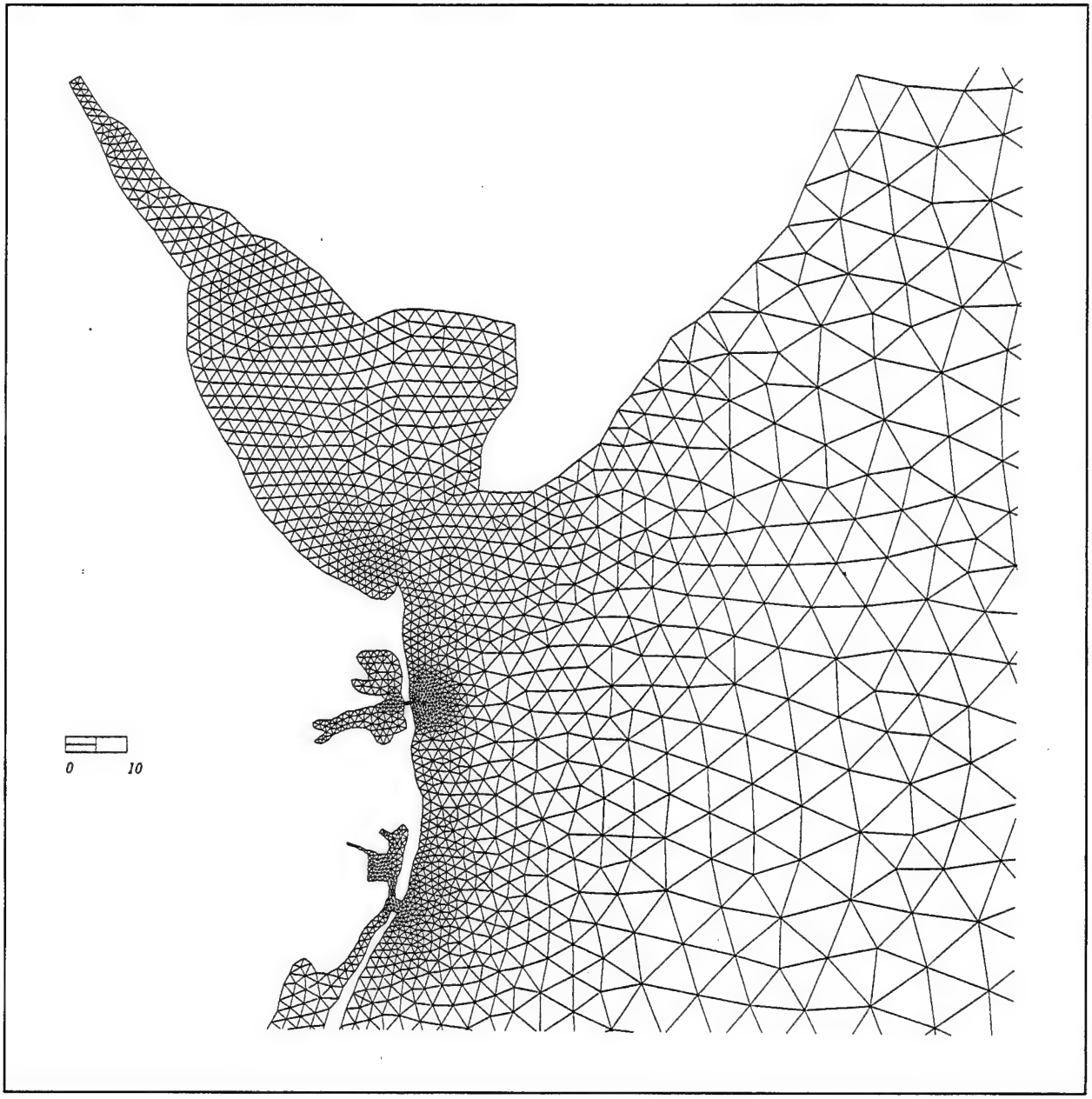

Figure 5. Numerical grid in vicinity of study area

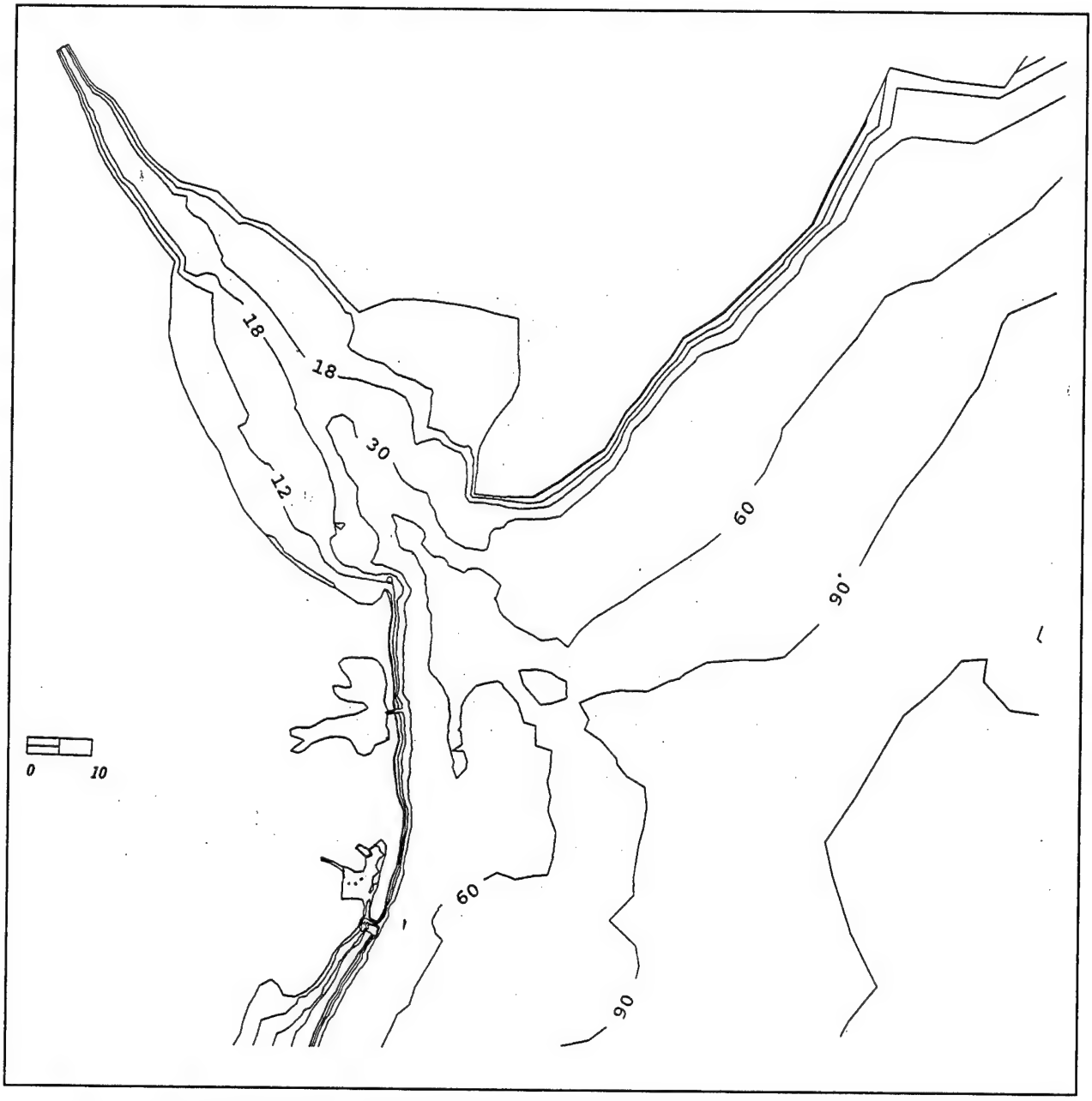

Figure 6. Bathymetric contours (in feet) in vicinity of study area

4 Implementation of Storm Surge Model

During construction of a numerical model, the model must undergo calibration and validation exercises to ensure that it accurately predicts hydrodynamic conditions within a given study area. Accuracy of model results is greatly influenced by the accuracy of boundary and forcing conditions, representation of the geometry of the study area (i.e., bathymetry and land/water interface), and to a lesser degree, the choice of certain "calibration" parameters. Calibration is the adjustments of certain model parameters, such as the bottom friction coefficient, to maximize agreement between model results and measured data.

Once the calibration procedure is completed, the model undergoes a validation procedure to ensure that the model can replicate conditions during a different time period than that used in the calibration procedure. In the validation procedure, the model is applied without adjusting those parameters determined in the calibration procedure. Obtaining a good comparison between model and measured data in the validation procedure provides confidence that the model can accurately predict hydrodynamic processes in the study area.

The strategy for calibrating and validating the storm surge model consists of two criteria. First, it must be demonstrated that the model can accurately predict tidal propagation in the study area. Second, in order to show that the model can replicate storm surge effects in the study area, storm surge for a medium-to-large intensity hurricane which impacted the coast of Delaware must be simulated. Procedures used in conducting model testing and results obtained in these tests are summarized in the following sections.

Calibration of Storm Surge Model

The hydrodynamic model was calibrated by adjusting model parameters (i.e., bottom friction coefficient and depths) so that model-generated water surface level time-series compared favorably to time-series reconstructed from tidal constituents. Locations at which comparisons were made include: Cape

May, NJ; Reedy Point, DE; Lewes, DE; Indian River Inlet, DE; and, Ocean City, MD. These locations are shown in Figure 7.

A model calibrated with time-series of water surface elevations synthesized using tidal constituents can simulate hydrodynamic conditions to the same degree of accuracy as one calibrated with measured water levels. Tidal constituents are derived from long-term tidal gaging measurements at a particular station; time-series of measured elevations are analyzed, using a Fourier series approach, to obtain a set of sine waves (with differing amplitudes, phases, and periods) which, when added together, reproduce the periodic signal of tides at that particular station. Because this analysis uses measured water surface elevations, the reconstructed tidal signal implicitly includes the effects of bathymetric gradients and shoreline configuration. However, wind effects are omitted in the reproduced signal.

Calibration simulations were conducted over a 30-day period beginning at 0:00 Eastern Standard Time on 1 September 1985. A 30-sec time-step was used in these simulations. Comparisons of computed and constituent-generated water surface levels are presented in Figures 8 through 12.

Parametric and non-parametric statistical tests were performed to quantitatively assess the model's ability to replicate the hydrodynamic processes occurring in the study area. One test is the root-mean-square (rms) difference calculations of the model- and constituent-generated water surface level time-series. One limitation of the rms difference test is that no information is provided as to the source of error being measured. For example, one source of error can be a shift in phase between measured and computed water oscillation periods, whereas a second source could be due to discrepancies in predicted water surface elevations. To overcome this limitation, a series of non-parametric or "skill" tests were used to differentiate between phase and magnitude errors (Hess and Bosley 1991).

Skill tests selected for analyzing the hydrodynamic model include statistical comparisons of the timing and amplitude of local water level extrema (minimum and maximum) computed with tidal constituents at the five gaging stations. These tests are average gain or ratio of predicted to measured extrema, the rms difference in amplitudes, average lag or phase shift between predicted and measured extrema, and the rms difference in lag.

The average gain can be expressed as:

$$G = \frac{1}{\nu} \Sigma \left(\frac{Y_c}{Y_m} \right) \tag{12}$$

where G represents the gain, υ is equal to the number of extrema pairs contained in the time-series data, and Y_c and Y_m signify the computed and measured (i.e., model- and constituent-generated) extrema values, respectively.

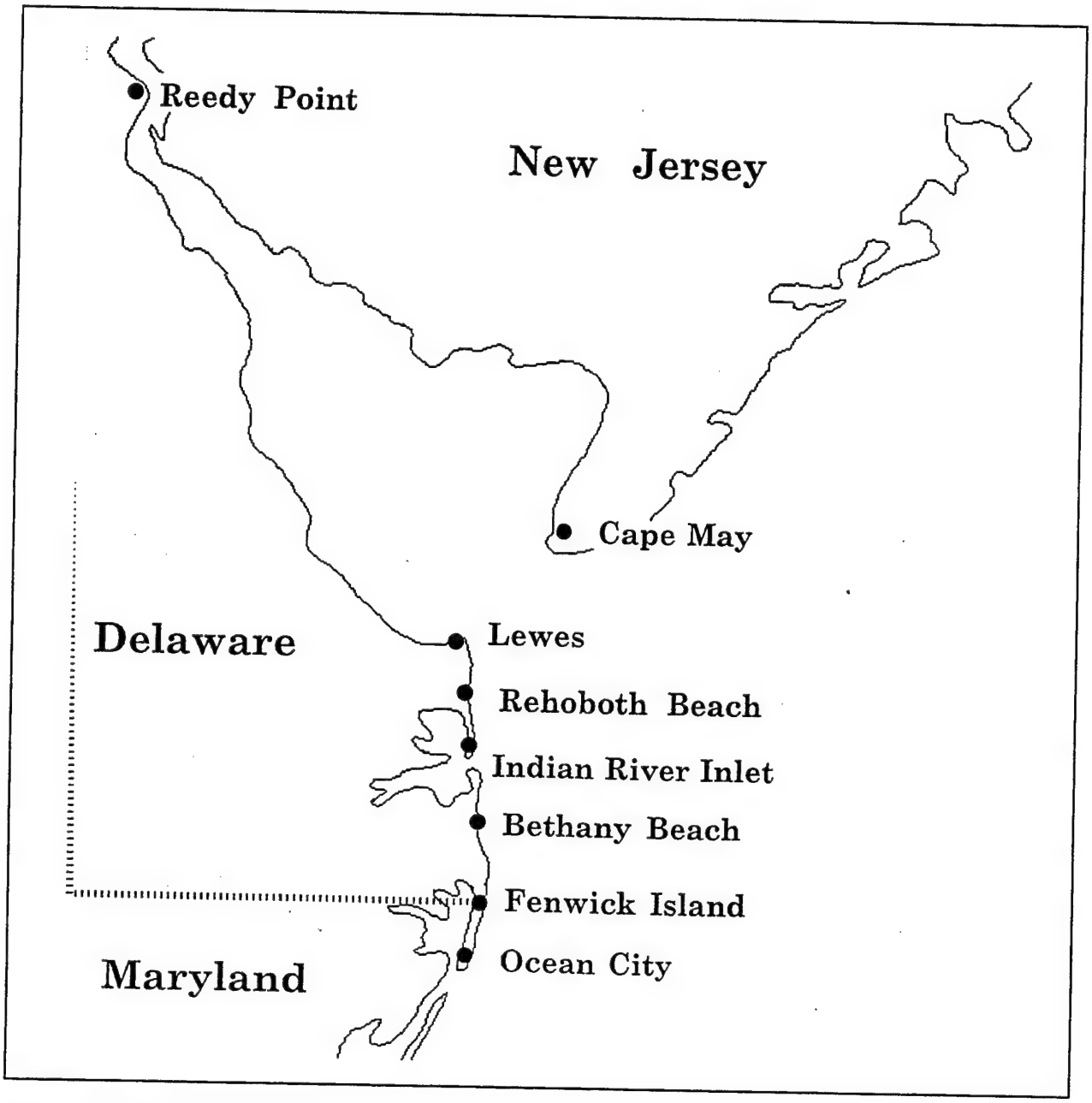

Figure 7. Vicinity of study area

The rms difference in amplitude has the following formulation:

$$A_{rms} = \left[\frac{1}{\nu} \Sigma \left(Y_c - Y_m\right)^2\right]^{1/2} \tag{13}$$

where A_{rms} represents the rms difference in amplitude and the remaining variables have been previously defined.

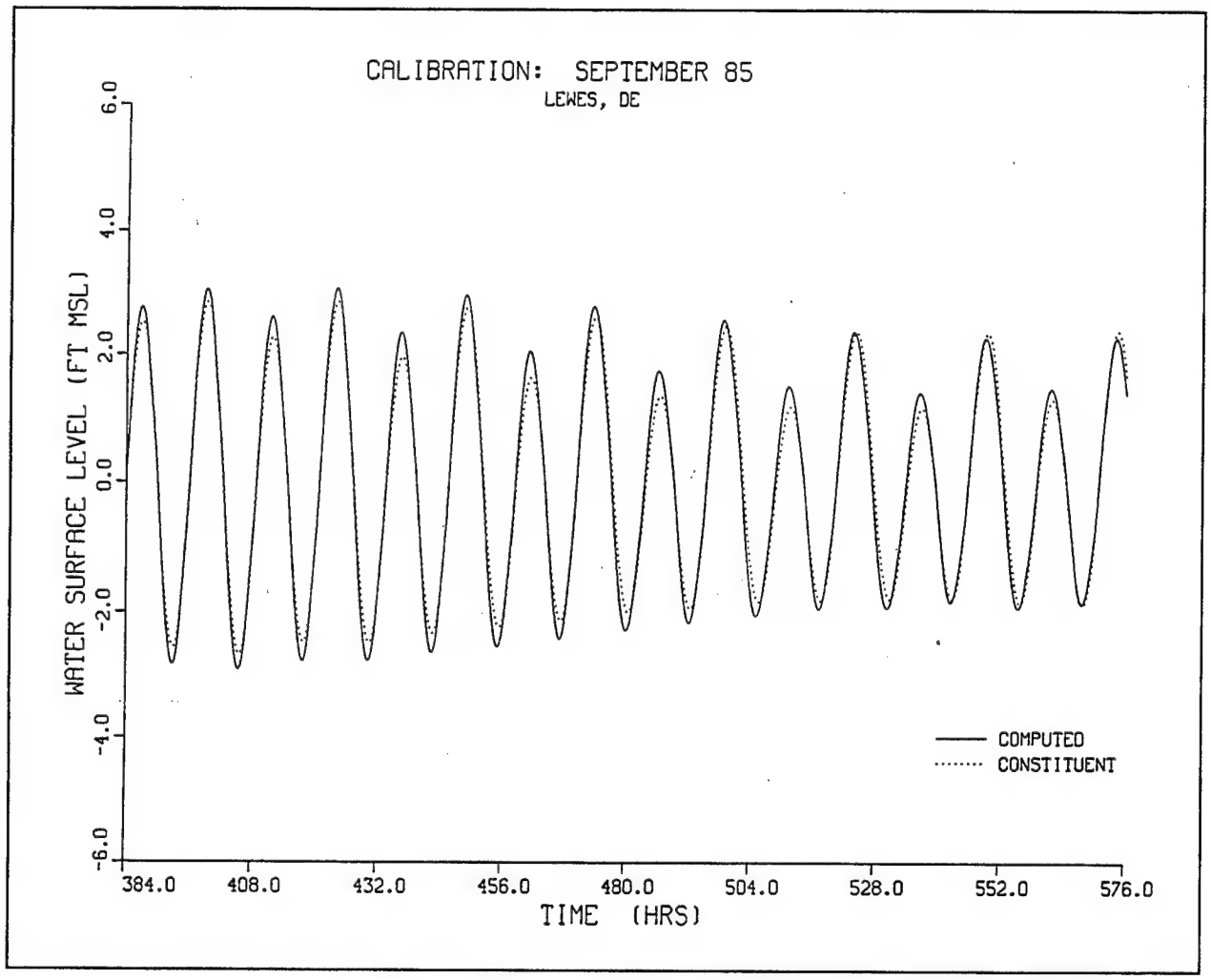

Figure 8. Comparison of water surface levels at Lewes station

The average lag between computed and measured extrema can be written as:

$$L_m = \frac{1}{\nu} \Sigma \left(T_c - T_m\right) \tag{14}$$

where L_m represents the average lag and T_c and T_m signify the time of extrema occurrence in the computed and measured time-series, respectively.

The rms difference in lag can be expressed as:

$$L_{rms} = \left[\frac{1}{\nu} \Sigma \left(T_c - T_m\right)^2\right]^{1/2} \tag{15}$$

where L_{rms} represents the rms lag.

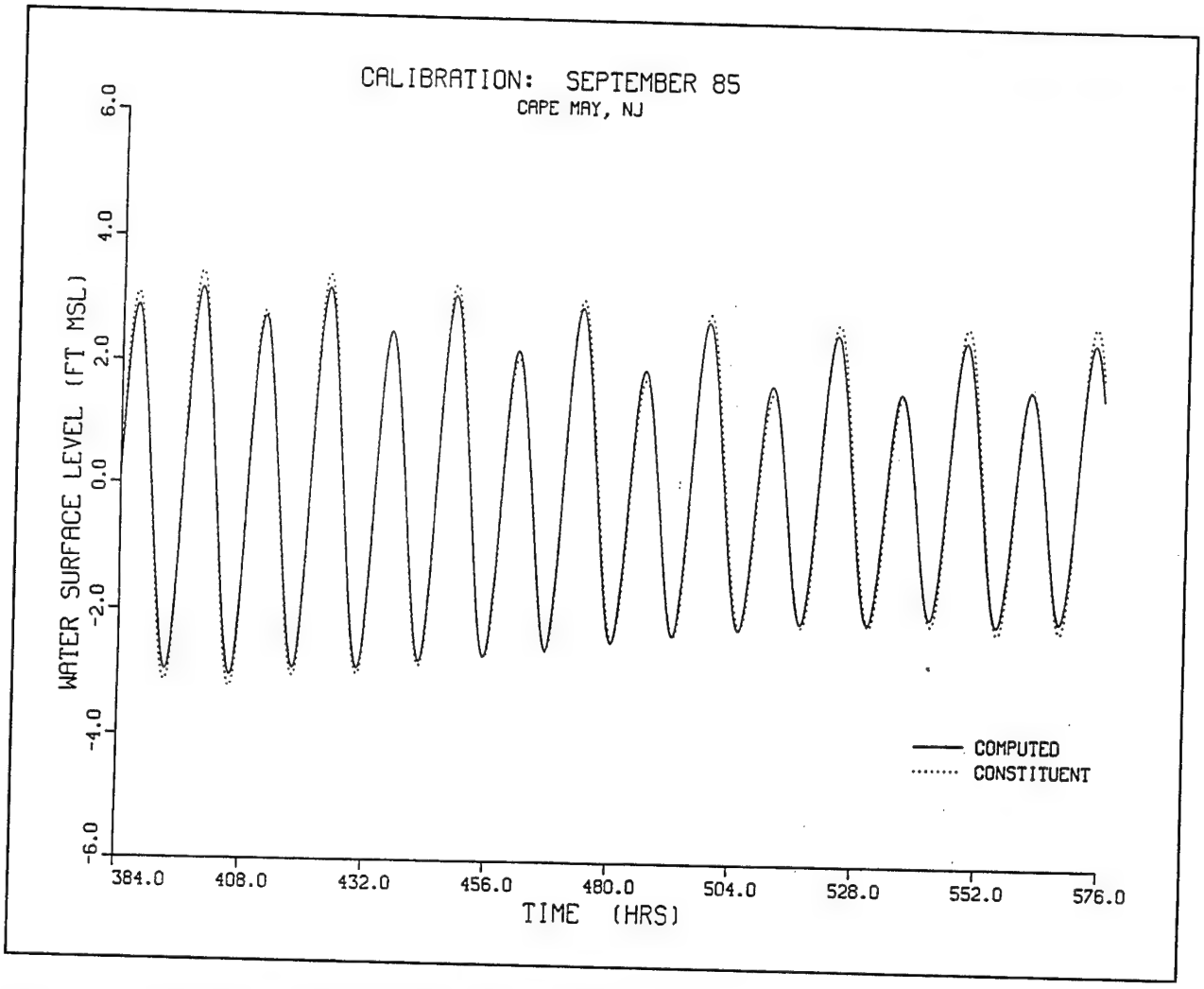

Figure 9. Comparison of water surface levels at Cape May station

Model-generated water surface level time-series at the five gauge locations were analyzed with the preceding skills tests. During the early stages of the calibration exercise, it was found that the model requires approximately 14 days to spin up, or dampen artificial oscillation modes generated by starting the model from static flow field conditions. Thus, skill tests were performed using time-series data "recorded" over the latter 16 days of the calibration period. Furthermore, tests were performed using a 15-min sampling interval. Table 2 presents a summary of this analysis.

The average gain in extrema water surface elevations for the five stations ranged from 0.96 to 1.11. (An average gain greater than 1.0 denotes that the model-generated extrema were greater than the constituent-generated extrema.) For the Cape May, Indian River Inlet, and Ocean City stations, the model-generated extrema were within 4 percent of the constituent-generated extrema. The greatest difference in gain was found at Reedy Point, which had a gain of 1.11. Furthermore, the greatest extrema rms was also found at the Reedy Point station (0.31 ft). This discrepancy is attributed to the placement of the

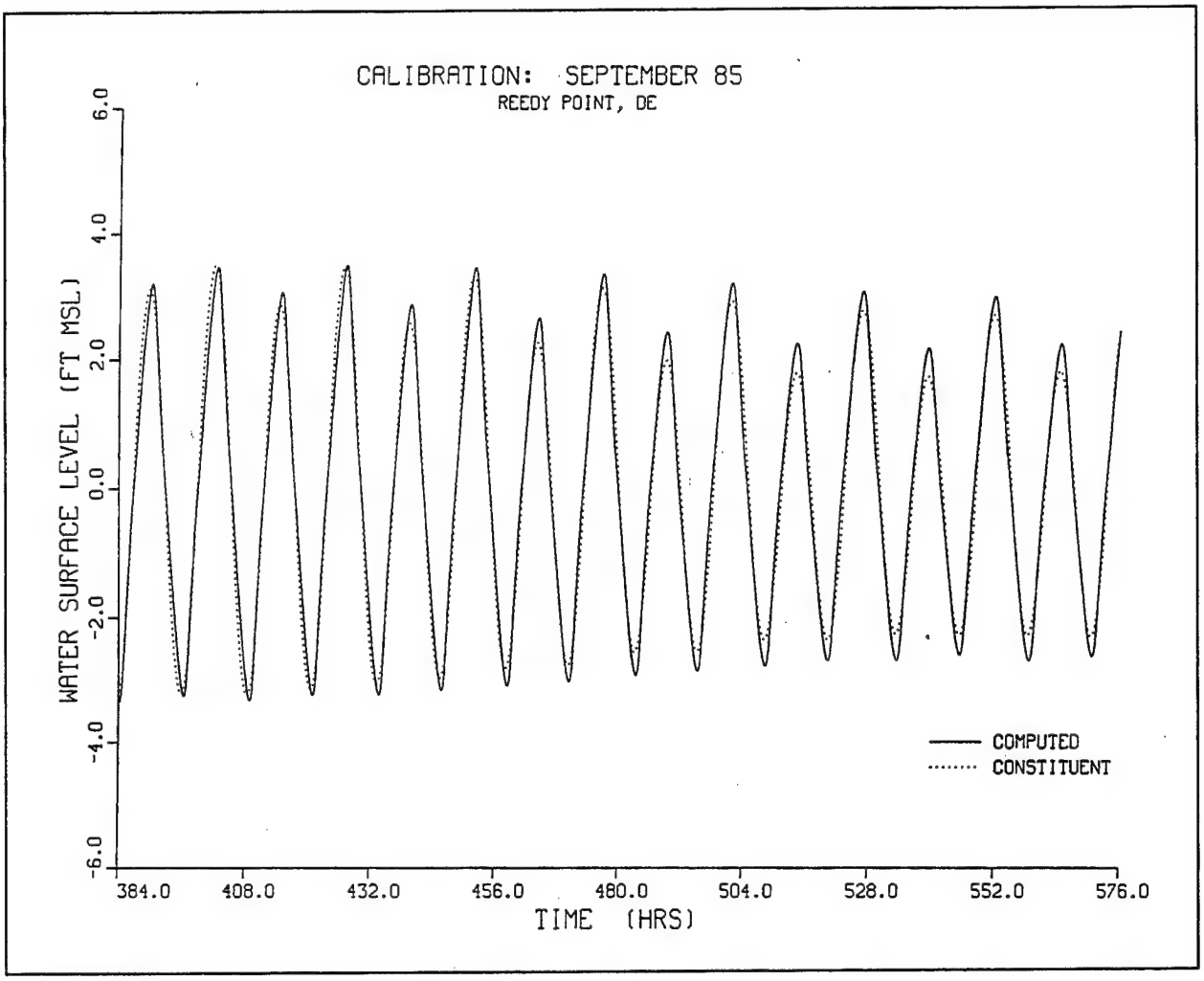

Figure 10. Comparison of water surface levels at Reedy Point station

upstream boundary of the Delaware Bay/River; extending the grid further upstream of its present limit would result in reducing water surface fluctuations via increasing the water storage volume of the upstream region. However, this step was not deemed necessary because the average tidal range over the simulation period at this station was approximately 5.8 ft; therefore, the discrepancy between model- and constituent-generated water surface levels was judged relatively small.

Phase differences between computed and constituent-generated tidal oscillations ranged from 0.14 to 0.66 hr. Computed tidal oscillations at the Cape May and Lewes stations tended to lead the constituent-generated oscillations, whereas at Reedy Point, Indian River Inlet, and Ocean City, the model-generated computed tidal phases lagged behind the constituent-generated phases. Except for the Indian River Inlet station, phase differences were within 45 min. The difference in phases at the Indian River Inlet station, which experienced the greatest discrepancy in phases, is attributed to the lack of grid resolution defining this inlet and its back-bay areas.

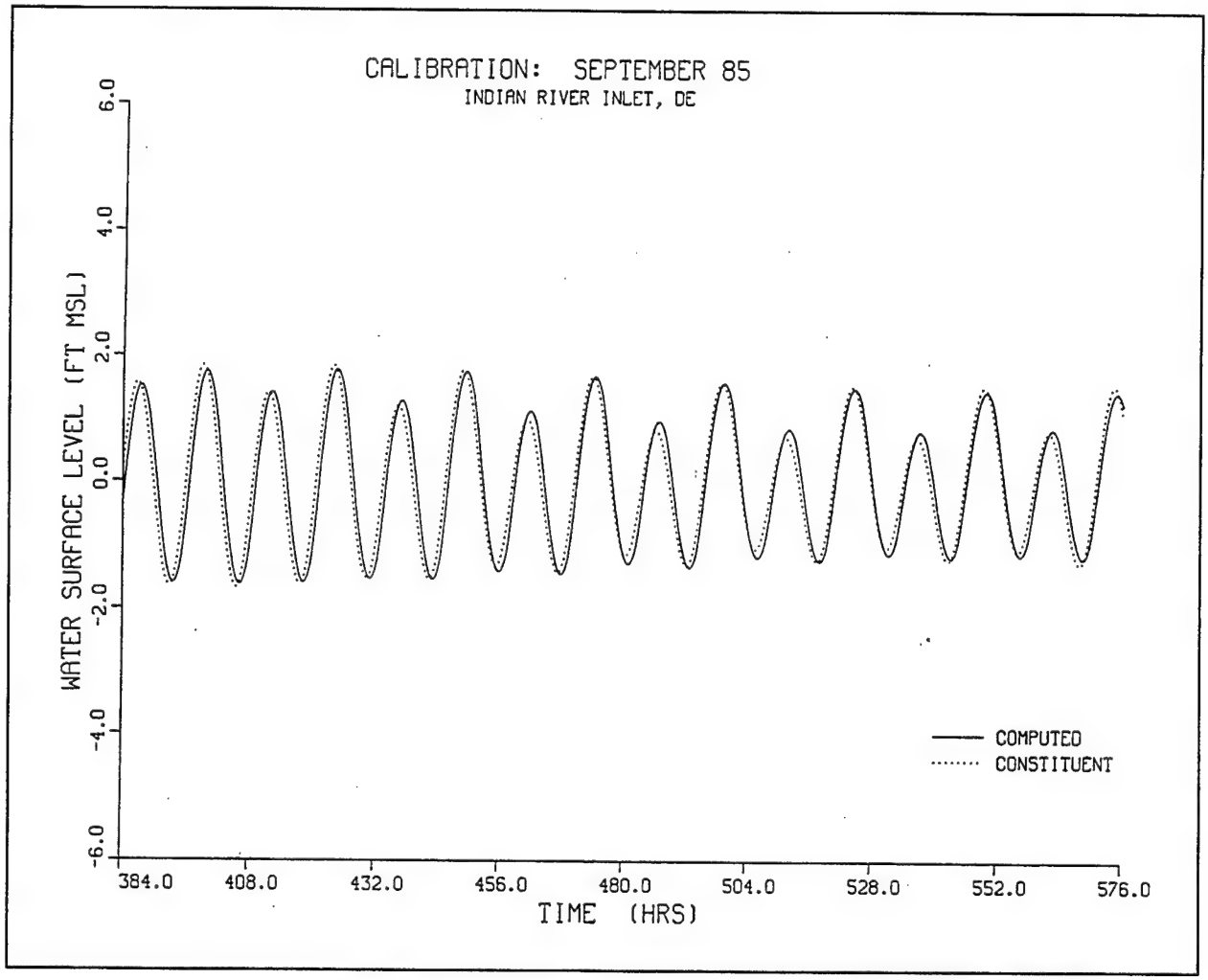

Figure 11. Comparison of water surface levels at Indian River Inlet station

Validation of Storm Surge Model

Model validation was achieved by performing a storm surge simulation of Hurricane Gloria, which impacted the study area in September 1985. The hindcast began on 1 September 1985 at 0000 GMT and ended on 1 October at 0000 GMT. A 30-sec time-step was used in the simulation and tidal forcing was specified at the open water boundary.

From the beginning of the hindcast simulation to 16 September at 1200 GMT, no wind or atmospheric pressures were included in the model. This 16-day period provided sufficient simulation time to develop an accurate tidal current field and to dampen any start-up errors. Thereafter, from 16 September at 1200 through the end of the hindcast at 0000 GMT on 1 October, wind and atmospheric pressure fields were supplied to the model at hourly increments. These fields were computed independently of adjacent weather systems (e.g., high pressure cells) using a constant far-field atmospheric pressure of

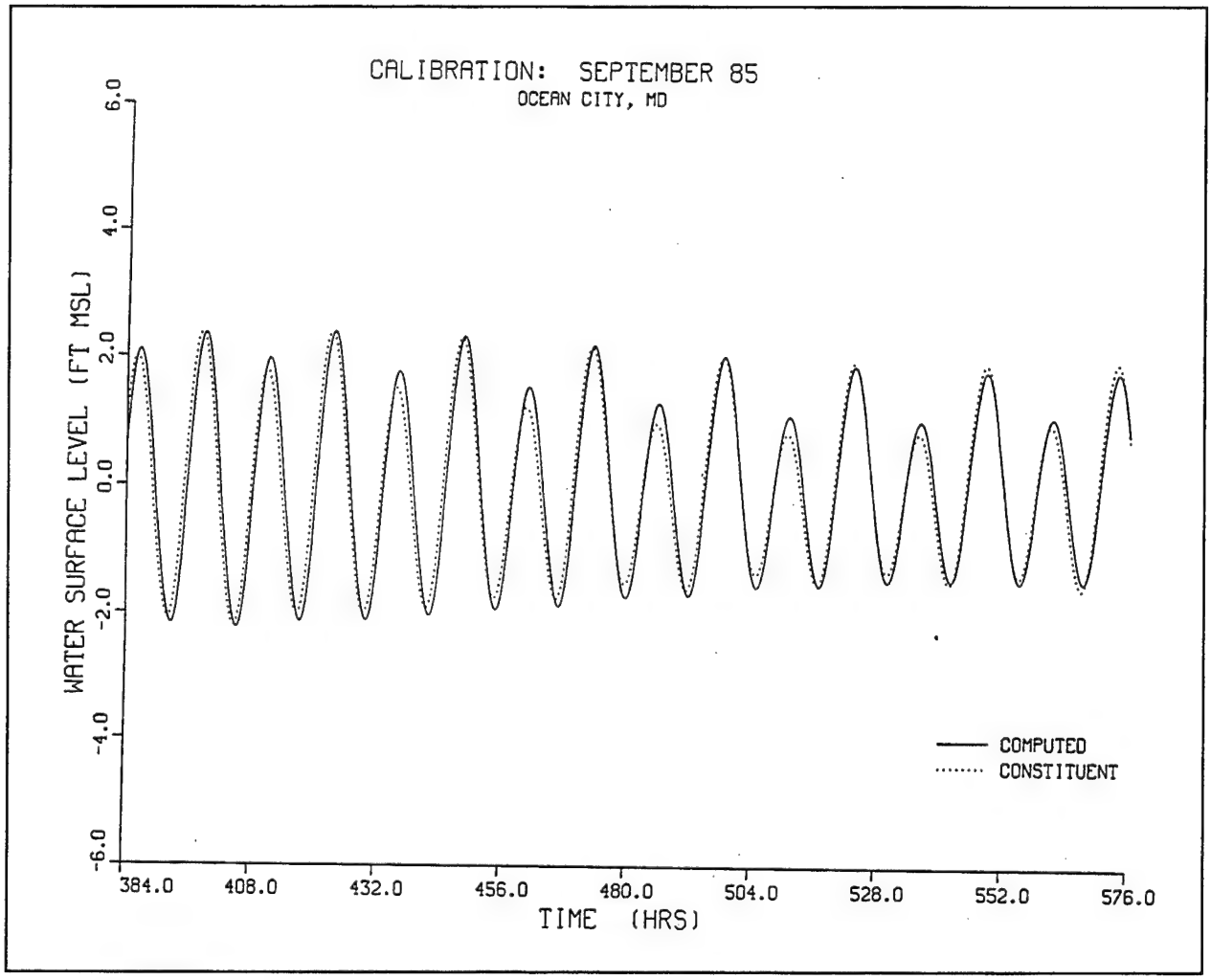

Figure 12. Comparison of water surface levels at Ocean City station

Table 2
Statistical Comparison of Model- and Constituent-Generated Tidal Time-Series[1]

Station	Gain	Extrema rms, ft	Average Lag, hr	Lag rms, hr
Cape May	0.96	0.16	-0.02	0.14
Lewes	1.07	0.20	-0.22	0.28
Reedy Point	1.11	0.31	0.39	0.44
Indian River Inlet	1.02	0.15	0.64	0.66
Ocean City	1.04	0.12	0.42	0.47

[1] A table of factors for converting non-SI units of measurement to SI units is presented on page v.

1,013 mb. In addition, nodal wind and pressure values were linearly interpolated at time-steps falling between whole hours.

Figure 13 presents a comparison of model-generated and measured water surface elevations recorded at Lewes, DE, for the period of 25 September at 0000 GMT to 0000 GMT on 30 September. The hydrodynamic model predicted a peak water surface elevation of approximately 6.21 ft mean sea level (msl), whereas the Lewes gaging station measured a peak elevation of 5.99 ft msl. Thus, the model overpredicted the peak water level by 0.2 ft. (No statistical analysis of the model's output was performed because the hurricane did not affect water surface elevations in the study area for a sufficient length of time to obtain reliable statistical comparisons.)

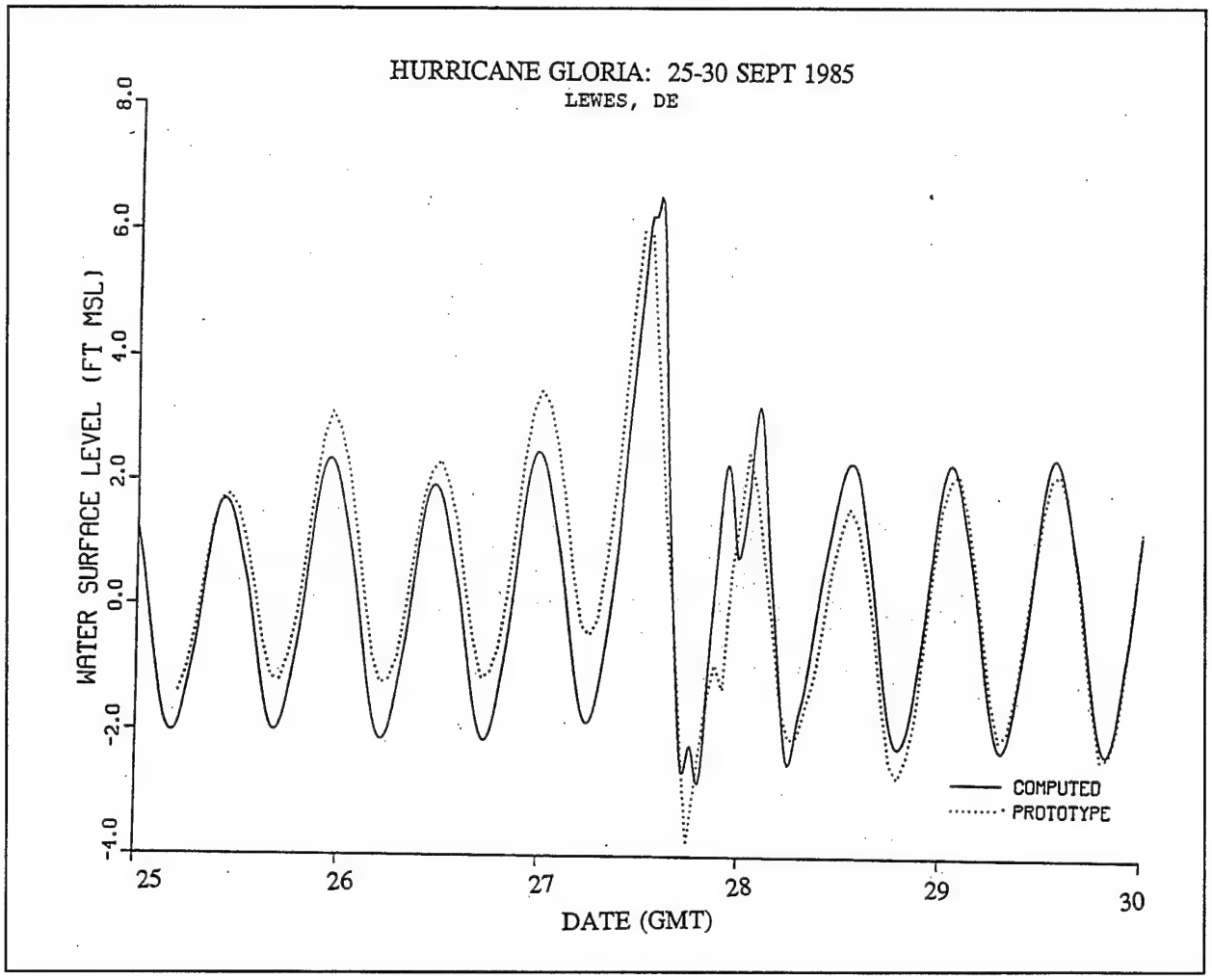

Figure 13. Comparison of computer and measured water surface levels at Lewes station

As shown in the figure, the hydrodynamic model predicted the peak storm surge elevation approximately 1 hr later than its measured occurrence. This lag is attributed to the assumption that the hurricane's forward speed was constant during the 6-hr period between "snapshots" or entries contained in the NHC database.

Whereas the model closely predicted the peak storm surge elevation, model-generated water surface elevations underpredicted the measured data by as much as 1 ft during the 36-hr period prior to the storm's passage. This discrepancy is believed to be due to differences between PBL-generated wind directions and those experienced during the storm. During this period, Hurricane Gloria was heading in the north-northeast direction or roughly parallel to the coastline; thus, winds would be directed in roughly the west-southwest direction or towards the southwest shore of Delaware Bay. A small deviation in PBL-generated wind directions (compared to actual winds) towards the west could result in greater water volumes being forced into the upper reaches of Delaware Bay, causing the hydrodynamic model to predict lower water levels along the bay's southwest shoreline (along which the Lewes gauging station is located) when compared to measured water levels.

5 Development of Stage-Frequency Relationships

The process of generating stage-frequency relationships for the coast of Delaware consisted of three sequential tasks. First, a set of historical hurricanes which impacted the study area were selected. The PBL wind field model was used to replicate the wind and atmospheric pressure fields generated by these storms. Second, using the output generated by the PBL model, storm surge elevations were computed. Time-series of storm surge elevations were stored at numerous locations along the coast of Delaware at which stage-frequency relationships are desired. Third, with descriptive parameters defining the simulated hurricane events together with resulting storm surge elevations, an empirical simulation technique was employed to compute the stage-frequency relationships. A description of the methodology used in performing these tasks is presented below.

Selection of Hurricanes

Because stage-frequency relationships are based on a statistical analysis of storm surge elevations resulting from historical storm events, a thorough analysis was required to define those storm events which have impacted the study area. To perform this task, track positions of all hurricanes in the NHC database were processed to determine those storms which affected the Mid-Atlantic states. Thus, any hurricane that did not track through the "box" extending from latitude 36°00'00"N, longitude 77°00'00"W to latitude 41°00'00"N, longitude 68°00'00"W were eliminated from consideration.

From this analysis, it was found that of the 875 hurricanes which occurred in the North Atlantic Ocean over the 104-year period of 1886 through 1989, only 66 hurricanes passed through this box. Furthermore, a review of these hurricanes showed that an additional 33 hurricanes could be eliminated from the storm ensemble. Reasons for eliminating the 33 hurricanes include the following: (a) some storms only "clipped" the edges of the box and did not come into close proximity with the study area; (b) a few hurricanes were downgraded to severe storm status before entering the box and were thus

ignored in the storm surge analysis; and, (c) because some storms tracked along the western edge of the box, they did not impact the coast of Delaware.

Through a process of elimination, 33 hurricanes over the 104-year period were judged to have impacted the study area. However, an additional 3 hurricanes were downgraded to severe storm status while in the vicinity of the study area. These hurricanes were also eliminated, reducing the number of storms from 33 to 30. However, because these storms entered the study area as hurricanes, statistical parameters such as mean frequency of hurricanes per year were computed using 33 as the number of storms impacting the study area.

With this set of 30 hurricanes, two approaches can be followed in performing the necessary storm surge simulations. In the first approach, storm surge simulations would be performed for each of the 30 hurricanes to obtain peak surge levels required in the statistical analysis procedure. In the second approach, a limited set of storms are selected and simulated by the storm surge model. This limited set of storms is referred to as the training set. Hurricanes composing the training set are selected such that the set is representative of the entire set of storms that impacted the study area. The second approach was chosen for this study.

Decisions regarding whether a storm is included in the training set focused primarily on a hurricane's path and its distance of closest approach to the study area. A cursory review of each hurricane's path shows one of three features: a track roughly parallel to the coast; a track veering towards the open sea once the storm passes Pamlico Sound; and, a path which loops around in a circle off the coast. Figures depicting the path of each hurricane are presented in Appendix C.

Storms were classified as to the type of path. Within each class, storms making closer approaches to the study area were generally chosen for inclusion into the training set. By weighting the training set towards storms making closer approaches to the study area, a better representation of the storm intensity/surge phenomena could be made. Storms more than 100 miles from the study area have little impact on surge levels along the coast of Delaware, regardless of storm intensity; response vectors for intense and weak storms would be essentially identical. However, to ensure that the effects of those storms veering towards the open ocean are represented in the HBOOT statistical procedure, five storms whose closest approaches to the study area exceeded 100 miles were included in the training set.

Storm surge elevations generated using the above information and the two models can be considered as approximations of the historical events. Although the frequencies associated with their maximum surge may be considered relatively accurate, the value of the peak surge may not correspond to historically observed surge elevations. The hydrographs should therefore not be considered as hindcast of the historical events for the following two reasons. First, the storm events were simulated without tides; therefore, peak

values do not reflect the stage of tide at the time of their occurrence. Second, the hurricane parameters estimated form the storm database are only approximate; all information necessary to numerically simulate each event is not known and has not been calibrated. For example, values of central pressure, radius to maximum winds, and far-field pressure are not known and were estimated from available data or observations. Because few data exist for the earlier storms, a consistent approach for selecting storm parameters was developed. This approach may not produce an accurate surge elevation for a particular event; however, it is felt that the final full population of storm data from which storm statistics are computed is representative of the range of historical events and should produce reliable and accurate hurricane stage-frequency relationships.

Application of Storm Surge Model

All 15 storms presented in Table 3, together with an additional 5 hypothetical hurricanes, were simulated with the storm surge model. Starting and ending times provided in this table correspond to the first and last entry contained in the NHC database for that particular storm. Furthermore, each storm surge simulation began with the hurricane residing at its initial position listed in the database and concluded at its ending position. Thus, each simulation began when the hurricane was far away from the study area and finished well after the occurrence of peak surge. For all hurricanes, including those which began outside of the grid domain, a temporal "ramp" function was used to slowly increase, over a 1-day period, wind stresses and pressure gradients from zero to their measured intensity. Using this feature eliminates spurious modes of oscillation caused by suddenly imposing a full-force wind stress and pressure gradient on the flow field.

All storm surge simulations were performed independently of tidal action, eliminating the task of extracting surge levels from a time-series of combined tide- and surge-induced water surface levels. Furthermore, the 15-day spin-up period needed to generate accurate current fields was no longer necessary. A 30-sec time-step was used in each simulation. Time-series of water surface elevations were recorded, at 15-min intervals, at 42 stations in the study area. Station locations are provided in Tables 4 and 5.

Eleven stations, including Reedy Point, reside in Delaware Bay and twenty-nine stations are located along the open coast. The locations of these stations are presented in Figures 14 and 15 for those along the open coast and in Figure 16 for those in the bay. Twenty-four of the open coast stations are referenced relative to the numerical grid's nodal numbers at which these stations were located. The remaining five open coast stations were placed in close proximity to existing coastal developments, including Lewes, Rehoboth Beach, Bethany Beach, Indian River Bay Inlet, and Fenwick Island. The remaining two stations are located in back-bay areas of Ocean City and Indian River Bay.

Table 3
Starting and Ending Times for Hurricanes Comprising Training Set

Hurricane		Starting Time		Ending Time	
Name	Number	Date	Time (GMT)	Date	Time (GMT)
Unnamed	327	8-17-33	0600	8-26-33	1800
Unnamed	332	9-08-33	1200	9-21-33	1800
Unnamed	370	9-08-36	0600	9-25-36	1800
Unnamed	386	9-10-38	0600	9-22-38	1800
Unnamed	436	9-09-44	0600	9-16-44	1800
Unnamed	440	10-12-44	1800	10-23-44	1800
Unnamed	476	8-21-49	0600	8-28-49	1800
Carol	535	8-25-54	1200	9-01-54	0600
Connie	545	8-03-55	0600	8-15-55	0600
Daisey	575	8-24-58	1200	8-31-58	1800
Donna	597	8-29-60	1800	9-14-60	0000
Doria	657	9-08-67	0000	9-21-67	1200
Belle	748	8-06-76	0600	8-10-76	1800
Gloria	835	9-16-85	1200	10-02-85	0000
Charley	842	8-13-86	1200	8-30-86	0000

Application of HBOOT Program

Input to the HBOOT program consists of hurricane parameters, or input vectors, describing each storm in the training set, together with their associated peak total water surface elevations (or response vectors). This data set is referred to as the training set of storms. Furthermore, the training set can be augmented with those storms that occurred in the study area but were omitted from the training set. This second set of storms is referred to as the statistical set. The combined storm set consisting of the training and statistical sets is referred to as the augmented storm set. No response vectors are specified with the statistical set of storms because HBOOT computes these vectors internally. Tables 6 and 7 present the training and statistical set input vectors for the Lewes gaging station.

Hurricane parameters used as input vectors in the HBOOT program are: maximum wind speed; radius to maximum winds; atmospheric pressure anomaly; translational or forward speed; track direction; and the minimum distance between the study area and the eye of the hurricane. Parameter values

Table 4
Station Positions for Stage-Frequency Relationships

Station	Latitude (N)	Longitude (W)
Cape May	38 58' 05"	74 57'35"
Lewes - Harbor	38 47'41"	75 08'09"
Reedy Point	39 24'43"	75 29'23"
Indian River Bay - Inlet	38 37'55"	75 04'19"
Lewes - Coast	38 46'25"	75 04'59"
Rehoboth Beach	38 43'00"	75 04'29"
Indian River Bay - Coast	38 36'29"	75 04'29"
Bethany Beach	38 32'12"	75 03'11"
Fenwick Island	38 27'45"	75 02'53"
Ocean City	38 19'59"	75 04'48"
Broadkill Beach	38 49'00"	75 12'29"
Mispillion River	38 56'30"	75 18'29"
St. Jones River	39 03'29"	75 23'44"
Mahon River	39 11'30"	75 23'44"
Cohansey River	39 20'44"	75 21'45"
Fortescue Creek	39 14'17"	75 10'54"
Maurice River	39 12'29"	75 02'17"
Bidwell Creek	39 07'14"	75 53'30"

are selected at the time a hurricane makes its closest approach to the study area.

The NHC database was processed to determine the necessary parameter values. Data contained in this database, however, are provided at 6-hr increments. Therefore, for each storm in the augmented storm set, a cubic spline interpolation or curve-fitting procedure was followed to compute hurricane positions at hourly intervals. Using the interpolated hurricane positions, the minimum distance between the hurricane's track and the study area was determined. The required hurricane parameters were then interpolated from NHC's 6-hr incremental data.

In developing response vectors, peak storm surge elevations were extracted from the storm surge time-histories created by simulating the storms in the training set. Each surge elevation was then combined with four tidal elevations. The basis for this procedure is that a storm surge event, and therefore its contribution to the peak total water surface elevation, is independent of the

Table 5
Open Coast Station Positions for Storm Surge Time-Series

Station	Latitude (N)	Longitude (W)
Node 10578	38 47'55"	75 04'37"
Node 10576	38 46'36"	75 04'15"
Node 10574	39 45'05"	75 04'15"
Node 10506	38 43'26"	75 04'19"
Node 10504	38 42'02"	75 04'09"
Node 10502	38 40'39"	75 03'51"
Node 10573	38 39'29"	75 03'40"
Node 10709	38 38'33"	75 03'42"
Node 10908	38 37'39"	75 03'37"
Node 10766	38 37'05"	75 03'29"
Node 10630	38 36'32"	75 03'21"
Node 10480	38 35'45"	75 03'11"
Node 10309	38 34'44"	75 03'10"
Node 10307	38 33'37"	75 03'27"
Node 10305	38 32'15"	75 03'17"
Node 10212	38 30'43"	75 03'02"
Node 10114	38 29'15"	75 02'23"
Node 10112	38 27'26"	75 02'25"
Node 10210	38 25'59"	75 02'34"
Node 10304	38 24'37"	75 02'45"
Node 10302	38 23'38"	75 03'06"
Node 10398	38 22'38"	75 03'17"
Node 10395	38 21'25"	75 03'34"
Node 10478	38 20'32"	75 03'50"

tidal cycle. In other words, peak storm surge levels can occur at any time during the tidal cycle. Thus, surge levels must be combined with a range of tidal elevations in order to accurately represent the temporal phasing of surge and tide.

Four tidal elevations were specified in the HBOOT program for representing the tidal water level component of the total water surface elevations. One elevation represented high tide elevations whereas a second depicted low tide levels. The two additional elevations equaled zero; thus, the combination of

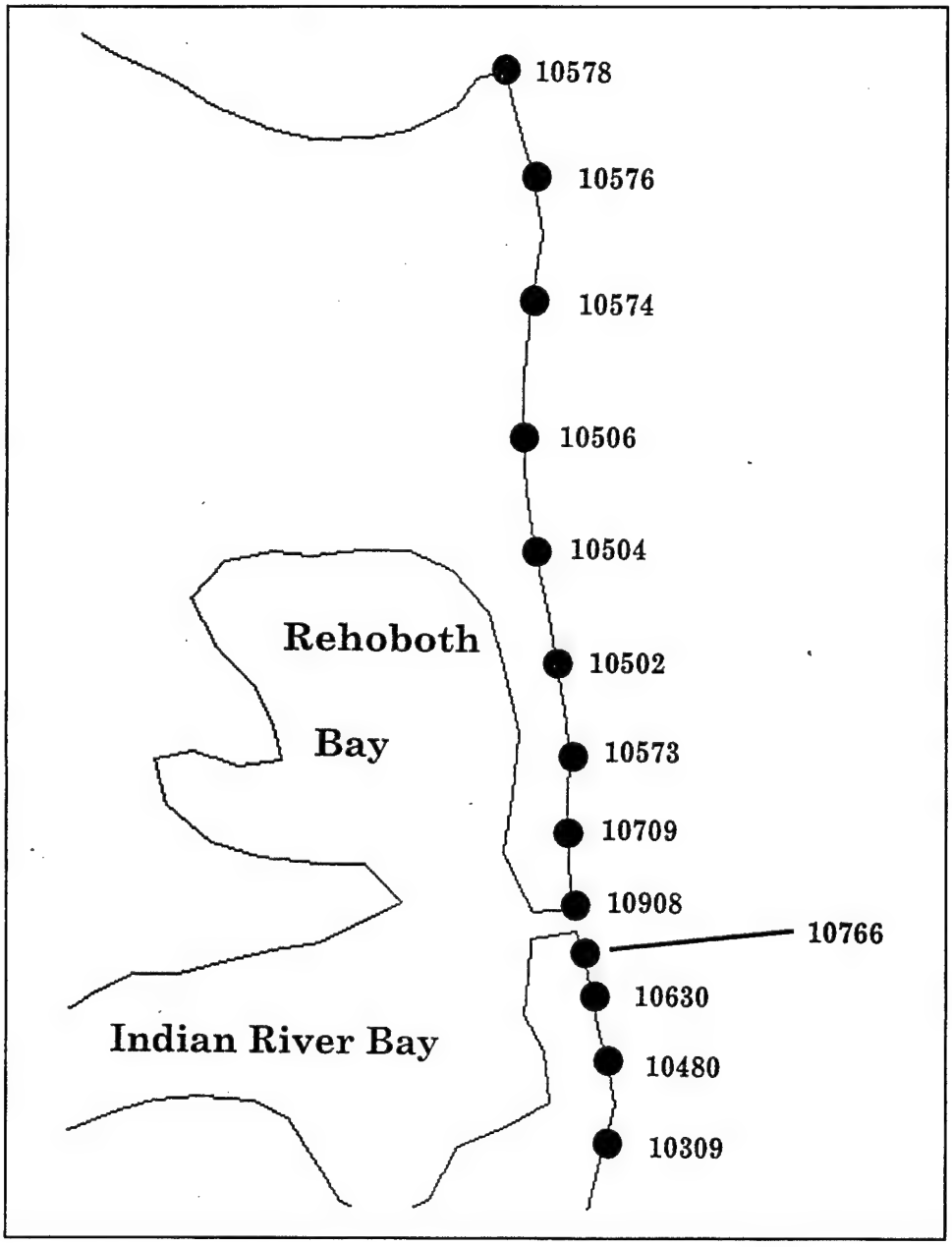

Figure 14. Locations of open coast stations (Northern Reach)

four elevations represents one tidal cycle. Furthermore, the HBOOT program randomly chooses the tide elevation, based on the four elevations, in the simulation procedure. For this study, it was assumed that the maximum and minimum tidal elevations were equal to the M_2 constituent amplitude, which represents approximately 70 percent of the maximum tidal amplitude. The M_2 constituent amplitude was selected because it is more representative of the average tidal range occurring over a one month lunar cycle; specifying spring tide levels as the maximum tidal elevation (or neap tide levels as the minimum

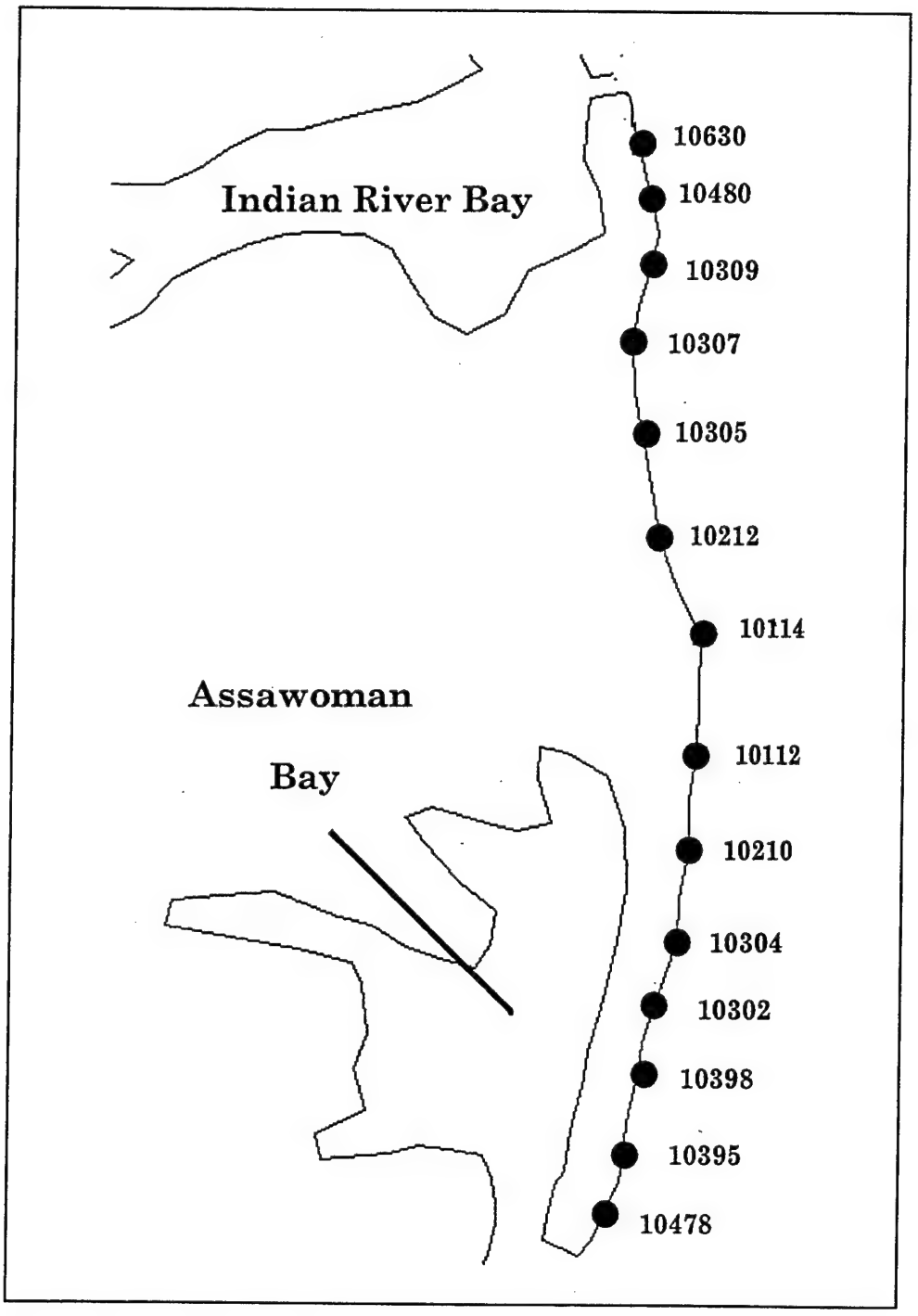

Figure 15. Locations of open coast stations (Southern Reach)

elevation) could cause biasing or unduly weighting the tidal water level component towards extreme tidal elevations.

With four tidal elevations being specified with each set of input/response vectors, the total number of storms in the training set was effectively

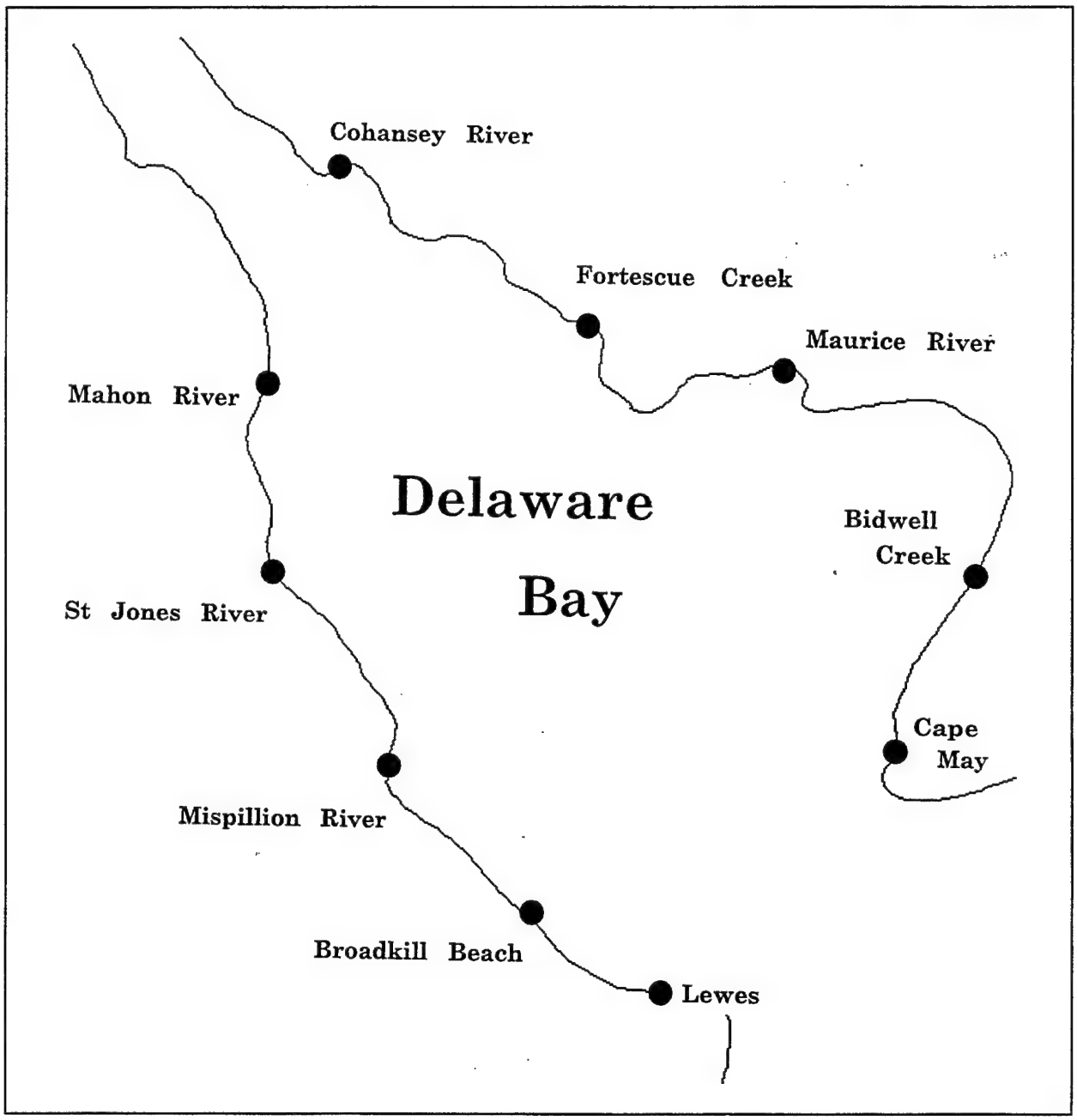

Figure 16. Location of stations in Delaware Bay

increased from 15 to 60 events. Because the training set was increased to 60 storms, the 15 storms in the statistical storm set were also increased to 60 storms. Four identical sets of input vectors or hurricanes were added to the data set. Adding the additional input vectors to the augmented storm set avoids biasing the training set's input vectors in the stage-frequency computations. Thus, the augmented storm set contained 120 storms.

Table 6
Summary of Hurricanes and Parameters Composing Training Set

Hurricane Name	Number	Distance Approach (miles)	Track Angle (deg)	Central Pressure (mb)	Maximum Velocity (knots)	Forward Speed (knots)	Radius to Winds (n.m.)
Unnamed	327	105.8	352.5	975.5	45.0	16.8	43.4
Unnamed	332	108.0	38.5	961.4	74.4	11.0	43.4
Unnamed	370	57.9	33.4	970.0	85.5	17.0	16.9
Unnamed	386	115.5	357.4	940.0	85.0	44.0	43.4
Unnamed	436	64.5	22.5	963.0	79.8	31.0	42.1
Unnamed	440	40.6	46.3	996.9	41.0	16.7	39.7
Unnamed	476	197.1	57.6	979.5	90.9	19.3	8.6
Carol	535	84.4	20.7	977.8	85.5	32.1	8.6
Connie	545	53.7	344.3	977.0	47.5	13.1	43.4
Daisey	575	131.0	31.1	968.8	110.0	21.5	8.6
Donna	597	67.6	26.0	967.7	94.3	29.6	8.6
Doria	657	82.3	253.2	988.2	58.8	7.8	20.7
Belle	748	71.8	8.8	977.0	80.0	22.7	10.4
Gloria	835	43.8	16.6	951.0	85.0	33.0	20.0
Charley	842	66.9	50.5	991.7	60.3	12.5	10.2
Unnamed[1]	370	37.9	33.4	970.0	85.0	17.0	16.9
Unnamed[1]	436	44.5	22.5	963.0	79.8	31.0	42.1
Donna[1]	597	67.6	26.0	967.7	94.3	29.6	20.0
Gloria[1]	835	23.8	16.6	951.0	85.0	33.0	20.0
Gloria[1]	835	43.8	16.6	951.0	85.0	33.0	43.4

[1] Superscript denotes hypothetical hurricane.

Using the HBOOT program and the data set discussed above, 100 simulations, each modeled over a 200-year period, were performed. The frequency of occurrence for a hurricane to impact the study area is 0.32 (33 storms per 104-year period) i.e., a hurricane-induced storm surge will impact the coast of Delaware, on average, once every 3.1 years.

Analysis of Stage-Frequency Relationships

Stage-frequency relationships were produced for the 42 stations presented in Tables 4 and 5. With the peak storm surge elevations computed from the

Table 7
Summary of Hurricanes and Parameters Composing Statistical Storm Set

Hurricane Name	Number	Distance Approach (miles)	Track Angle (deg)	Central Pressure (mb)	Maximum Velocity (knots)	Forward Speed (knots)	Radius to Winds (n.m.)
Unnamed	112	123.7	54.3	974.6	70.6	6.8	31.1
Unnamed	299	219.0	49.5	978.7	76.1	10.1	13.2
Barbara	520	85.5	43.3	990.7	68.9	15.0	8.6
Esther	604	156.9	18.8	969.2	114.0	15.3	8.6
Alma	611	151.2	38.0	990.7	76.8	23.9	8.6
Dora	630	164.5	51.0	998.7	50.0	17.0	24.7
Gladys	633	234.9	36.4	979.8	73.9	14.0	14.3
Alma	643	119.0	35.5	1002.0	44.9	6.7	33.2
Gladys	669	198.4	53.0	981.5	70.6	26.2	15.9
Gerda	676	168.9	35.3	984.5	107.0	30.6	8.6
Doria	702	9.4	25.1	993.6	48.9	27.4	26.6
Agnes	712	113.1	1.0	976.5	59.9	19.8	43.4
Carrie	714	215.0	6.9	1000.0	48.5	9.6	27.2
Unnamed	805	208.8	24.5	978.4	59.9	7.7	40.9
Unnamed	807	164.7	50.6	992.0	60.0	31.7	10.3
Unnamed[1]	370	72.9	33.4	970.0	85.5	17.0	16.9
Unnamed[1]	370	42.9	33.4	970.0	85.5	17.0	16.9
Unnamed[1]	436	79.5	22.5	963.0	79.8	31.0	42.1
Unnamed[1]	436	49.5	22.5	963.0	79.8	31.0	42.1
Unnamed[1]	440	55.6	46.3	996.9	41.0	16.7	39.7
Unnamed[1]	440	25.6	46.3	996.9	41.0	16.7	39.7
Doria[1]	657	97.3	253.2	988.2	58.8	7.8	20.7
Doria[1]	657	67.3	253.2	988.2	58.8	7.8	20.7
Gloria[1]	835	58.8	16.6	951.0	85.0	33.0	20.0
Gloria[1]	835	28.8	16.6	951.0	85.0	33.0	20.0

[1] Superscript denotes hypothetical hurricane.

100 simulations, average stages were computed for each 1-year return period in the 200-year simulation period. Standard deviations were also calculated. Figure 17 presents an example of the stage-frequency relationship for Lewes, DE. Additional figures for the remaining stations are contained in Appendix B. Tabular results for each station are presented in Appendix A.

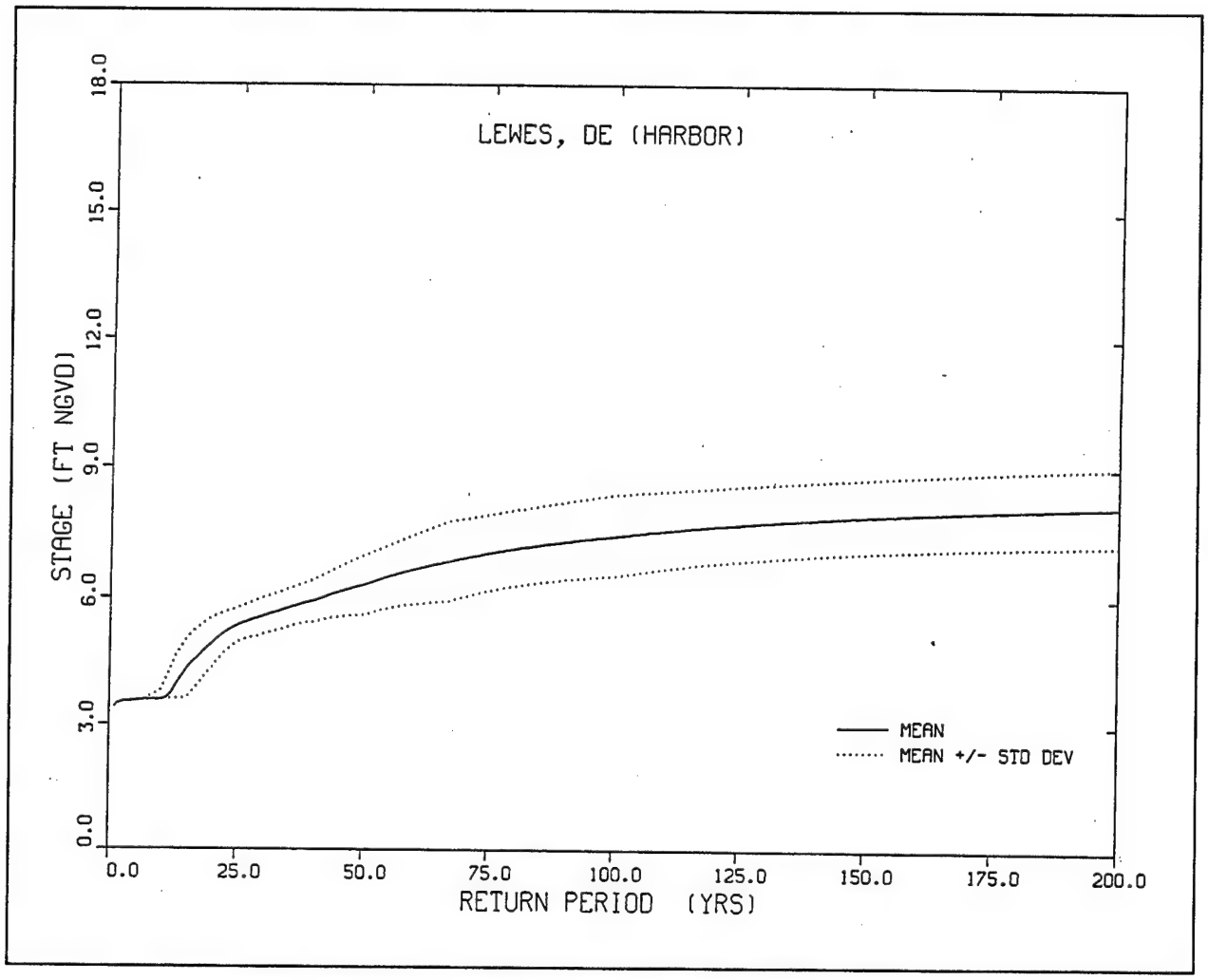

Figure 17. Stage-frequency relationship for Lewes (harbor)

Tables contained in this appendix present the average water surface elevation, in feet (National Geodetic Vertifcal Datum (NGVD)), and standard deviation for return periods of 5, 10, 25, 50, 75, 100, 150, and 200 years.

Average total water surface elevations (combined tide and storm surge elevations) were relatively constant along the coast of Delaware. As shown in Figures 18 and 19, which display the 100-year return period elevation, water surface levels ranged from a minimum stage of 6.12 ft NGVD along Fenwick Island to a maximum of 6.86 ft NGVD in the vicinity of Indian River Bay Inlet. Towards Cape Henlopen, the 100-year return period elevation was 6.84 ft NGVD. Thus, the maximum difference in the 100-year elevation for stations along the coast was less than 1 ft.

Differences in total water surface elevations between the coastal stations are attributed to variations in water depths. In general, depths along the northern coast of Delaware tend to be deeper than along Fenwick Island. Thus,

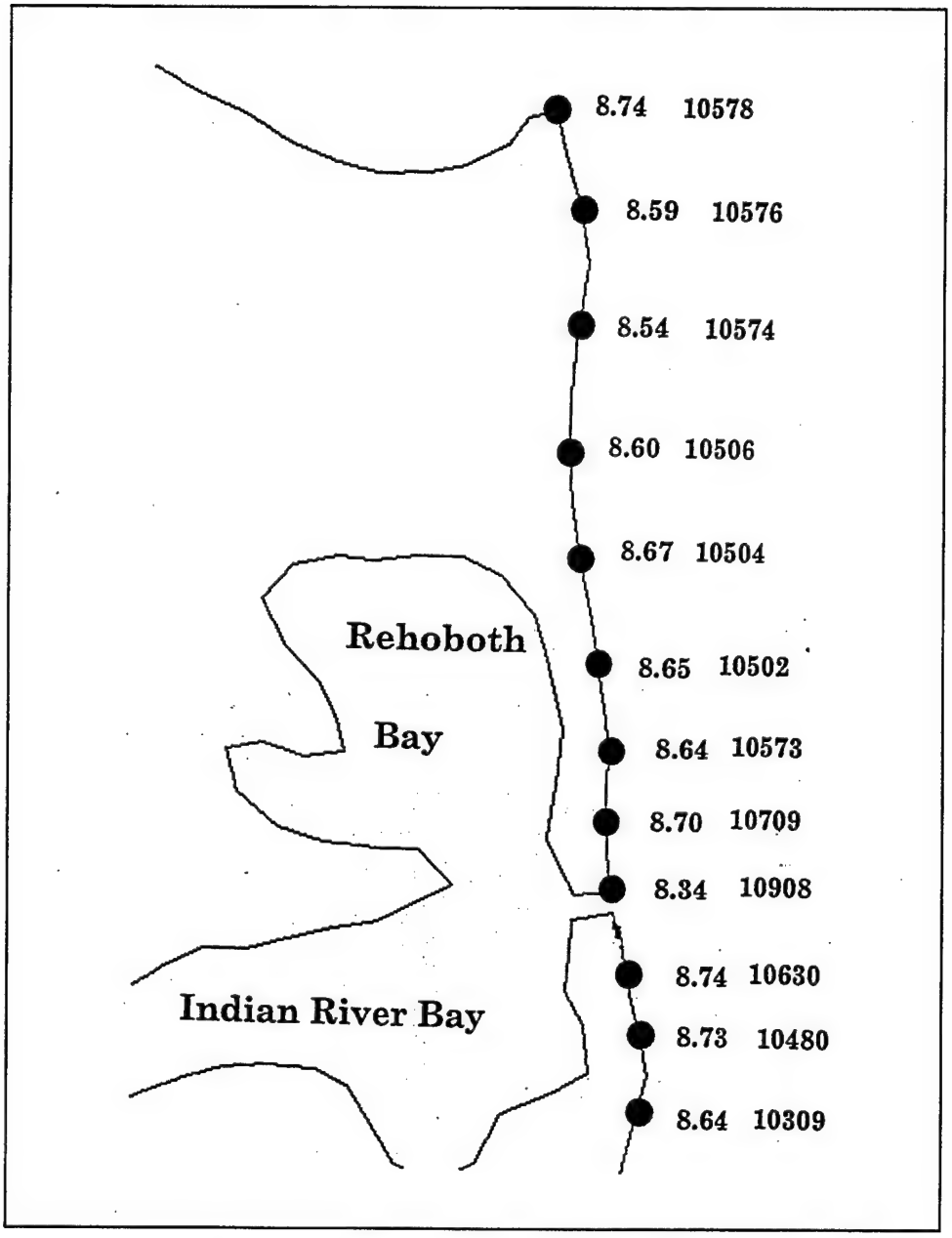

Figure 18. Average total water surface elevation (NGVD) along coast of Delaware for 100-year return period storm (Northern Reach)

increased shoaling of storm surges can be expected in shallower water, resulting in higher storm surge elevations.

The 100-year return period elevations in Delaware Bay, shown in Figure 20, tend to be higher along the southwest shore than along the northeast bank. Furthermore, stations towards the confluence of the Delaware River tend to have greater stages than those stations close to the inlet. Higher surge levels can be expected along the southwest shore of Delaware Bay because

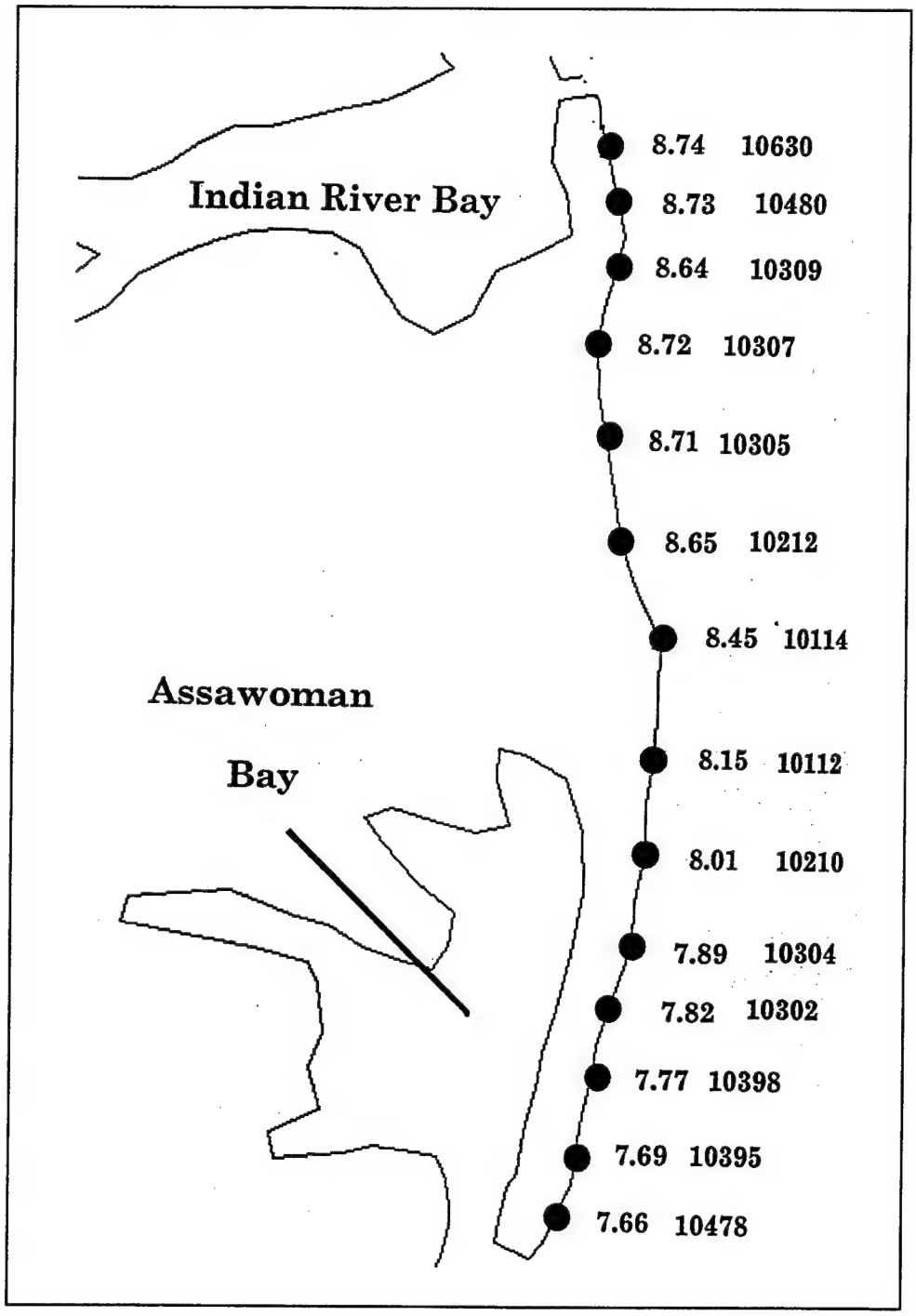

Figure 19. Average total water surface elevation (NGVD) along coast of Delaware for 100-year return period storm (Southern Reach)

hurricanes tend to track in the north-northeast direction; therefore, counter-clockwise winds are directed towards the southwest as the hurricanes pass the bay, forcing water to the southwest shore.

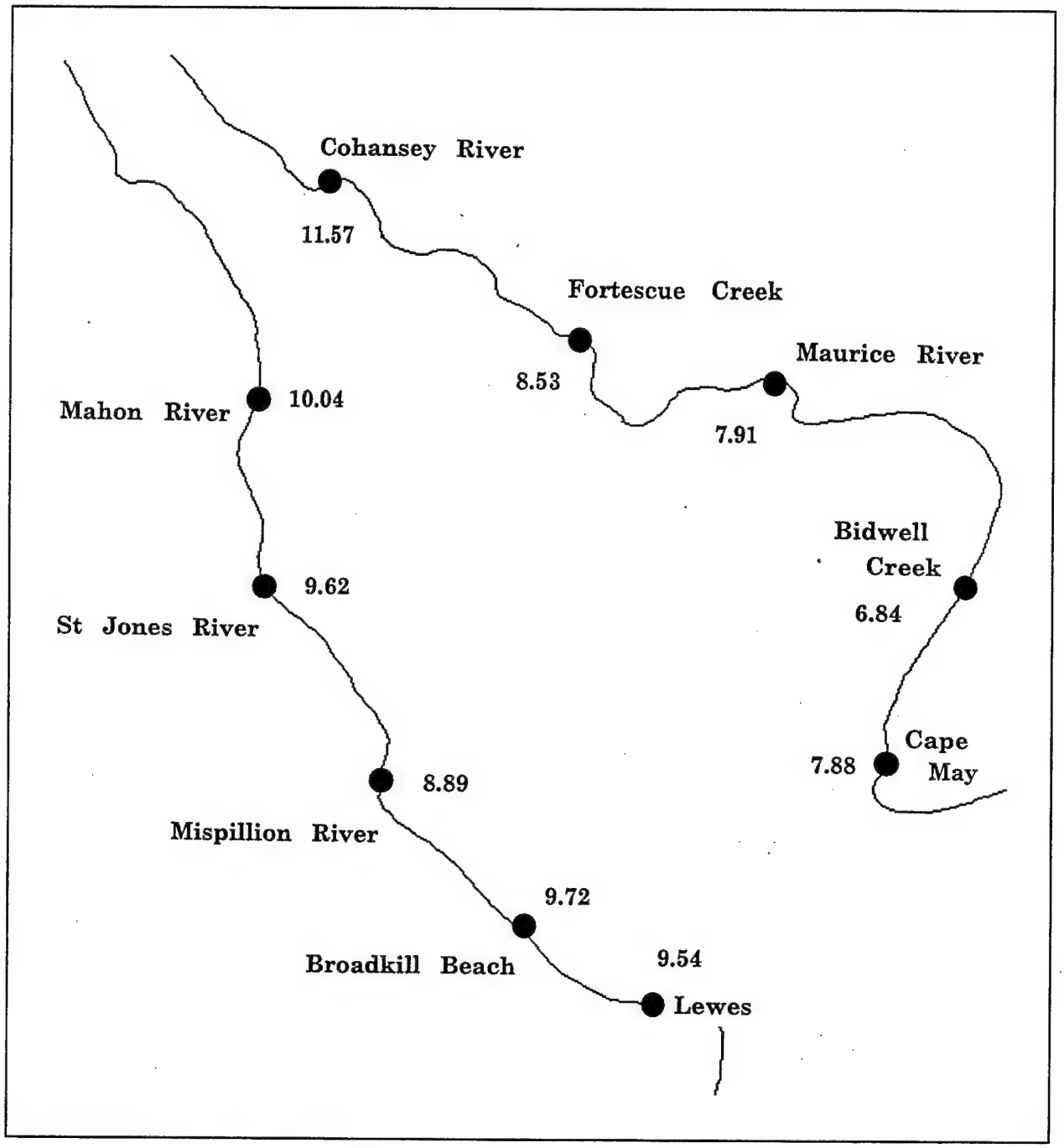

Figure 20. Average total water surface elevation (NGVD) in Delaware Bay for 100-year return period storm

Higher surge levels towards the north of the bay can be attributed to its planform geometry, which is shaped like a funnel. For example, the 100-year return period elevations at the Lewes (Breakwater Harbor), Cohansey River Mouth, and Reedy Point were 7.45, 11.56, and 13.36 ft NGVD, respectively. As the bay's width decreases going towards the north, the funnel-shaped geometry constricts the water volumes being driven upstream during storm

surge events; thus, water surface levels will increase due to conservation of mass and momentum considerations.

Datum Adjustments to Peak Surge Levels

In the storm surge model, water depths and predicted water surface elevations are referenced relative to a spherical surface that approximates mean sea level. However, stage-frequency relationships are presented with stage elevations referenced relative to the NGVD of 1929. For NOS-established gauging stations, stage elevations were adjusted using their published values. These stations are: Cape May, NJ; Reedy Point, DE; Lewes, DE (Breakwater Harbor); Indian River Bay, DE (Inlet); and Ocean City, MD. Additional stations, located in Delaware Bay, for which datum adjustment heights are available include Woodland Beach, Murderkill River entrance, and Mispillion River entrance.

For open coast stations, a linear interpolation procedure was used to approximate datum adjustment heights. Datum adjustment heights for Ocean City and Lewes served as the pivotal values in this procedure, and the distance between Ocean City and Lewes was computed via a rhumble line extending from one station to the other. Incremental distances were also computed via a rhumble line and extended from Ocean City to the respective station. Furthermore, all distances were computed as a function of latitude only; thus, all stations were assumed to have identical longitudes.

A similar interpolation procedure could not be used for stations situated in Delaware Bay because datum adjustment heights between the inlet and river mouth do not monotonically increase/decrease. For example, the adjustment height at Mispillion River entrance gage is 0.99 ft, whereas these heights for Lewes and Woodland Beach gages are 0.51 ft and 0.73 ft, respectively. The datum adjustment height for Broadkill Beach was linearly interpolated using heights from Lewes and Mispillion River entrance, whereas the height for Mahon River entrance was assumed equal to the simple average of heights at Woodland Beach and the Murderkill River entrance.

Datum adjustment height for Cohansey River entrance was assumed equal to the adjustment for Woodland Beach, whereas the adjustment for Fortesque Creek was assumed equal to that at the Mahon River entrance. The adjustment height for Bidwell Creek was linearly interpolated using heights established for Cape May and Mispillion River entrance gages, and the adjustment for Maurice River entrance was assumed to equal the adjustment for the Mispillion River entrance gages. Table 8 summarizes the adjustment heights for all stations. Tidal epochs, which are the 19-year periods used in obtaining mean values for tidal datums, are presented in Table 9.

Table 8
Datum Adjustment Between Mean Sea Level (msl) and National Geodetic Vertical Datum (NGVD) (1929)[1]

Station	Displacement (ft)
Cape May	0.62
Lewes - Harbor	0.52
Reedy Point	0.40
Indian River Bay - Inlet	0.50
Lewes - Coast	0.51
Rehoboth Beach	0.47
Indian River Bay - Coast	0.41
Batheny Beach	0.37
Fenwick Island	0.33
Ocean City	0.26
Broadkill Beach	0.67
Mispillion River	0.99
St. Jones River	0.87
Mahon River	0.80
Cohansey River	0.73
Fortescue Creek	0.80
Maurice River	0.99
Bidwell Creek	0.81
Node 10578	0.52
Node 10576	0.51
Node 10574	0.49
Node 10506	0.48
Node 10504	0.47
Node 10502	0.45
Node 10573	0.44
Node 10709	0.43
Node 10908	0.42
Node 10766	0.42
Node 10630	0.41
Node 10480	0.41
Node 10309	0.40
Node 10307	0.39
Node 10305	0.37
Node 10212	0.36
Node 10114	0.35
Node 10112	0.33
Node 10210	0.32
Node 10304	0.30
Node 10302	0.30
Node 10398	0.29
Node 10395	0.27
Node 10478	0.27

[1] NGVD = msl + displacement.

Table 9
Tidal Epochs for Selected Gauging Stations

Station	Tidal Epoch
Cape May	1960-1978
Lewes - Harbor	1960-1978
Reedy Point	1960-1978
Indian River Inlet	1960-1978
Ocean City	1960-1978
Woodland Beach	1941-1959
Fortescue Creek	1960-1978
Murderkill River	1960-1978
Mispillion River	1960-1978

6 Summary and Conclusions

A hurricane stage-frequency analysis was conducted for the open coast of Delaware. Three models were employed in this analysis, including: a wind and atmospheric pressure field model; a long wave hydrodynamic model; and, an empirical simulation model. The PBL model was used for generating hurricane-induced wind and atmospheric pressure fields subsequently used as input to the hydrodynamic model. Data supplied to the PBL model were obtained from the NHC's HURDAT database.

The ADCIRC numerical model was used for simulating the long-wave hydrodynamic processes in the study area. This program employs a two-dimensional, depth-integrated, finite-element solution of the GWCE. The fundamental components of the GWCE equation are the depth-integrated continuity and Navier-Stokes equations for conservation of mass and momentum.

The ADCIRC model was calibrated by adjusting local bottom friction coefficients in order that model-generated water surface level time-series favorably matched those reconstructed from NOAA-published tidal constituents. Comparisons were made at Cape May, NJ; Lewes, DE; Reedy Point, DE; Indian River Inlet, DE; and Ocean City, MD. Parametric and nonparametric statistical tests were used to quantitatively assess the model's accuracy. Furthermore, model validation was achieved by performing a storm surge simulation of Hurricane Gloria, which impacted the study area in September 1985.

An EST procedure was used for determining the stage-frequency relationships. The EST is a statistical resampling procedure which uses historical data to develop joint probability relationships among the various measured storm parameters (e.g., maximum wind speed). The EST generates a database of peak storm surge elevations by simulating multiple-year periods (e.g., 200-year periods) of storm activity a multiple number of times. Stage-frequency relationships are then generated using the database of peak storm surge elevations computed with the ADCIRC model.

In generating the stage-frequency relationships, 15 hurricanes which impacted the coast of Delaware were simulated using the PBL and ADCIRC models. Peak storm surge levels produced by these storms were subsequently

processed using the EST model to generate frequency-of-occurrence relationships at 42 locations along the open coast of Delaware and within Delaware Bay.

References

Borgman, L. E., and Scheffner, N. W. (1991). "Simulation of time sequences of wave height, period, and direction," Technical Report DRP-91-2, U.S. Army Engineer Waterways Experiment Station, Vicksburg, MS.

Borgman, L., Miller, M., Butler, L., and Reinhard, R. (1992). "Empirical simulation of future hurricane storm histories as a tool in engineering and economic analysis." *Fifth International Conference on Civil Engineering in the Oceans*, ASCE, College Station, TX, 2-5 November 1992.

Cardone, V. J., Greenwood, C. V., and Greenwood, J. A. (1992). "Unified program for the specification of hurricane boundary layer winds over surface of specified roughness." Contract Report CERC-92-1, U.S. Army Engineer Waterways Experiment Station, Vicksburg, MS.

Gumbel, E. J. (1954). *Statistical theory of extreme values and some practical applications; a series of lectures.* U.S. Government Printing Office, Washington, DC.

Hess, K., and Bosley, K. (1991). "Validation of a Tampa Bay circulation model," *2nd International Conference on Estuarine and Coastal Modeling.* Tampa, FL, 13-15 November 1991.

Jarvinen, B. R., Neumann, C. J., and Davis, M. A. (1988). "A tropical cyclone data tape for the North Atlantic Basin, 1886-1983: Contents, limitations, and uses," NOAA Technical Memorandum NWS NHC 22, National Hurricane Center, Miami, FL.

Jelesnianski, C. P., and Taylor, A. D. (1973). "A preliminary view of storm surges before and after storm modifications," NOAA Technical Memorandum ERL WMPO-3, Weather Modification Program Office, Boulder, CO.

Scheffner, N. W., and Borgman, L. E. (1992). "A stochastic time series representation of wave data." *J. Wtrwy. Port, Coast. and Oc. Engrg.* 118(4), 337-351.

Scheffner, N. W., and Borgman, L. E. (1993). "Stochastic time-series representation of wave data," *Journal of Waterway, Port, Coastal and Ocean Engineering*, American Society of Civil Engineers, 118(4), 337-351.

Schwiderski, E. W., and Szeto, L. T. (1981). "The NSWC global ocean tide data tape, its features and application, random-point tide program," Technical Report NSWC 81-254, Naval Surface Weapons Center, Dahlgren, VA.

Westerink, J. J., Luettich, A. M., Baptista, A. M., Scheffner, N. W., and Farrar, P. (1992). "Tide and storm surge predictions using finite element model," *Journal of Hydraulic Engineering*, American Society of Civil Engineers, 118(10), 1373-1390.

Appendix A
Stage-Frequency Relationship Tables

Table A1
Hurricane Stage-Frequency Relationship for Cape May, NJ

Return Period (yr)	Water Surface Elevation (ft NGVD)	Standard Deviation (ft)
5	4.37	0.0
10	4.47	0.0
25	5.65	0.52
50	7.00	0.94
75	7.64	0.74
100	7.88	0.70
150	8.14	0.53
200	8.27	0.51

Table A2
Hurricane Stage-Frequency Relationship for Lewes, DE (Harbor)

Return Period (yr)	Water Surface Elevation (ft NGVD)	Standard Deviation (ft)
5	3.55	0.0
10	4.78	0.72
25	6.94	0.55
50	8.43	1.02
75	9.19	0.87
100	9.54	0.86
150	9.98	0.68
200	10.21	0.68

Table A3
Hurricane Stage-Frequency Relationship for Reedy Point, DE

Return Period (yr)	Water Surface Elevation (ft NGVD)	Standard Deviation (ft)
5	4.13	0.0
10	4.25	1.32
25	6.62	0.87
50	9.72	2.27
75	11.85	2.37
100	13.29	2.56
150	14.70	2.24
200	15.40	2.40

Table A4
Hurricane Stage-Frequency Relationship for Indian River Bay, DE (Inlet)

Return Period (yr)	Water Surface Elevation (ft NGVD)	Standard Deviation (ft)
5	2.46	0.0
10	3.24	0.42
25	4.45	0.29
50	5.22	0.51
75	5.59	0.42
100	5.78	0.41
150	5.95	0.36
200	6.04	0.36

Table A5
Hurricane Stage-Frequency Relationship for Lewes, DE (Open Coast)

Return Period (yr)	Water Surface Elevation (ft NGVD)	Standard Deviation (ft)
5	3.55	0.0
10	4.88	0.67
25	7.44	0.63
50	9.01	1.12
75	9.84	0.96
100	10.20	0.90
150	10.61	0.68
200	10.81	0.67

Table A6
Hurricane Stage-Frequency Relationship for Rehoboth Beach, DE

Return Period (yr)	Water Surface Elevation (ft NGVD)	Standard Deviation (ft)
5	3.53	0.0
10	4.32	0.75
25	6.17	0.49
50	7.63	1.03
75	8.35	0.84
100	8.64	0.79
150	8.97	0.62
200	9.14	0.60

Table A7
Hurricane Stage-Frequency Relationship for Indian River Inlet, DE (Open Coast)

Return Period (yr)	Water Surface Elevation (ft NGVD)	Standard Deviation (ft)
5	3.49	0.0
10	3.86	0.41
25	5.41	0.35
50	6.26	0.58
75	6.71	0.53
100	6.97	0.52
150	7.21	0.39
200	7.32	0.38

Table A8
Hurricane Stage-Frequency Relationship for Bethany Beach, DE

Return Period (yr)	Water Surface Elevation (ft NGVD)	Standard Deviation (ft)
5	3.46	0.0
10	4.22	0.75
25	6.15	0.43
50	7.58	1.10
75	8.38	0.91
100	8.69	0.84
150	9.00	0.63
200	9.15	0.60

Table A9
Hurricane Stage-Frequency Relationship for Fenwick Island, DE (Open Coast)

Return Period (yr)	Water Surface Elevation (ft NGVD)	Standard Deviation (ft)
5	3.44	0.0
10	4.10	0.70
25	5.92	0.47
50	7.28	0.96
75	7.98	0.80
100	8.25	0.76
150	8.59	0.59
200	8.76	0.58

Table A10
Hurricane Stage-Frequency Relationship for Ocean City, MD.

Return Period (yr)	Water Surface Elevation (ft NGVD)	Standard Deviation (ft)
5	3.39	0.0
10	3.57	0.56
25	5.24	0.48
50	6.32	0.72
75	6.86	0.62
100	7.09	0.63
150	7.42	0.53
200	7.59	0.54

Table A11
Hurricane Stage-Frequency Relationship for Broadkill Beach, DE

Return Period (yr)	Water Surface Elevation (ft NGVD)	Standard Deviation (ft)
5	3.20	0.14
10	5.19	0.64
25	7.40	0.63
50	8.65	0.84
75	9.34	0.80
100	9.72	0.88
150	10.26	0.74
200	10.53	0.78

Table A12
Hurricane Stage-Frequency Relationship for Mispillion River, DE

Return Period (yr)	Water Surface Elevation (ft NGVD)	Standard Deviation (ft)
5	3.69	0.0
10	4.88	0.50
25	6.88	0.51
50	7.84	0.61
75	8.47	0.77
100	8.89	0.84
150	9.34	0.70
200	9.56	0.71

Table A13
Hurricane Stage-Frequency Relationship for St. Jones River, DE

Return Period (yr)	Water Surface Elevation (ft NGVD)	Standard Deviation (ft)
5	3.72	0.0
10	4.71	0.59
25	6.79	0.50
50	8.05	0.88
75	8.96	1.96
100	9.62	1.29
150	10.48	1.35
200	10.92	1.56

Table A14
Hurricane Stage-Frequency Relationship for Mahon River, DE

Return Period (yr)	Water Surface Elevation (ft NGVD)	Standard Deviation (ft)
5	3.95	0.0
10	3.11	0.76
25	6.33	0.36
50	7.61	1.32
75	8.99	1.61
100	10.04	1.88
150	11.11	1.75
200	11.65	1.91

Table A15
Hurricane Stage-Frequency Relationship for Cohansey River, NJ

Return Period (yr)	Water Surface Elevation (ft NGVD)	Standard Deviation (ft)
5	4.18	0.0
10	4.18	1.09
25	6.21	0.62
50	8.56	1.80
75	10.34	2.00
100	11.57	2.19
150	12.80	1.93
200	13.41	2.06

Table A16
Hurricane Stage-Frequency Relationship for Fortescue Creek, NJ

Return Period (yr)	Water Surface Elevation (ft NGVD)	Standard Deviation (ft)
5	4.30	0.0
10	4.30	0.09
25	5.43	0.26
50	6.46	1.01
75	7.66	1.40
100	8.53	1.67
150	9.52	1.49
200	10.01	1.59

Table A17
Hurricane Stage-Frequency Relationship for Maurice River, NJ

Return Period (yr)	Water Surface Elevation (ft NGVD)	Standard Deviation (ft)
5	4.34	0.0
10	4.34	0.01
25	5.53	0.24
50	6.17	0.73
75	7.16	1.25
100	7.91	1.56
150	8.82	1.36
200	9.28	1.46

Table A18
Hurricane Stage-Frequency Relationship for Bidwell Creek, NJ

Return Period (yr)	Water Surface Elevation (ft NGVD)	Standard Deviation (ft)
5	3.49	0.0
10	3.49	0.48
25	5.35	0.54
50	6.30	0.46
75	6.65	0.44
100	6.84	0.41
150	7.09	0.33
200	7.22	0.35

Table A19
Hurricane Stage-Frequency Relationship for Grid Node 10578

Return Period (yr)	Water Surface Elevation (ft NGVD)	Standard Deviation (ft)
5	3.56	0.0
10	4.40	0.73
25	6.26	0.50
50	7.70	1.03
75	8.44	0.84
100	8.74	0.81
150	9.11	0.63
200	9.30	0.62

Table A20
Hurricane Stage-Frequency Relationship for Grid Node 10576

Return Period (yr)	Water Surface Elevation (ft NGVD)	Standard Deviation (ft)
5	3.55	0.0
10	4.33	0.73
25	6.14	0.51
50	7.58	1.01
75	8.31	0.81
100	8.59	0.78
150	8.93	0.62
200	9.11	0.61

Table A21
Hurricane Stage-Frequency Relationship for Grid Node 10574

Return Period (yr)	Water Surface Elevation (ft NGVD)	Standard Deviation (ft)
5	3.54	0.0
10	4.31	0.73
25	6.11	0.50
50	7.56	1.00
75	8.26	0.82
100	8.54	0.79
150	8.88	0.62
200	9.05	0.61

Table A22
Hurricane Stage-Frequency Relationship for Grid Node 10506

Return Period (yr)	Water Surface Elevation (ft NGVD)	Standard Deviation (ft)
5	3.53	0.0
10	4.31	0.74
25	6.13	0.50
50	7.58	1.02
75	8.32	0.83
100	8.60	0.80
150	8.93	0.61
200	9.10	0.60

Table A23
Hurricane Stage-Frequency Relationship for Grid Node 10504

Return Period (yr)	Water Surface Elevation (ft NGVD)	Standard Deviation (ft)
5	3.52	0.0
10	4.32	0.76
25	6.16	0.47
50	7.63	0.06
75	8.38	0.87
100	8.67	0.82
150	9.00	0.61
200	9.16	0.59

Table A24
Hurricane Stage-Frequency Relationship for Grid Node 10502

Return Period (yr)	Water Surface Elevation (ft NGVD)	Standard Deviation (ft)
5	3.51	0.0
10	4.28	0.77
25	6.12	0.47
50	7.60	1.08
75	8.36	0.88
100	8.65	0.83
150	8.96	0.63
200	9.12	0.60

Table A25
Hurricane Stage-Frequency Relationship for Grid Node 10573

Return Period (yr)	Water Surface Elevation (ft NGVD)	Standard Deviation (ft)
5	3.51	0.0
10	4.54	0.77
25	6.10	0.47
50	7.57	1.09
75	8.34	0.89
100	8.64	0.82
150	8.94	0.62
200	9.09	0.60

Table A26
Hurricane Stage-Frequency Relationship for Grid Node 10709

Return Period (yr)	Water Surface Elevation (ft NGVD)	Standard Deviation (ft)
5	3.50	0.0
10	4.28	0.77
25	6.14	0.46
50	7.62	1.10
75	8.40	0.90
100	8.70	0.83
150	9.00	0.63
200	9.16	0.59

Table A27
Hurricane Stage-Frequency Relationship for Grid Node 10908

Return Period (yr)	Water Surface Elevation (ft NGVD)	Standard Deviation (ft)
5	3.50	0.0
10	4.13	0.74
25	5.91	0.44
50	7.31	0.05
75	8.06	0.86
100	8.34	0.80
150	8.63	0.60
200	8.78	0.57

Table A28
Hurricane Stage-Frequency Relationship for Grid Node 10766

Return Period (yr)	Water Surface Elevation (ft NGVD)	Standard Deviation (ft)
5	3.49	0.0
10	4.25	0.75
25	6.13	0.45
50	7.57	1.10
75	6.42	0.89
100	6.80	0.84
150	7.32	0.61
200	7.57	0.59

Table A29
Hurricane Stage-Frequency Relationship for Grid Node 10630

Return Period (yr)	Water Surface Elevation (ft NGVD)	Standard Deviation (ft)
5	3.49	0.0
10	4.53	0.76
25	6.19	0.44
50	7.64	1.11
75	8.44	0.90
100	8.74	0.84
150	9.05	0.63
200	9.20	0.61

Table A30
Hurricane Stage-Frequency Relationship for Grid Node 10480

Return Period (yr)	Water Surface Elevation (ft NGVD)	Standard Deviation (ft)
5	3.48	0.0
10	4.26	0.76
25	6.17	0.44
50	7.63	1.11
75	8.42	0.91
100	8.73	0.83
150	9.03	0.63
200	9.18	0.60

Table A31
Hurricane Stage-Frequency Relationship for Grid Node 10309

Return Period (yr)	Water Surface Elevation (ft NGVD)	Standard Deviation (ft)
5	3.48	0.0
10	4.23	0.75
25	6.10	0.45
50	7.56	1.10
75	8.34	0.91
100	8.64	0.84
150	8.94	0.63
200	9.09	0.59

Table A32
Hurricane Stage-Frequency Relationship for Grid Node 10307

Return Period (yr)	Water Surface Elevation (ft NGVD)	Standard Deviation (ft)
5	3.47	0.0
10	4.26	0.74
25	6.18	0.44
50	7.61	1.10
75	8.41	0.91
100	8.72	0.85
150	9.02	0.64
200	9.18	0.60

Table A33
Hurricane Stage-Frequency Relationship for Grid Node 10305

Return Period (yr)	Water Surface Elevation (ft NGVD)	Standard Deviation (ft)
5	3.46	0.0
10	4.23	0.74
25	6.17	0.44
50	7.59	1.10
75	8.39	0.91
100	8.71	0.85
150	9.02	0.64
200	9.17	0.61

Table A34
Hurricane Stage-Frequency Relationship for Grid Node 10212

Return Period (yr)	Water Surface Elevation (ft NGVD)	Standard Deviation (ft)
5	3.45	0.0
10	4.21	0.73
25	6.13	0.44
50	7.56	1.09
75	8.35	0.89
100	8.65	0.84
150	8.97	0.62
200	9.12	0.60

Table A35
Hurricane Stage-Frequency Relationship for Grid Node 10114

Return Period (yr)	Water Surface Elevation (ft NGVD)	Standard Deviation (ft)
5	3.45	0.0
10	4.14	0.73
25	5.98	0.45
50	7.40	1.06
75	8.16	0.87
100	8.45	0.80
150	8.76	0.60
200	8.91	0.58

Table A36
Hurricane Stage-Frequency Relationship for Grid Node 10112

Return Period (yr)	Water Surface Elevation (ft NGVD)	Standard Deviation (ft)
5	3.44	0.0
10	4.04	0.70
25	5.82	0.48
50	7.19	0.97
75	7.88	0.79
100	8.15	0.76
150	8.48	0.58
200	8.65	0.57

Table A37
Hurricane Stage-Frequency Relationship for Grid Node 10210

Return Period (yr)	Water Surface Elevation (ft NGVD)	Standard Deviation (ft)
5	3.43	0.0
10	3.99	0.67
25	5.76	0.49
50	7.06	0.91
75	7.72	0.75
100	8.01	0.73
150	8.37	0.59
200	8.55	0.59

Table A38
Hurricane Stage-Frequency Relationship for Grid Node 10304

Return Period (yr)	Water Surface Elevation (ft NGVD)	Standard Deviation (ft)
5	3.42	0.0
10	3.93	0.66
25	5.69	0.50
50	6.96	0.87
75	7.61	0.72
100	7.89	0.72
150	8.26	0.59
200	8.44	0.60

Table A39
Hurricane Stage-Frequency Relationship for Grid Node 10302

Return Period (yr)	Water Surface Elevation (ft NGVD)	Standard Deviation (ft)
5	3.41	0.0
10	3.91	0.63
25	5.69	0.50
50	6.92	0.84
75	7.54	0.71
100	7.82	0.71
150	8.20	0.59
200	8.39	0.60

Table A40
Hurricane Stage-Frequency Relationship for Grid Node 10398

Return Period (yr)	Water Surface Elevation (ft NGVD)	Standard Deviation (ft)
5	3.41	0.0
10	3.88	0.64
25	5.65	0.49
50	6.88	0.83
75	7.50	0.70
100	7.77	0.71
150	8.15	0.58
200	8.33	0.60

Table A41
Hurricane Stage-Frequency Relationship for Grid Node 10395

Return Period (yr)	Water Surface Elevation (ft NGVD)	Standard Deviation (ft)
5	3.40	0.0
10	3.83	0.63
25	5.58	0.50
50	6.80	0.83
75	7.42	0.70
100	7.69	0.71
150	8.06	0.58
200	8.24	0.59

Table A42
Hurricane Stage-Frequency Relationship for Grid Node 10478

Return Period (yr)	Water Surface Elevation (ft NGVD)	Standard Deviation (ft)
5	3.39	0.0
10	3.81	0.63
25	5.57	0.48
50	6.78	0.88
75	7.38	0.70
100	7.66	0.70
150	8.02	0.57
200	8.20	0.58

Appendix B
Stage-Frequency Relationship Figures

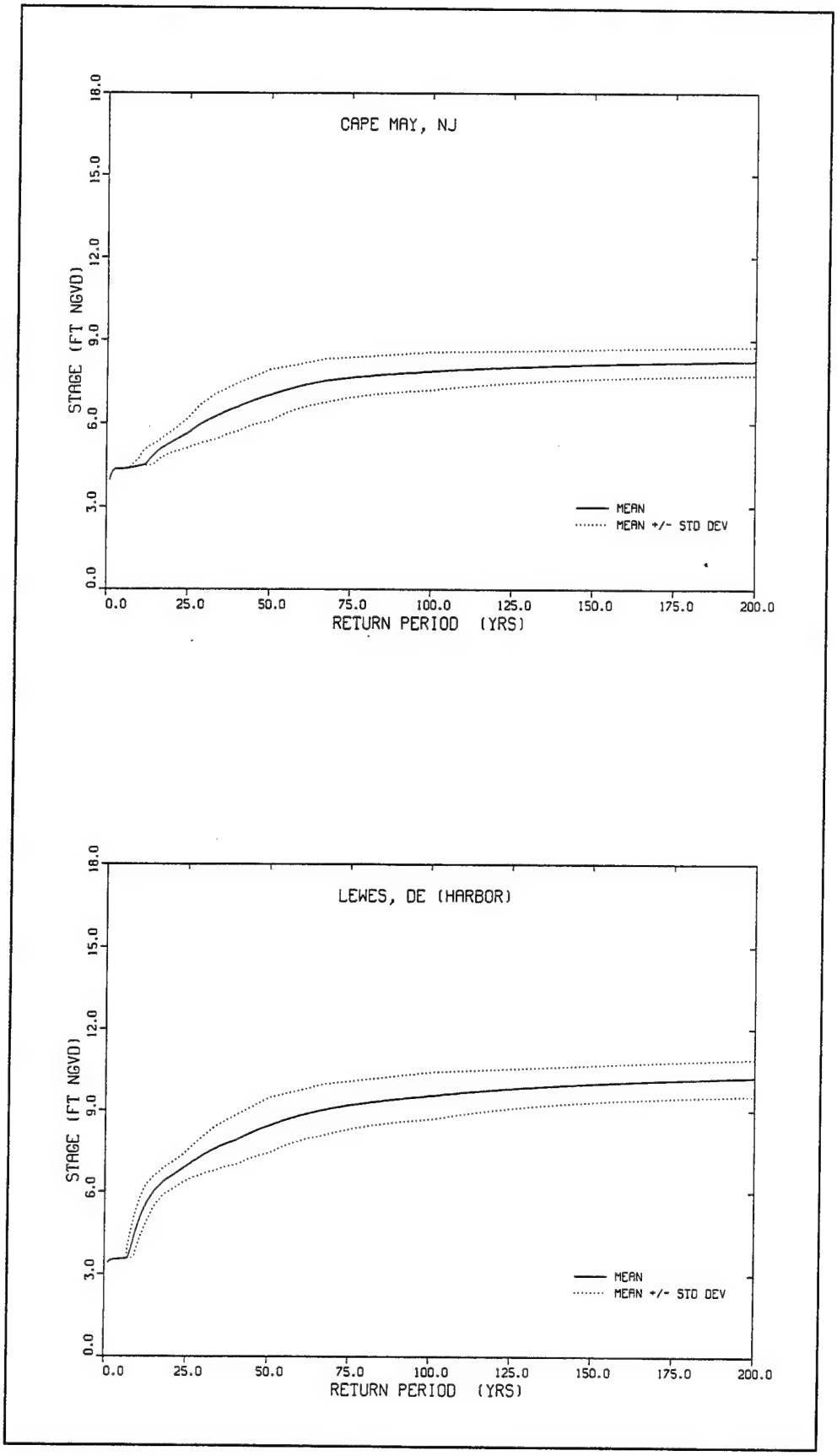
CAPE MAY, NJ
STAGE (FT NGVD)
0.0
3.0
6.0
9.0
12.0
15.0
18.0
0.0
25.0
50.0
75.0
100.0
125.0
150.0
175.0
200.0
RETURN PERIOD (YRS)
MEAN
MEAN +/- STD DEV
LEWES, DE (HARBOR)
STAGE (FT NGVD)
0.0
3.0
6.0
9.0
12.0
15.0
18.0
0.0
25.0
50.0
75.0
100.0
125.0
150.0
175.0
200.0
RETURN PERIOD (YRS)
MEAN
MEAN +/- STD DEV

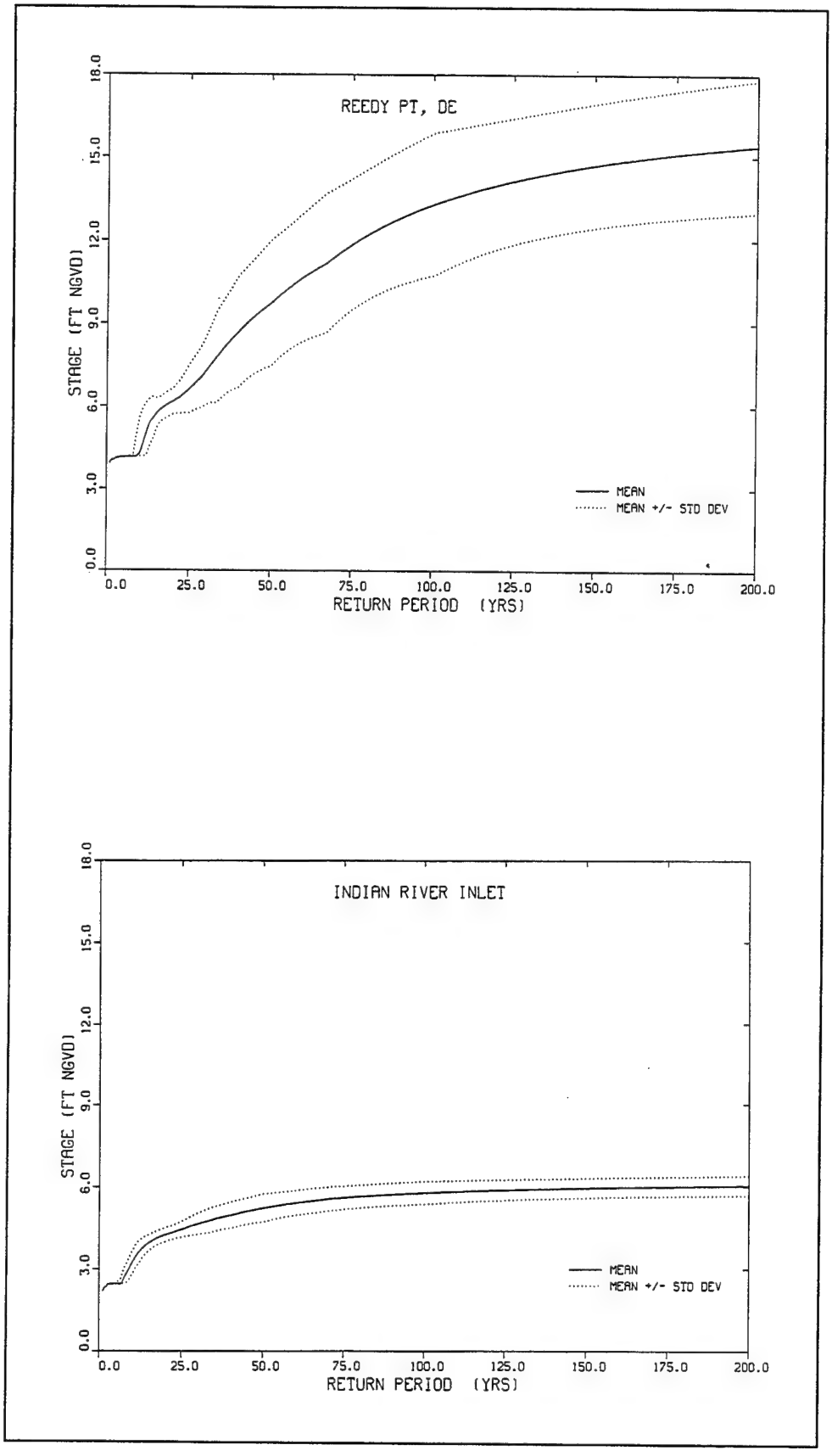
REEDY PT, DE
STAGE (FT NGVD)
0.0
3.0
6.0
9.0
12.0
15.0
18.0
0.0
25.0
50.0
75.0
100.0
125.0
150.0
175.0
200.0
RETURN PERIOD (YRS)
MEAN
MEAN +/- STD DEV
INDIAN RIVER INLET
STAGE (FT NGVD)
RETURN PERIOD (YRS)
MEAN
MEAN +/- STD DEV

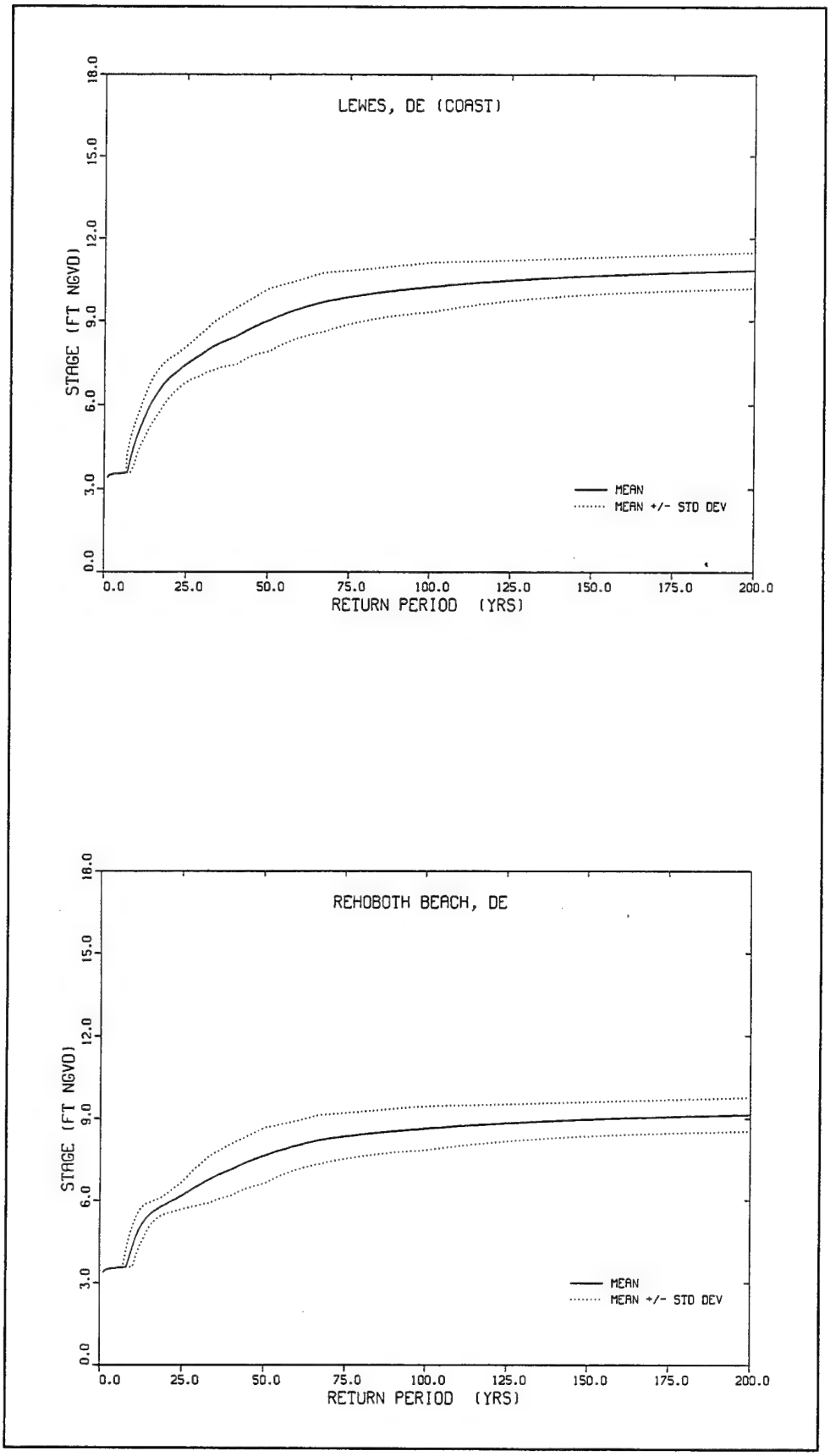
LEWES, DE (COAST)
STAGE (FT NGVD)
0.0
3.0
6.0
9.0
12.0
15.0
18.0
0.0
25.0
50.0
75.0
100.0
125.0
150.0
175.0
200.0
RETURN PERIOD (YRS)
MEAN
MEAN +/- STD DEV
REHOBOTH BEACH, DE
STAGE (FT NGVD)
0.0
3.0
6.0
9.0
12.0
15.0
18.0
0.0
25.0
50.0
75.0
100.0
125.0
150.0
175.0
200.0
RETURN PERIOD (YRS)
MEAN
MEAN +/- STD DEV

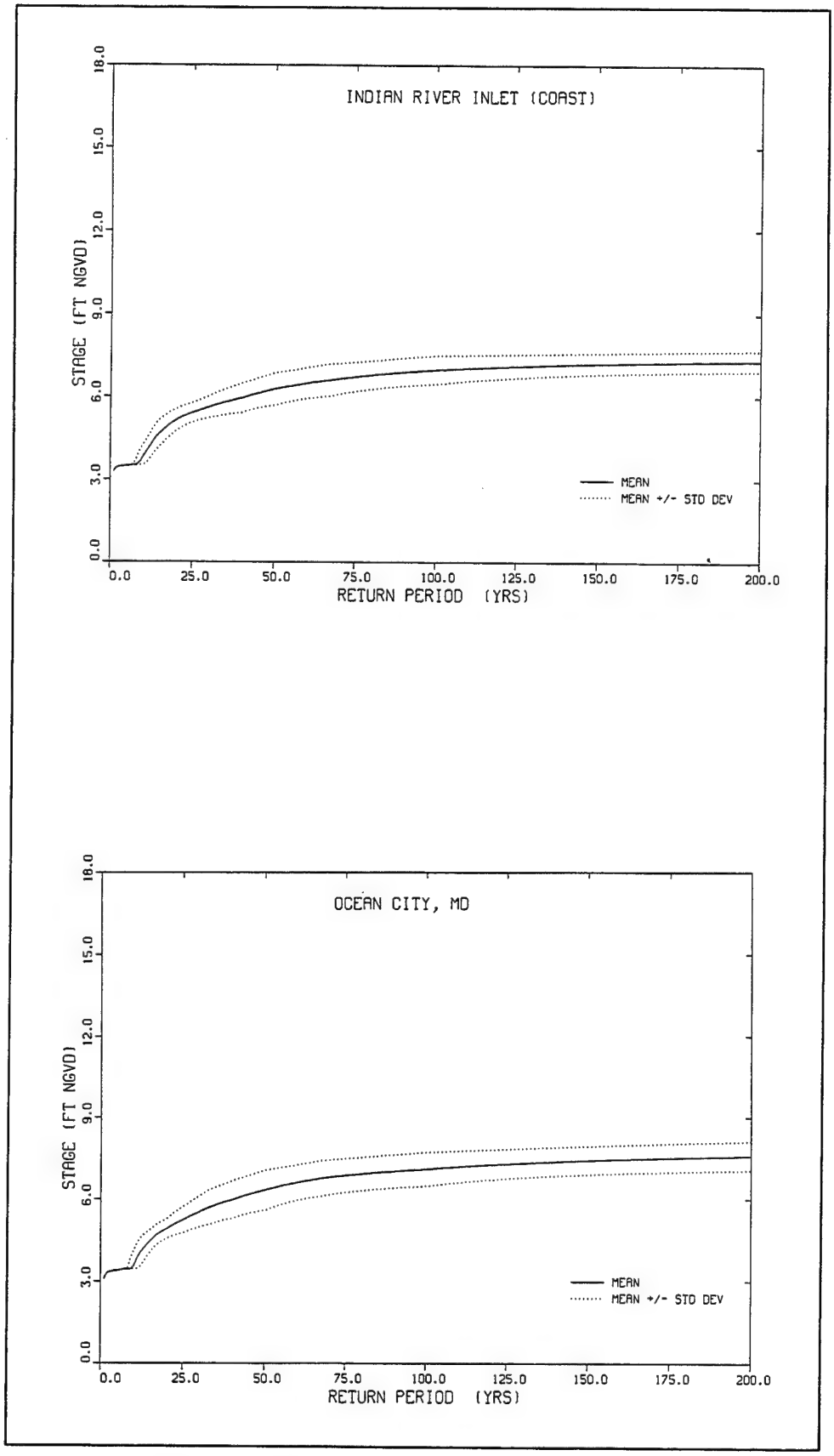
INDIAN RIVER INLET (COAST)
STAGE (FT NGVD)
0.0
3.0
6.0
9.0
12.0
15.0
18.0
0.0
25.0
50.0
75.0
100.0
125.0
150.0
175.0
200.0
RETURN PERIOD (YRS)
MEAN
MEAN +/- STD DEV
OCEAN CITY, MD
STAGE (FT NGVD)
0.0
3.0
6.0
9.0
12.0
15.0
18.0
0.0
25.0
50.0
75.0
100.0
125.0
150.0
175.0
200.0
RETURN PERIOD (YRS)
MEAN
MEAN +/- STD DEV

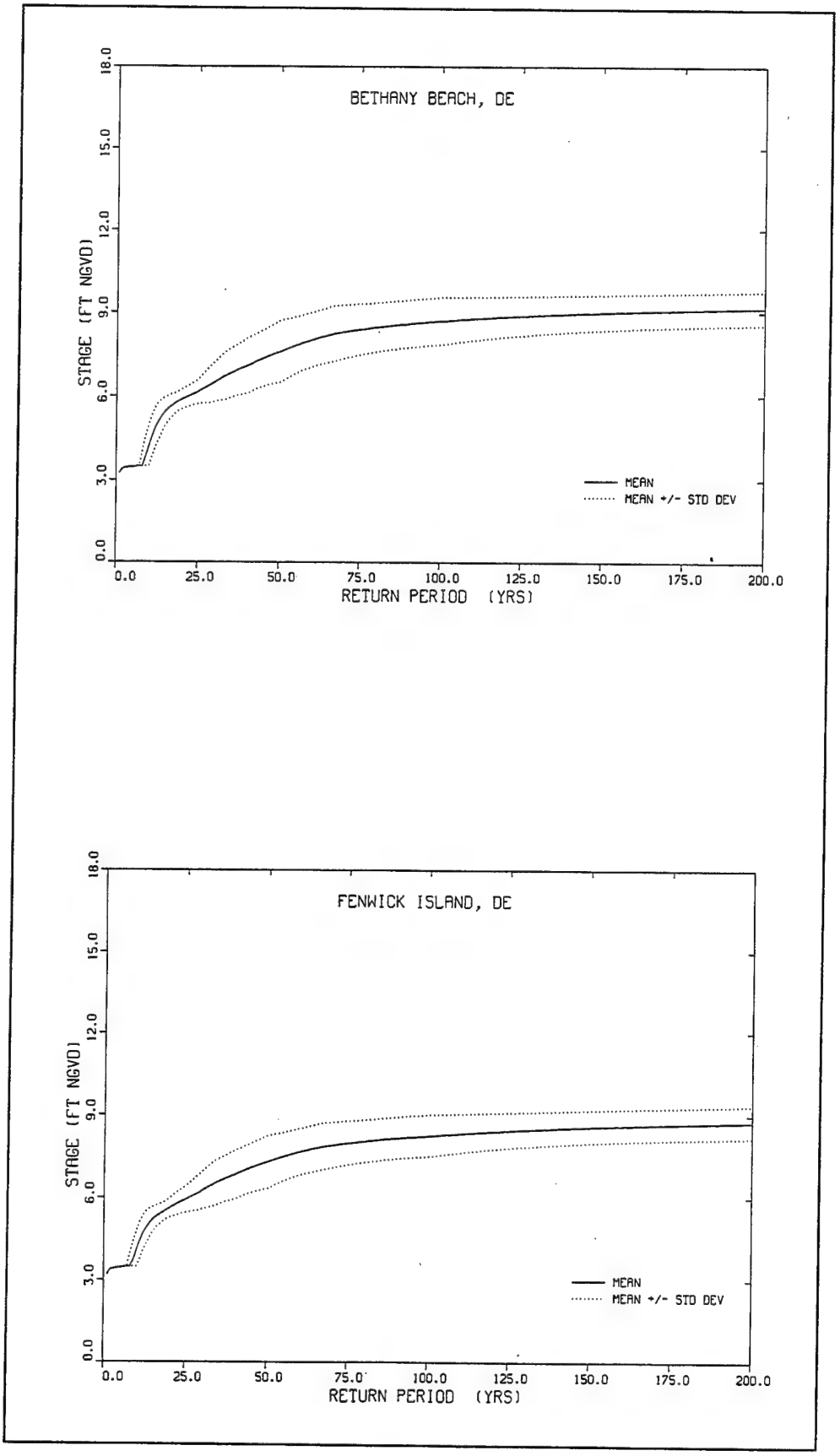
BETHANY BEACH, DE
STAGE (FT NGVD)
0.0
3.0
6.0
9.0
12.0
15.0
18.0
0.0
25.0
50.0
75.0
100.0
125.0
150.0
175.0
200.0
RETURN PERIOD (YRS)
MEAN
MEAN +/- STD DEV
FENWICK ISLAND, DE
STAGE (FT NGVD)
0.0
3.0
6.0
9.0
12.0
15.0
18.0
0.0
25.0
50.0
75.0
100.0
125.0
150.0
175.0
200.0
RETURN PERIOD (YRS)
MEAN
MEAN +/- STD DEV

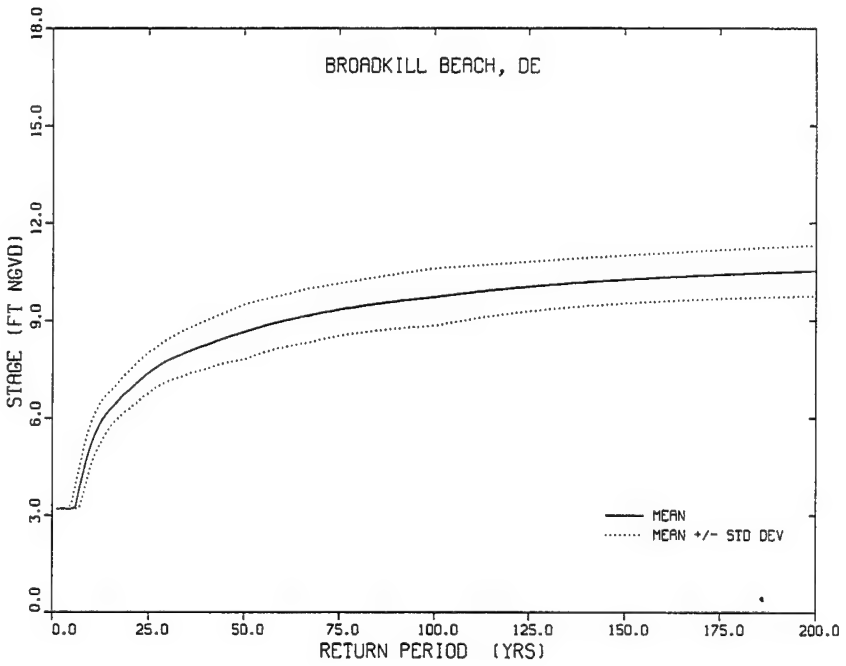
BROADKILL BEACH, DE
STAGE (FT NGVD)
0.0
3.0
6.0
9.0
12.0
15.0
18.0
0.0
25.0
50.0
75.0
100.0
125.0
150.0
175.0
200.0
RETURN PERIOD (YRS)
MEAN
MEAN +/- STD DEV

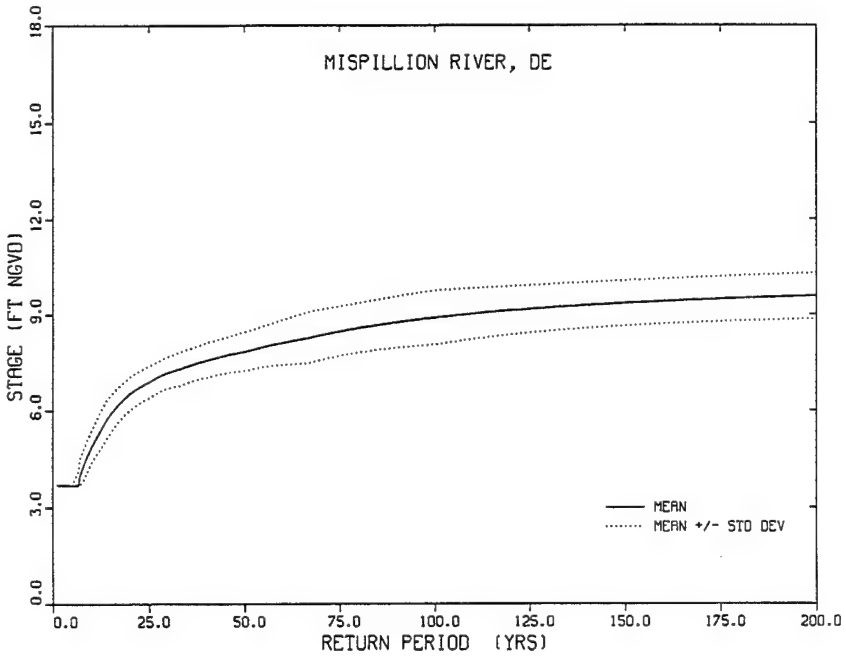
MISPILLION RIVER, DE
STAGE (FT NGVD)
0.0
3.0
6.0
9.0
12.0
15.0
18.0
0.0
25.0
50.0
75.0
100.0
125.0
150.0
175.0
200.0
RETURN PERIOD (YRS)
MEAN
MEAN +/- STD DEV

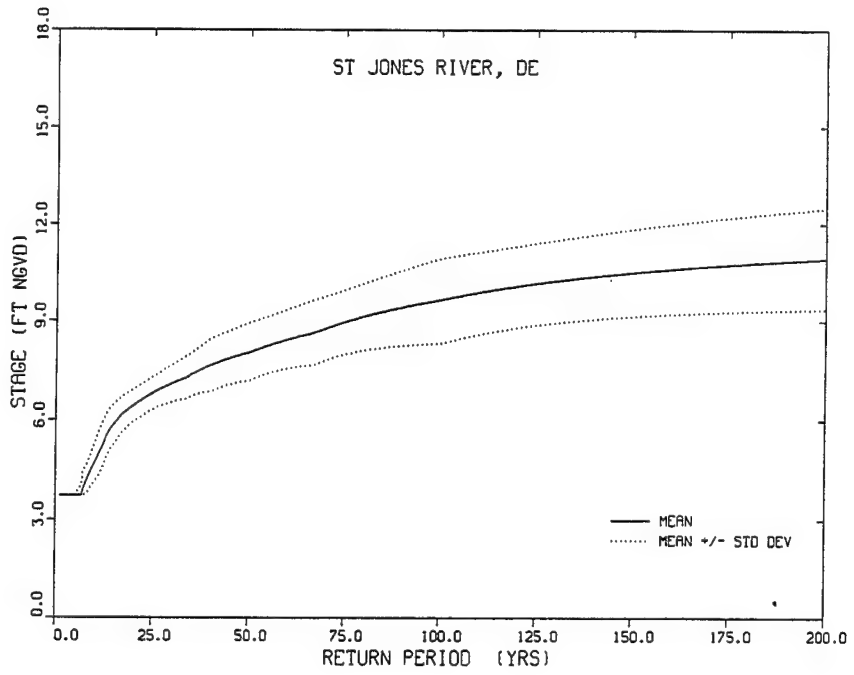
ST JONES RIVER, DE
STAGE (FT NGVD)
0.0
3.0
6.0
9.0
12.0
15.0
18.0
0.0
25.0
50.0
75.0
100.0
125.0
150.0
175.0
200.0
RETURN PERIOD (YRS)
MEAN
MEAN +/- STD DEV

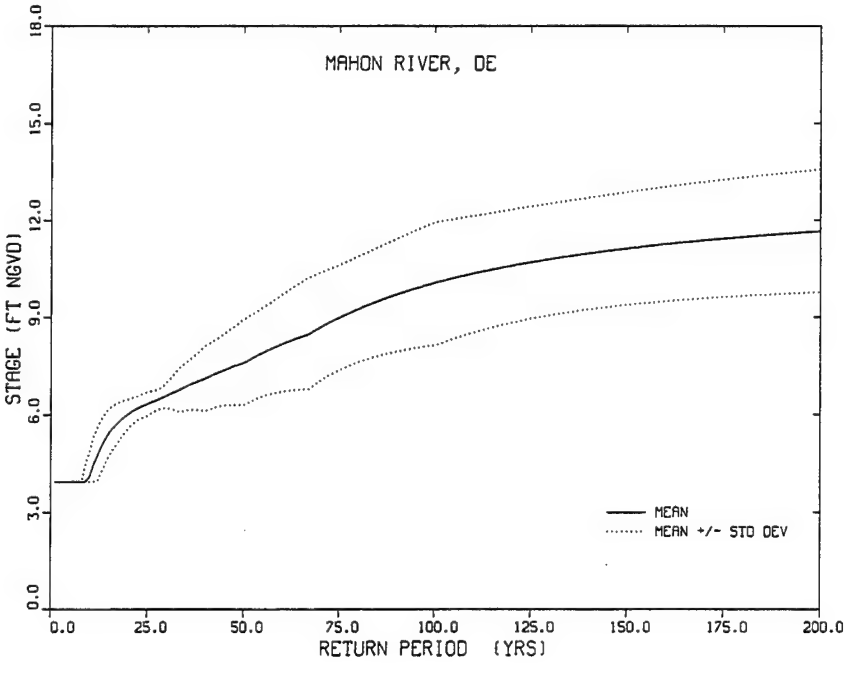
MAHON RIVER, DE
STAGE (FT NGVD)
0.0
3.0
6.0
9.0
12.0
15.0
18.0
0.0
25.0
50.0
75.0
100.0
125.0
150.0
175.0
200.0
RETURN PERIOD (YRS)
MEAN
MEAN +/- STD DEV

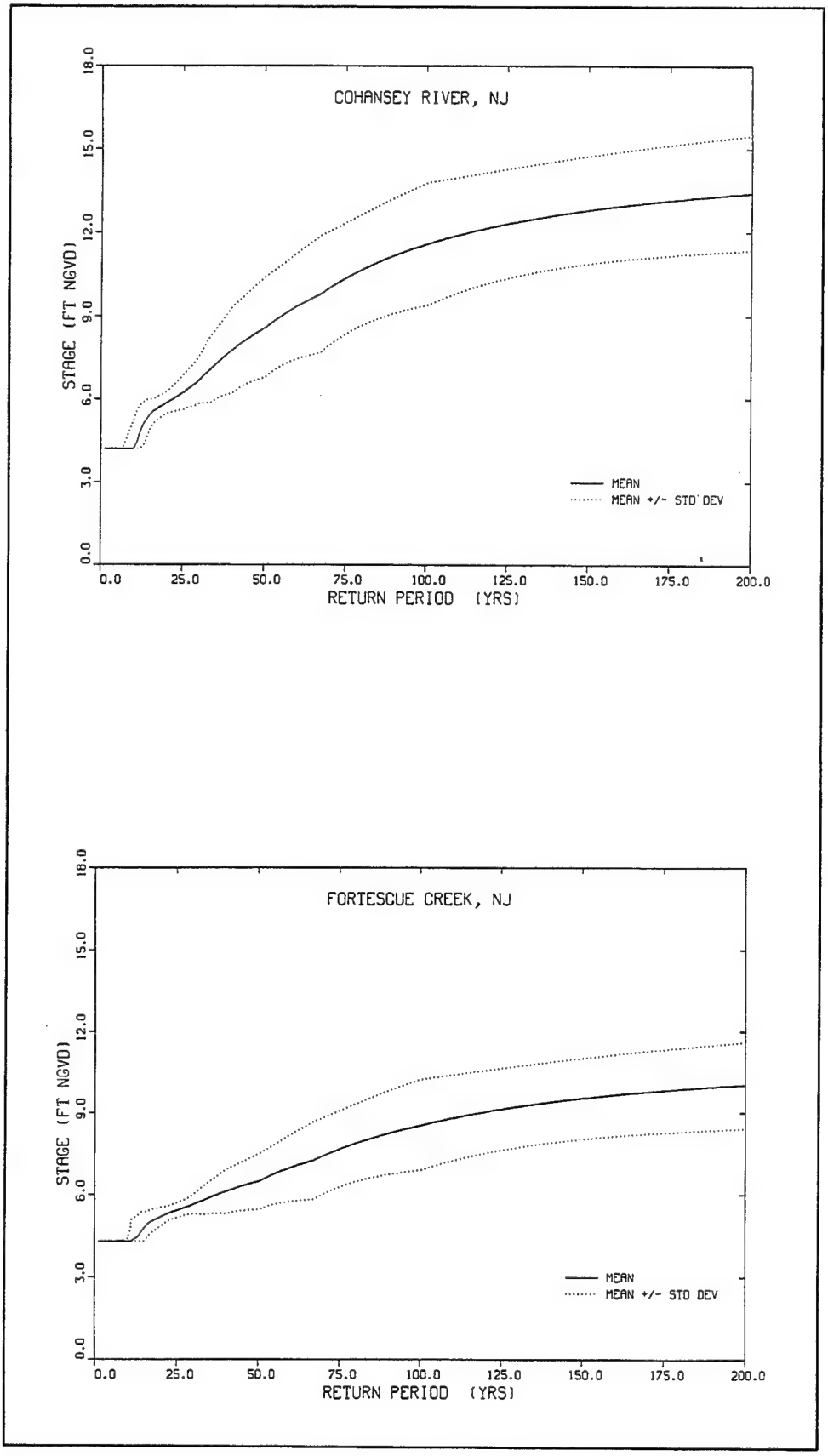
COHANSEY RIVER, NJ
STAGE (FT NGVD)
0.0
3.0
6.0
9.0
12.0
15.0
18.0
0.0
25.0
50.0
75.0
100.0
125.0
150.0
175.0
200.0
RETURN PERIOD (YRS)
MEAN
MEAN +/- STD DEV
FORTESCUE CREEK, NJ
STAGE (FT NGVD)
0.0
3.0
6.0
9.0
12.0
15.0
18.0
0.0
25.0
50.0
75.0
100.0
125.0
150.0
175.0
200.0
RETURN PERIOD (YRS)
MEAN
MEAN +/- STD DEV

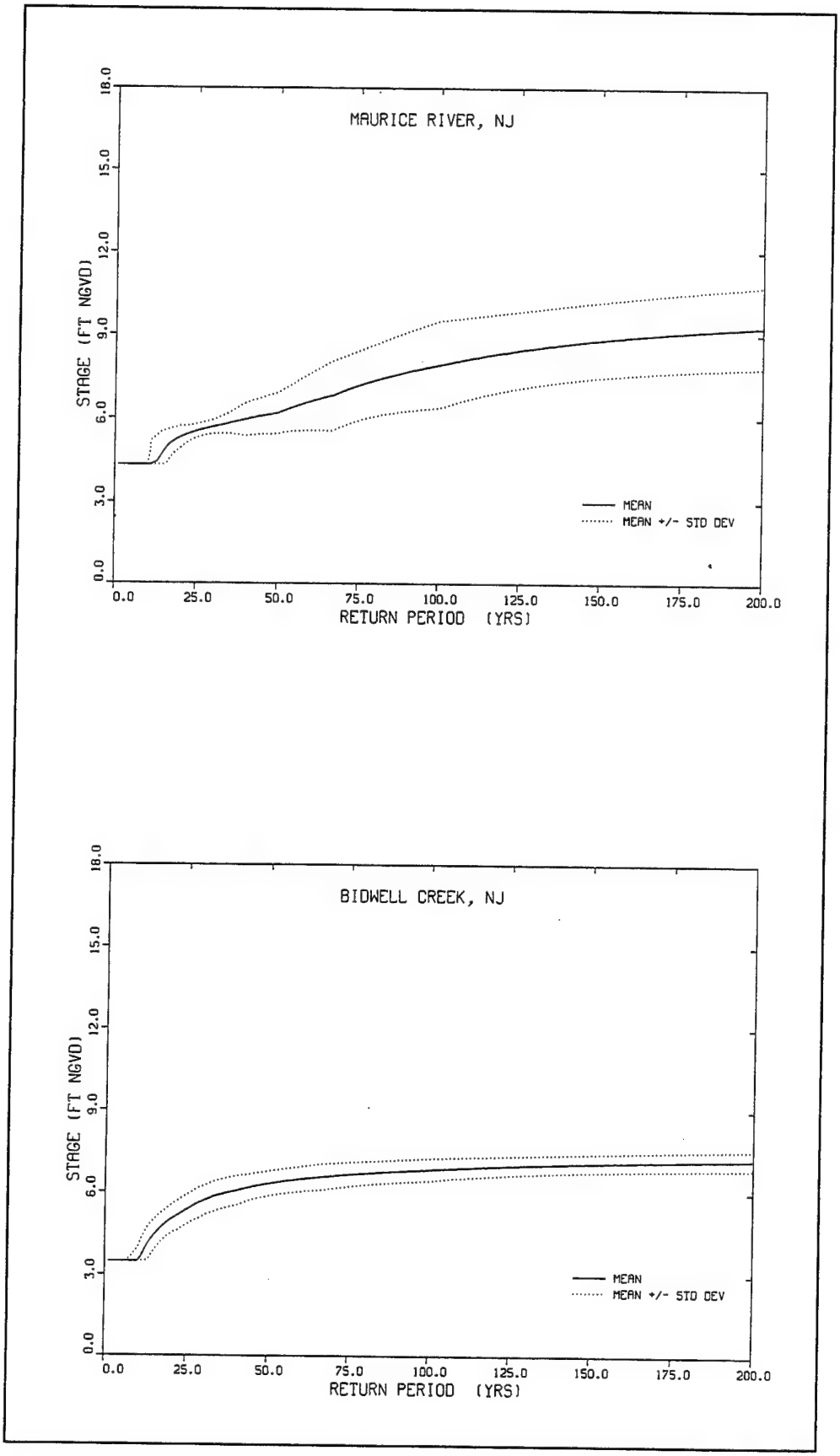
MAURICE RIVER, NJ
STAGE (FT NGVD)
0.0
3.0
6.0
9.0
12.0
15.0
18.0
0.0
25.0
50.0
75.0
100.0
125.0
150.0
175.0
200.0
RETURN PERIOD (YRS)
MEAN
MEAN +/- STD DEV
BIDWELL CREEK, NJ
STAGE (FT NGVD)
0.0
3.0
6.0
9.0
12.0
15.0
18.0
0.0
25.0
50.0
75.0
100.0
125.0
150.0
175.0
200.0
RETURN PERIOD (YRS)
MEAN
MEAN +/- STD DEV

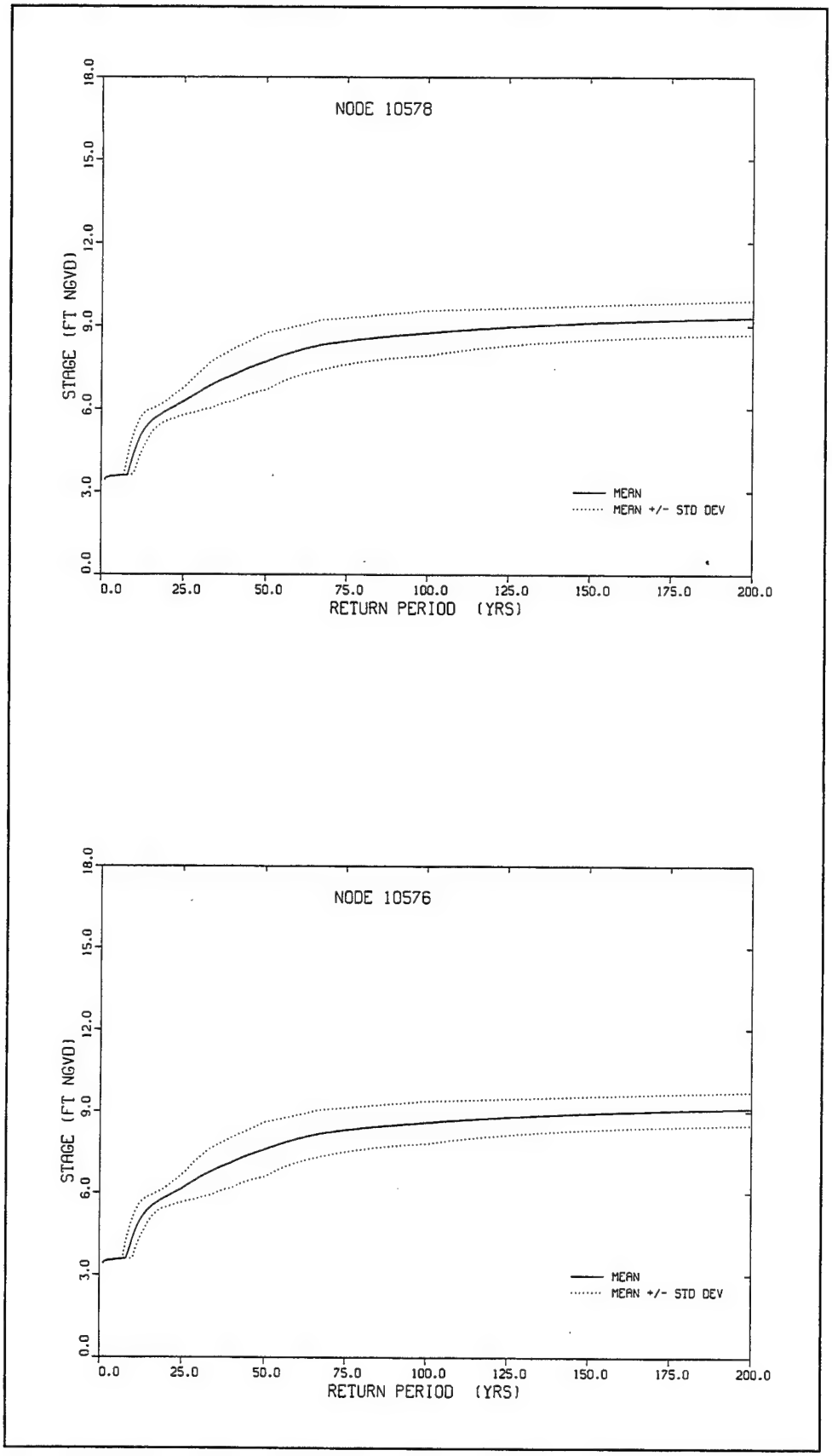
NODE 10578
STAGE (FT NGVD)
0.0
3.0
6.0
9.0
12.0
15.0
18.0
0.0
25.0
50.0
75.0
100.0
125.0
150.0
175.0
200.0
RETURN PERIOD (YRS)
MEAN
MEAN +/- STD DEV
NODE 10576
STAGE (FT NGVD)
RETURN PERIOD (YRS)
MEAN
MEAN +/- STD DEV

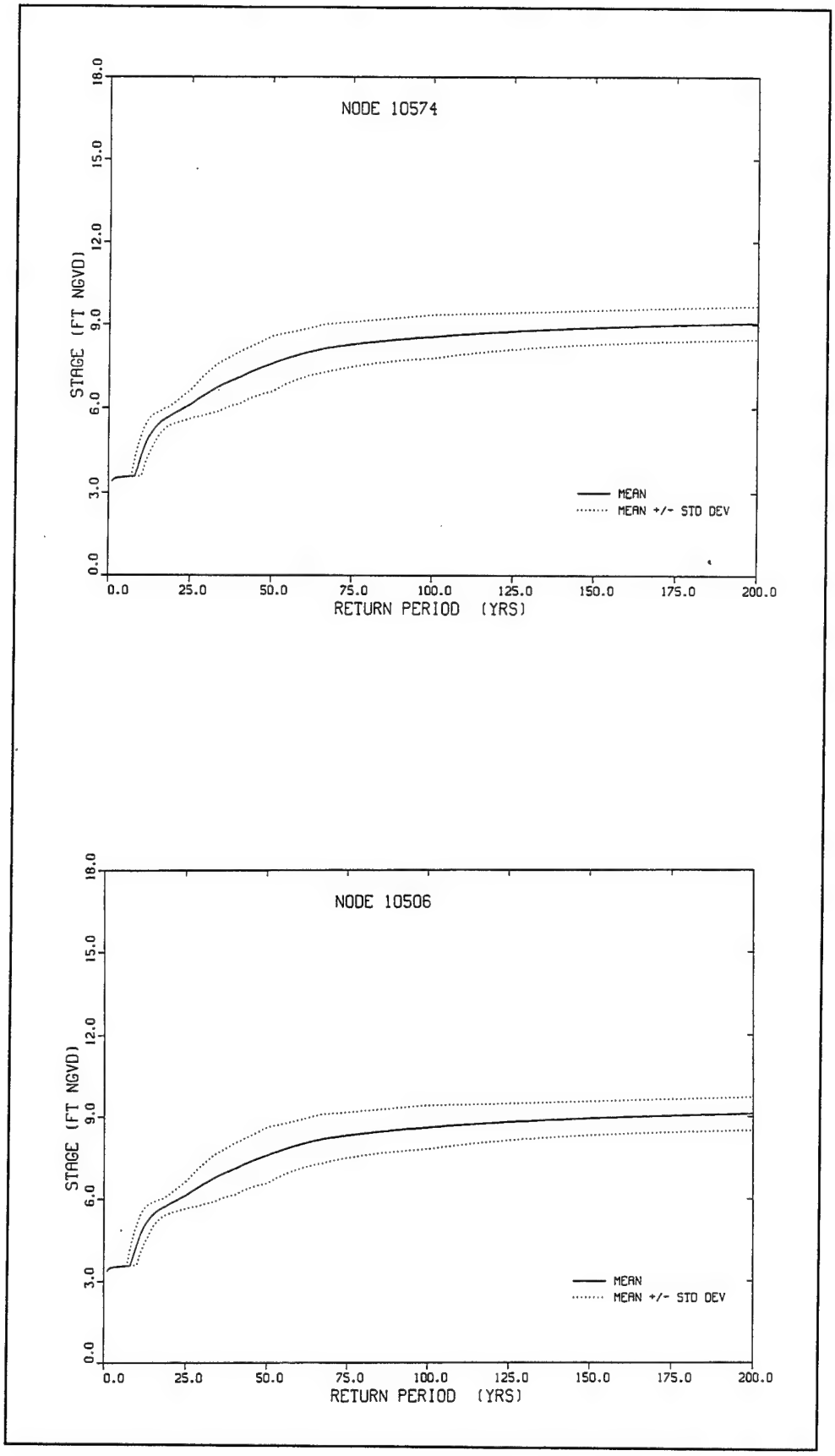
NODE 10574
STAGE (FT NGVD)
0.0
3.0
6.0
9.0
12.0
15.0
18.0
0.0
25.0
50.0
75.0
100.0
125.0
150.0
175.0
200.0
RETURN PERIOD (YRS)
MEAN
MEAN +/- STD DEV
NODE 10506
STAGE (FT NGVD)
RETURN PERIOD (YRS)
MEAN
MEAN +/- STD DEV

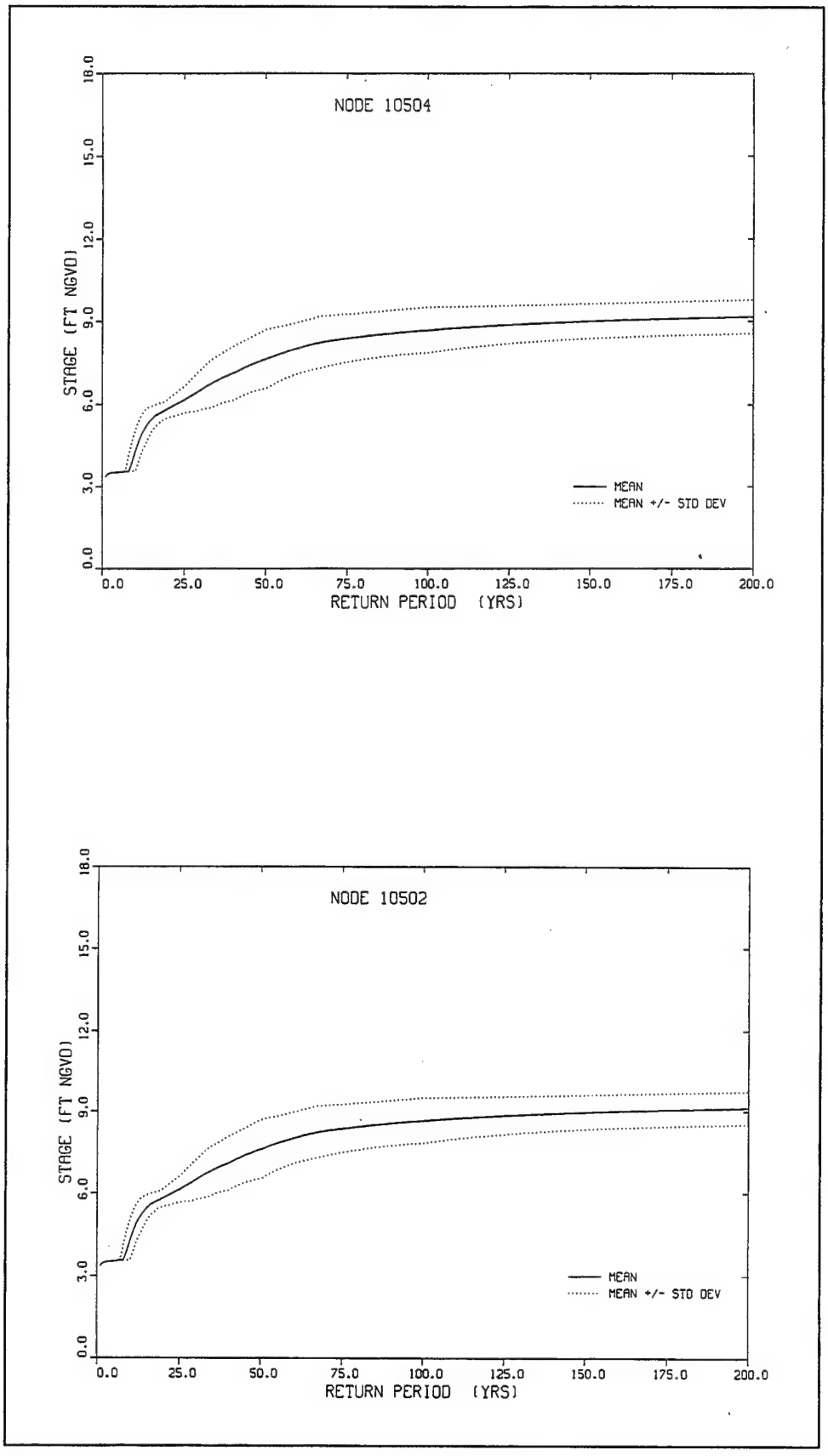
NODE 10504
STAGE (FT NGVD)
0.0
3.0
6.0
9.0
12.0
15.0
18.0
0.0
25.0
50.0
75.0
100.0
125.0
150.0
175.0
200.0
RETURN PERIOD (YRS)
MEAN
MEAN +/- STD DEV
NODE 10502
STAGE (FT NGVD)
RETURN PERIOD (YRS)
MEAN
MEAN +/- STD DEV

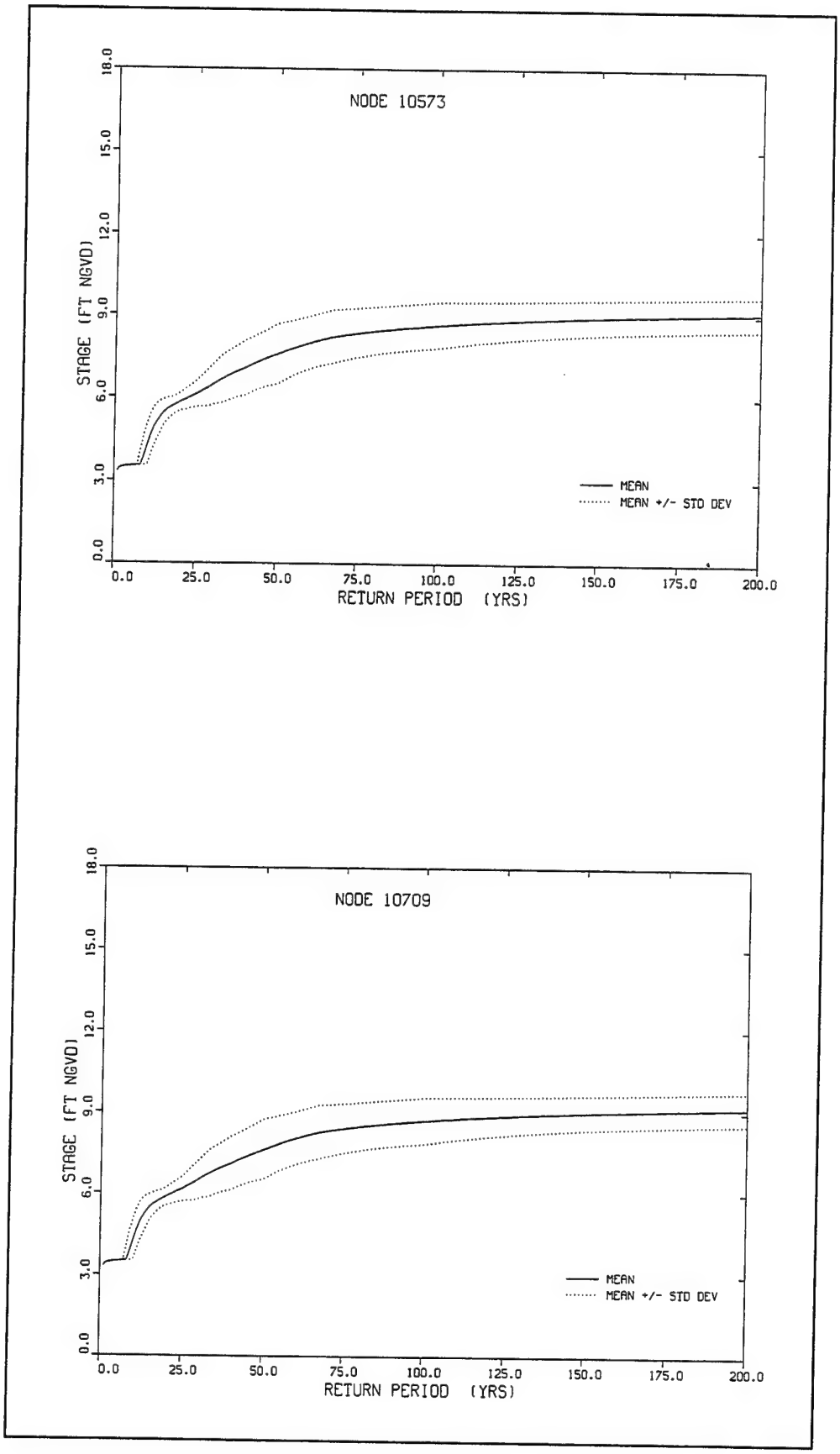
NODE 10573
STAGE (FT NGVD)
0.0
3.0
6.0
9.0
12.0
15.0
18.0
0.0
25.0
50.0
75.0
100.0
125.0
150.0
175.0
200.0
RETURN PERIOD (YRS)
MEAN
MEAN +/- STD DEV
NODE 10709
STAGE (FT NGVD)
RETURN PERIOD (YRS)
MEAN
MEAN +/- STD DEV

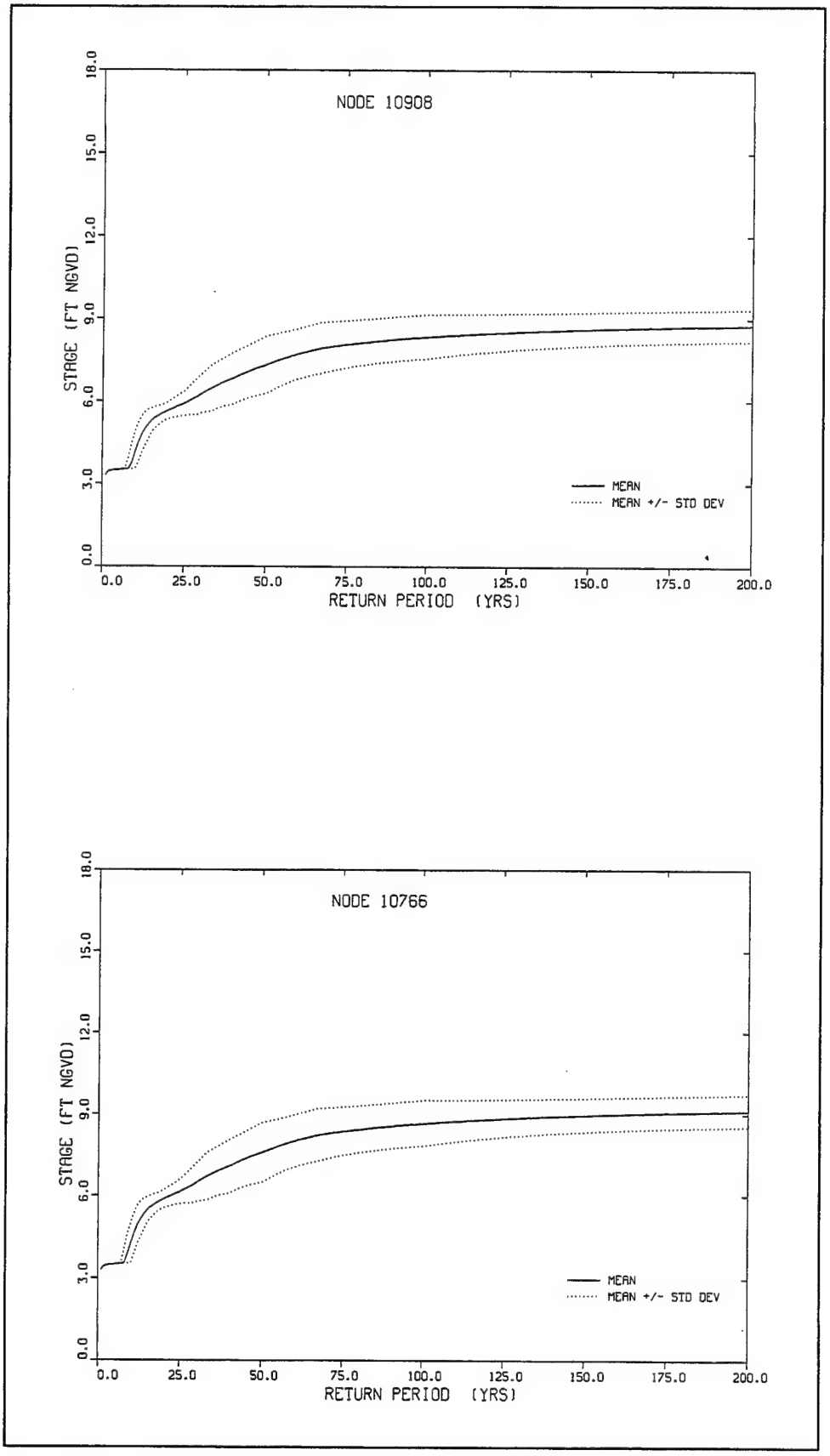
NODE 10908
STAGE (FT NGVD)
0.0
3.0
6.0
9.0
12.0
15.0
18.0
0.0
25.0
50.0
75.0
100.0
125.0
150.0
175.0
200.0
RETURN PERIOD (YRS)
MEAN
MEAN +/- STD DEV
NODE 10766
STAGE (FT NGVD)
RETURN PERIOD (YRS)
MEAN
MEAN +/- STD DEV

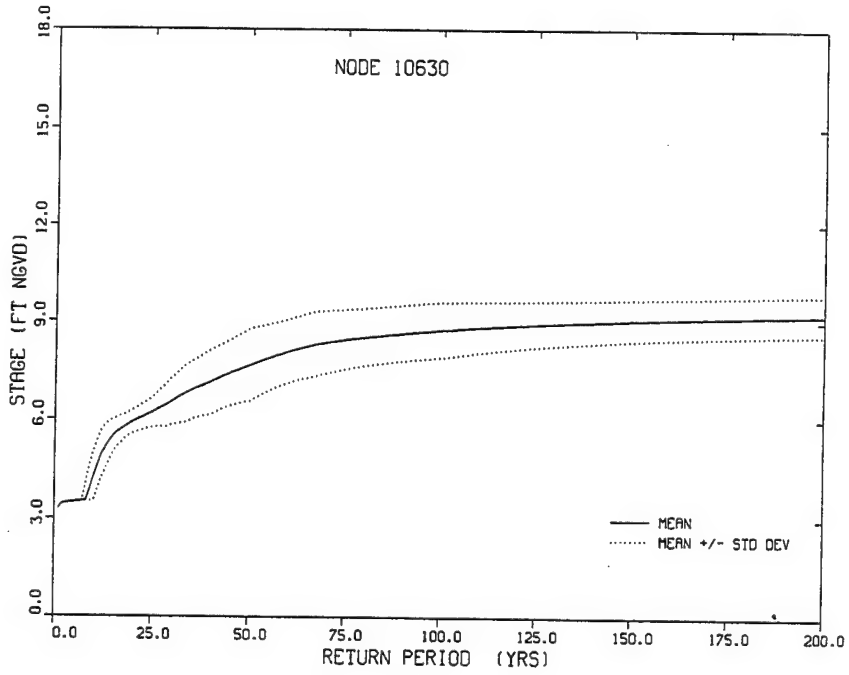
NODE 10630
STAGE (FT NGVD)
0.0
3.0
6.0
9.0
12.0
15.0
18.0
0.0
25.0
50.0
75.0
100.0
125.0
150.0
175.0
200.0
RETURN PERIOD (YRS)
MEAN
MEAN +/- STD DEV

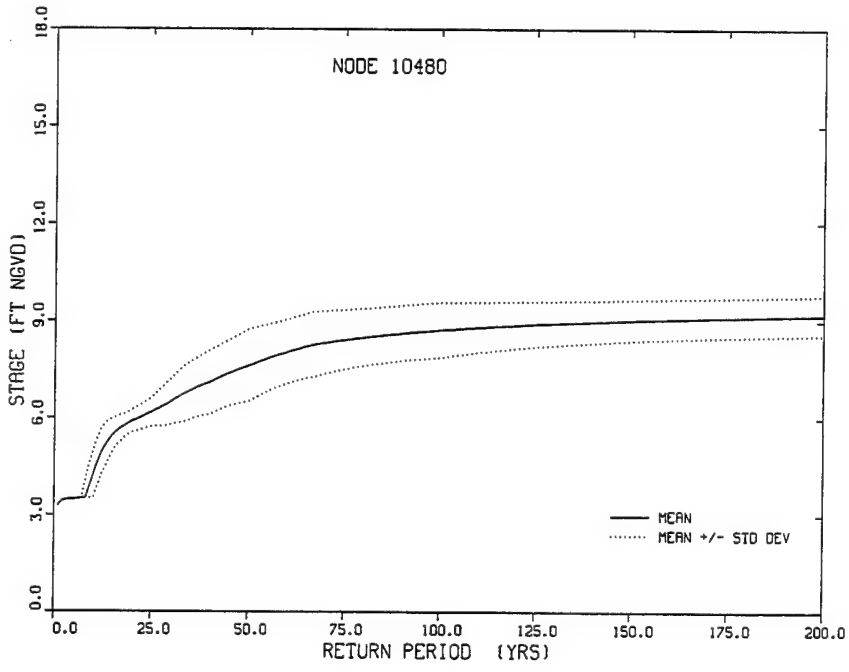
NODE 10480
STAGE (FT NGVD)
0.0
3.0
6.0
9.0
12.0
15.0
18.0
0.0
25.0
50.0
75.0
100.0
125.0
150.0
175.0
200.0
RETURN PERIOD (YRS)
MEAN
MEAN +/- STD DEV

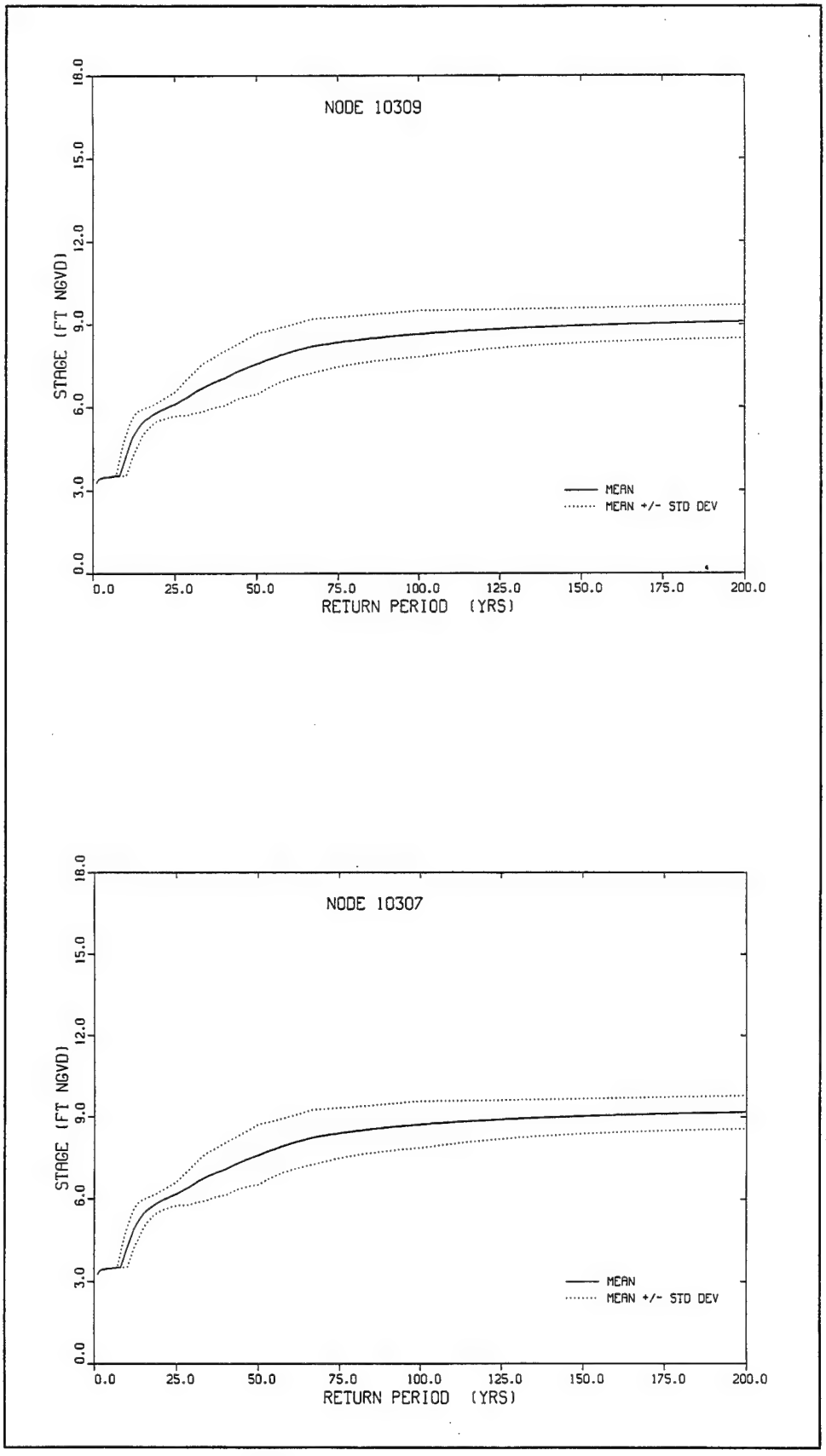
NODE 10309
STAGE (FT NGVD)
0.0
3.0
6.0
9.0
12.0
15.0
18.0
0.0
25.0
50.0
75.0
100.0
125.0
150.0
175.0
200.0
RETURN PERIOD (YRS)
MEAN
MEAN +/- STD DEV
NODE 10307
STAGE (FT NGVD)
RETURN PERIOD (YRS)
MEAN
MEAN +/- STD DEV

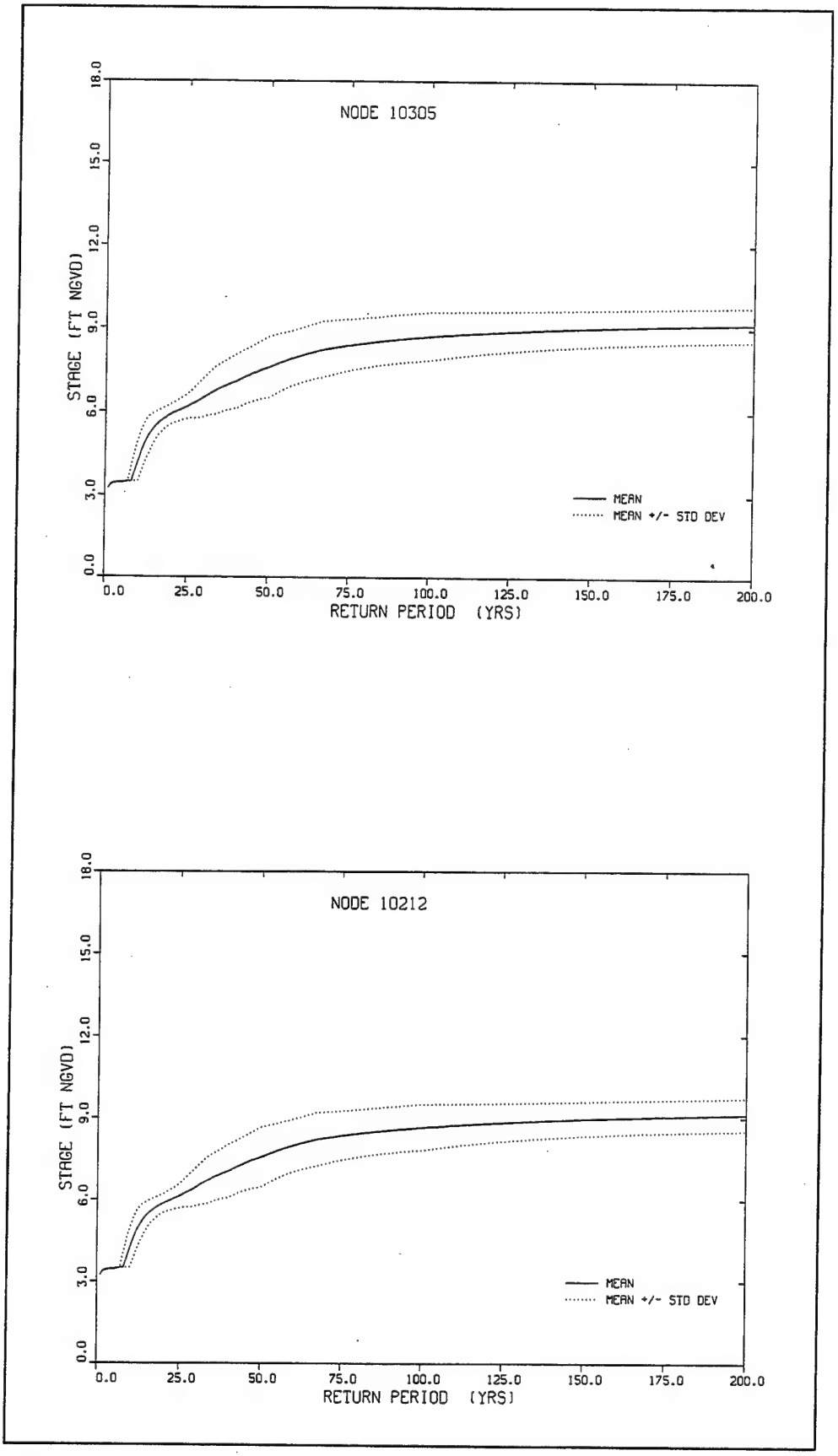
NODE 10305
STAGE (FT NGVD)
0.0
3.0
6.0
9.0
12.0
15.0
18.0
0.0
25.0
50.0
75.0
100.0
125.0
150.0
175.0
200.0
RETURN PERIOD (YRS)
MEAN
MEAN +/- STD DEV
NODE 10212
STAGE (FT NGVD)
RETURN PERIOD (YRS)
MEAN
MEAN +/- STD DEV

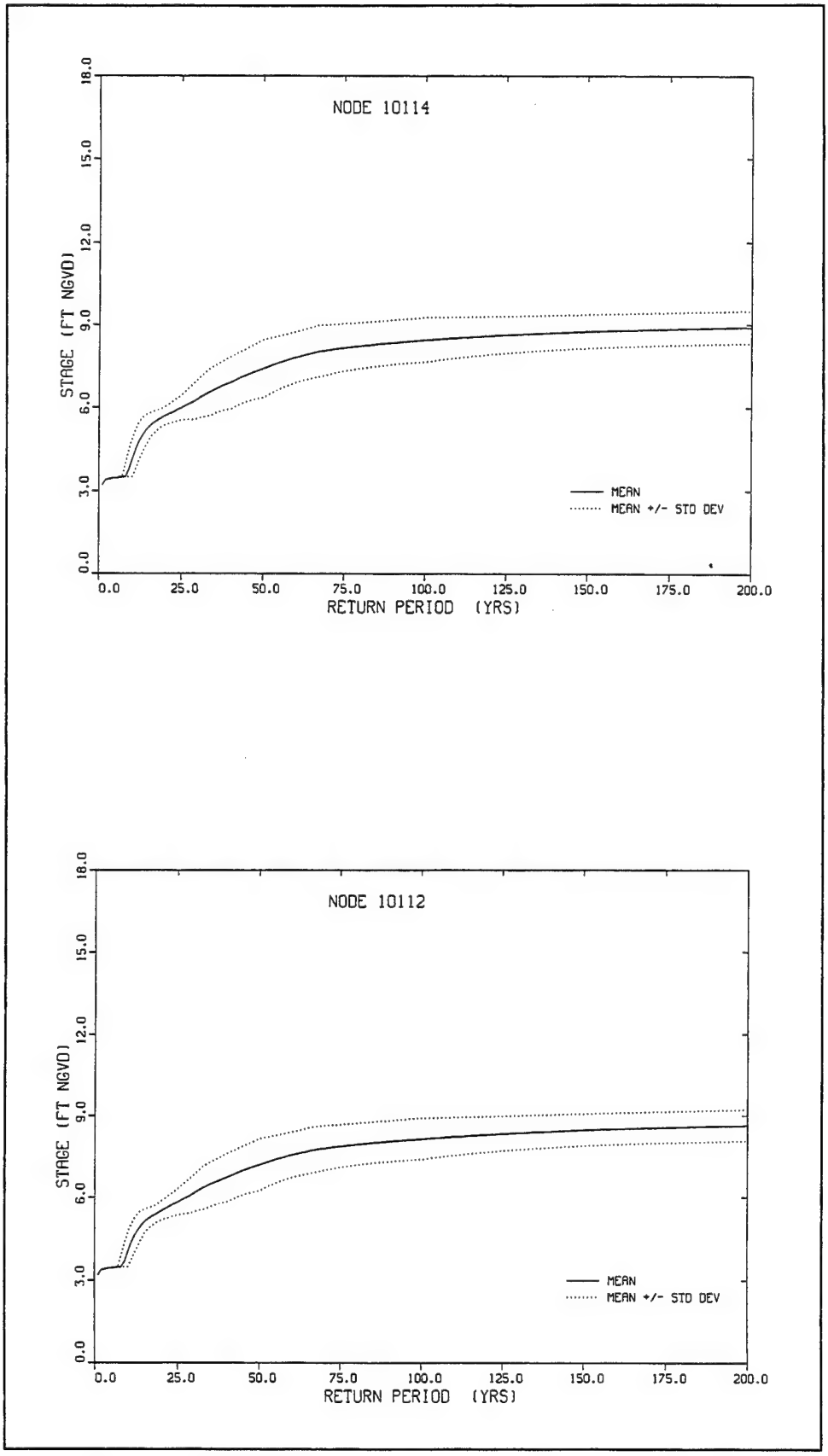
NODE 10114
STAGE (FT NGVD)
0.0
3.0
6.0
9.0
12.0
15.0
18.0
0.0
25.0
50.0
75.0
100.0
125.0
150.0
175.0
200.0
RETURN PERIOD (YRS)
MEAN
MEAN +/- STD DEV
NODE 10112
STAGE (FT NGVD)
RETURN PERIOD (YRS)
MEAN
MEAN +/- STD DEV

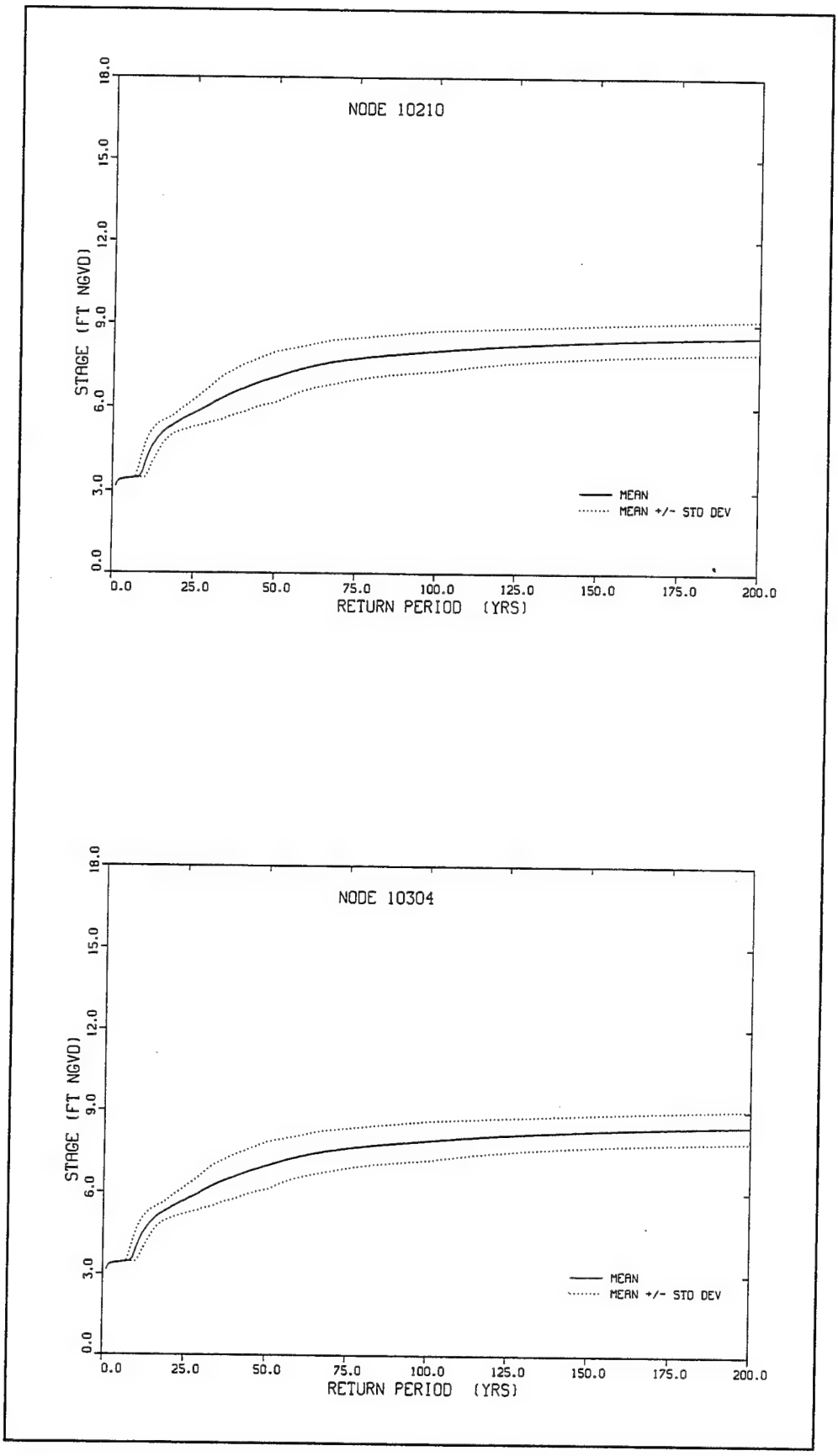
NODE 10210
STAGE (FT NGVD)
0.0
3.0
6.0
9.0
12.0
15.0
18.0
0.0
25.0
50.0
75.0
100.0
125.0
150.0
175.0
200.0
RETURN PERIOD (YRS)
MEAN
MEAN +/- STD DEV
NODE 10304
STAGE (FT NGVD)
RETURN PERIOD (YRS)
MEAN
MEAN +/- STD DEV

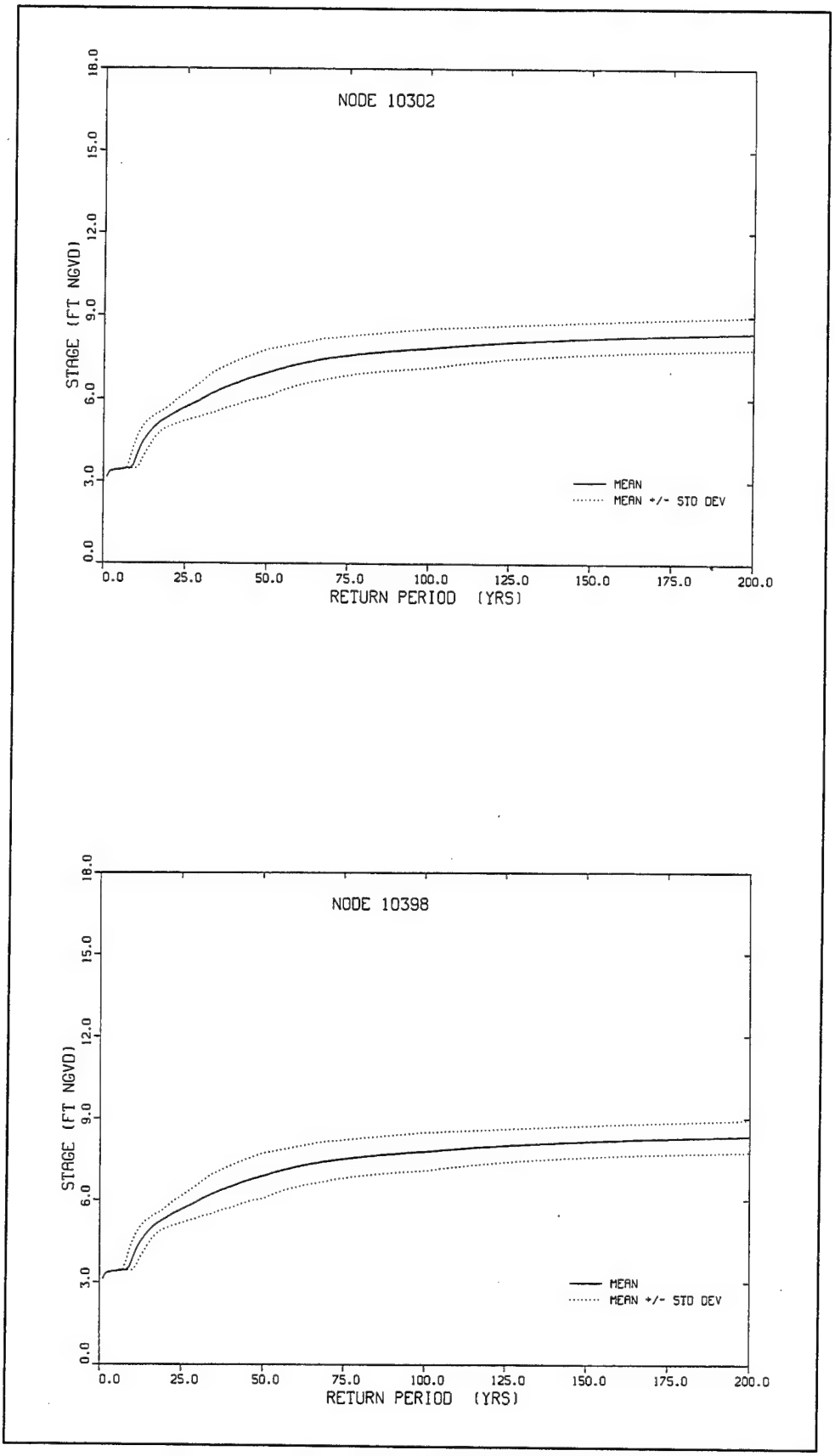
NODE 10302
STAGE (FT NGVD)
0.0
3.0
6.0
9.0
12.0
15.0
18.0
0.0
25.0
50.0
75.0
100.0
125.0
150.0
175.0
200.0
RETURN PERIOD (YRS)
MEAN
MEAN +/- STD DEV
NODE 10398
STAGE (FT NGVD)
RETURN PERIOD (YRS)
MEAN
MEAN +/- STD DEV

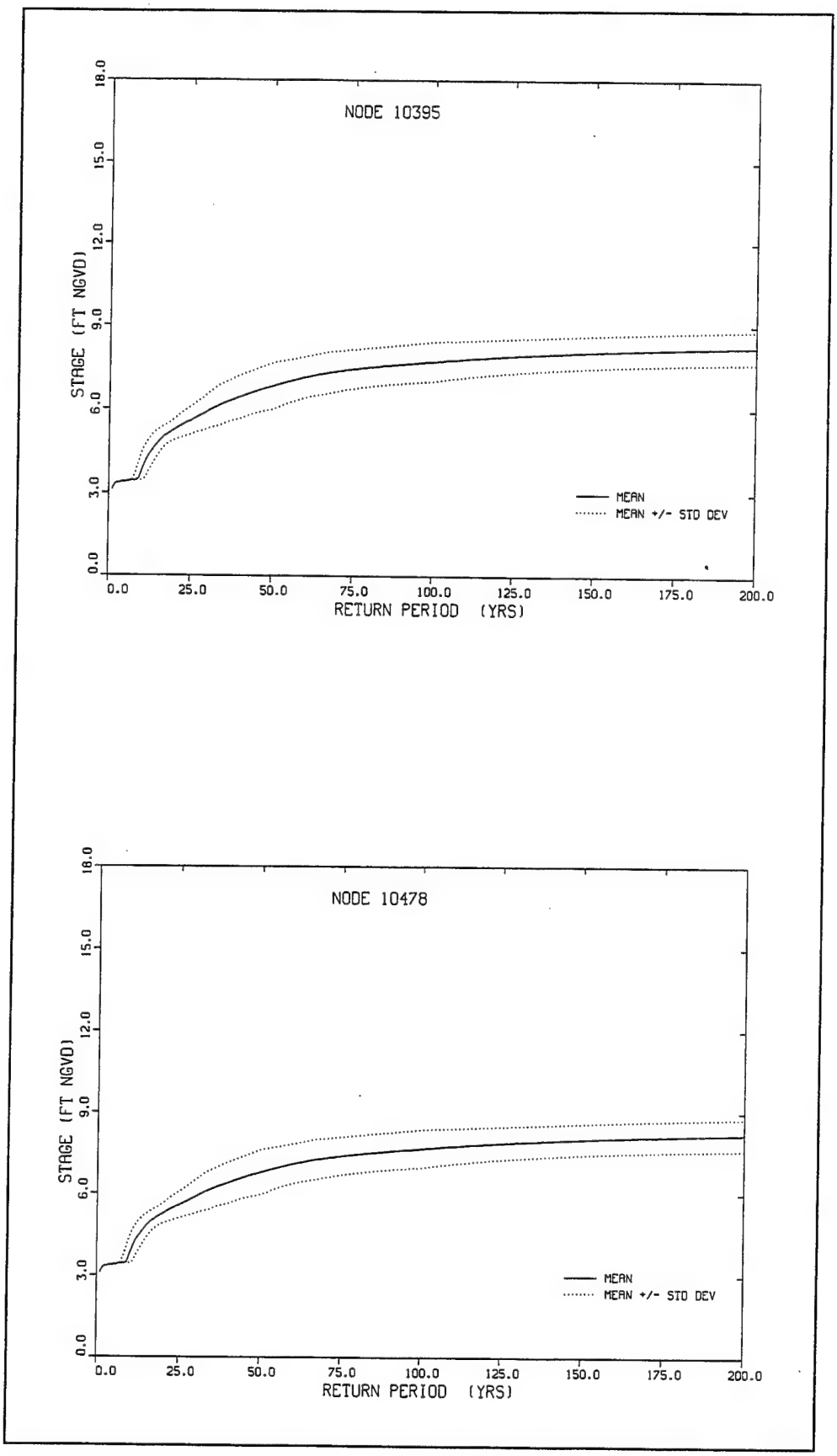
NODE 10395
STAGE (FT NGVD)
0.0
3.0
6.0
9.0
12.0
15.0
18.0
0.0
25.0
50.0
75.0
100.0
125.0
150.0
175.0
200.0
RETURN PERIOD (YRS)
MEAN
MEAN +/- STD DEV
NODE 10478
STAGE (FT NGVD)
0.0
3.0
6.0
9.0
12.0
15.0
18.0
0.0
25.0
50.0
75.0
100.0
125.0
150.0
175.0
200.0
RETURN PERIOD (YRS)
MEAN
MEAN +/- STD DEV

Appendix C
Hurricane Track Figures

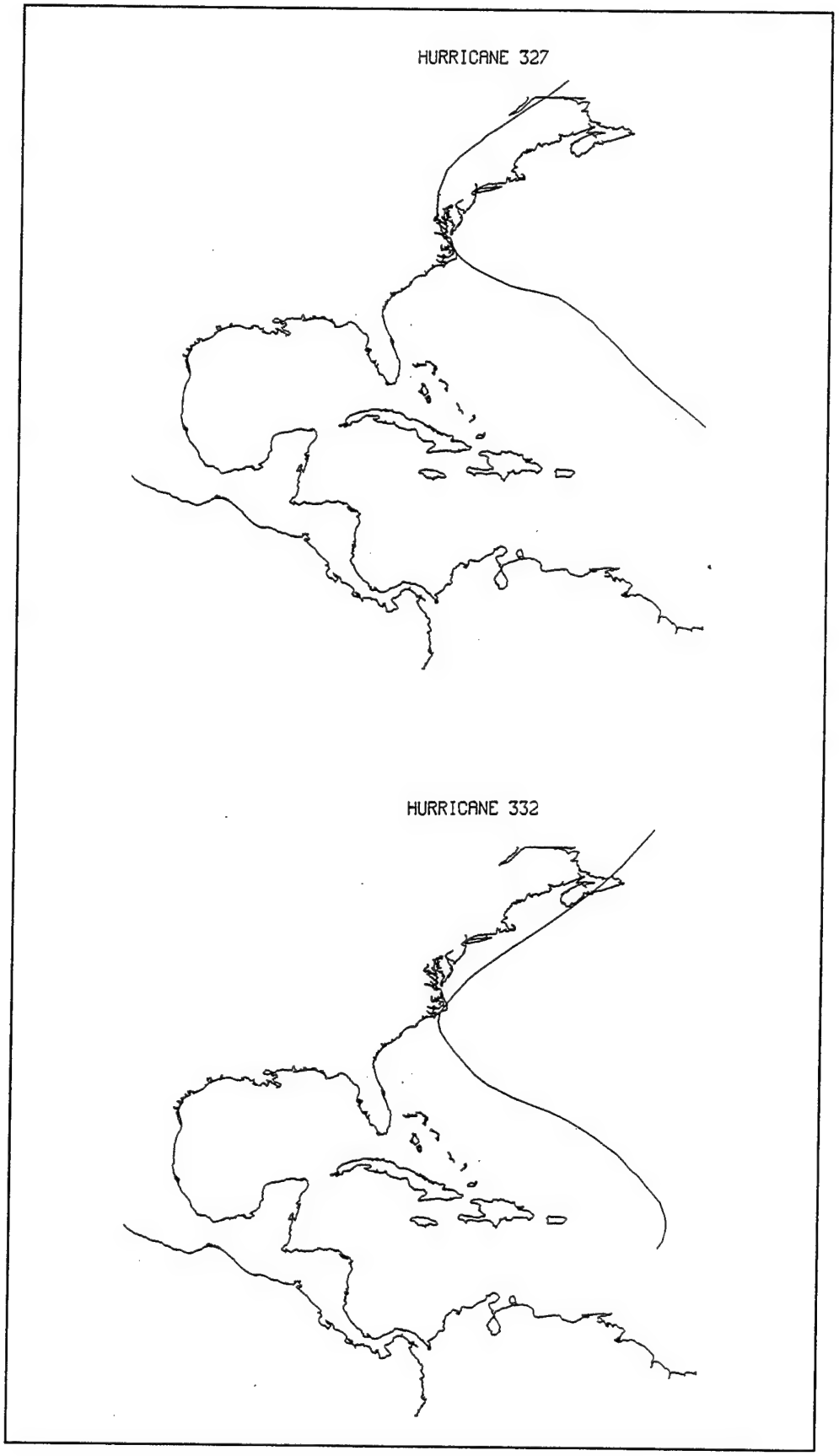
HURRICANE 327
HURRICANE 332

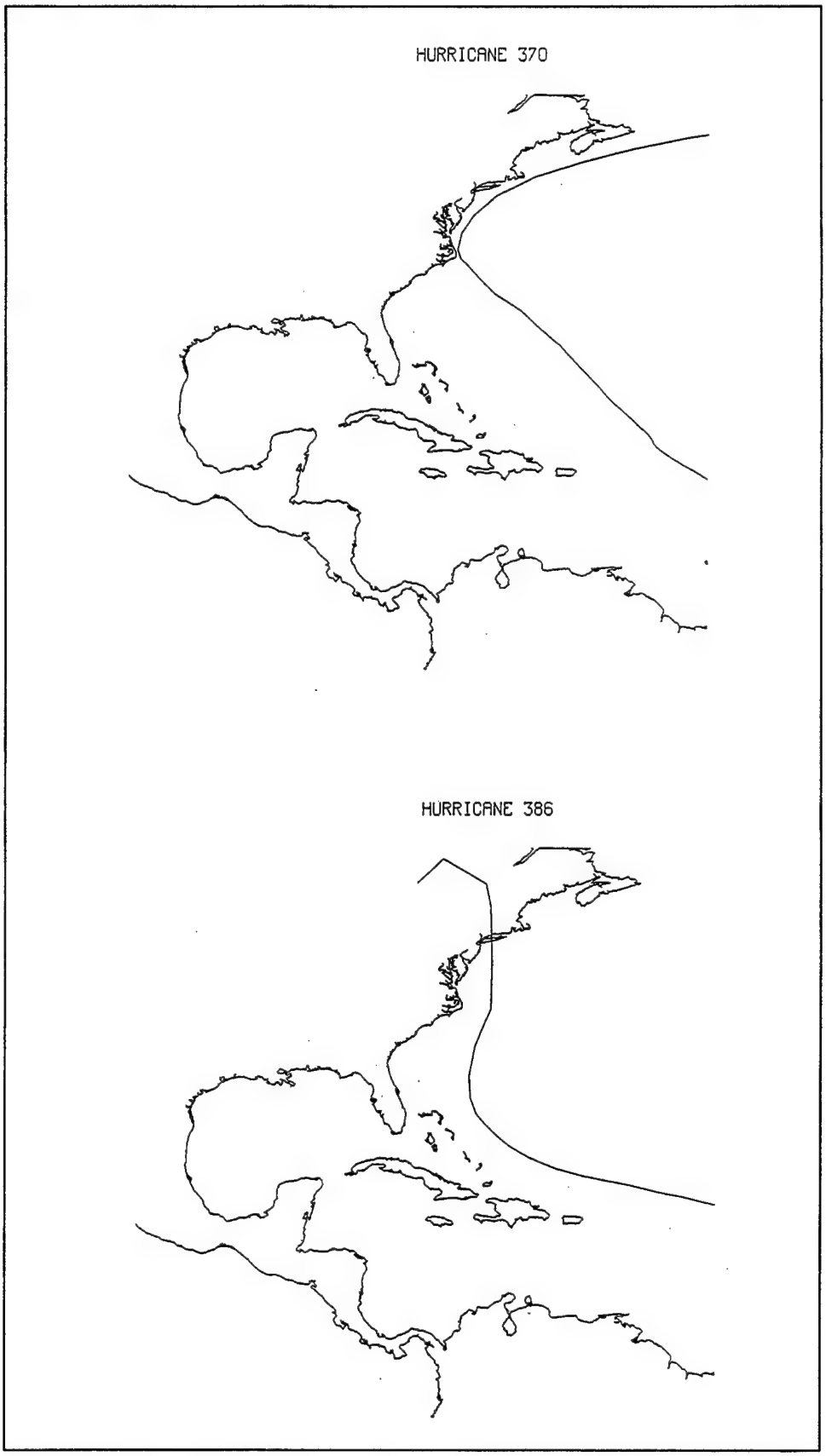
HURRICANE 370
HURRICANE 386

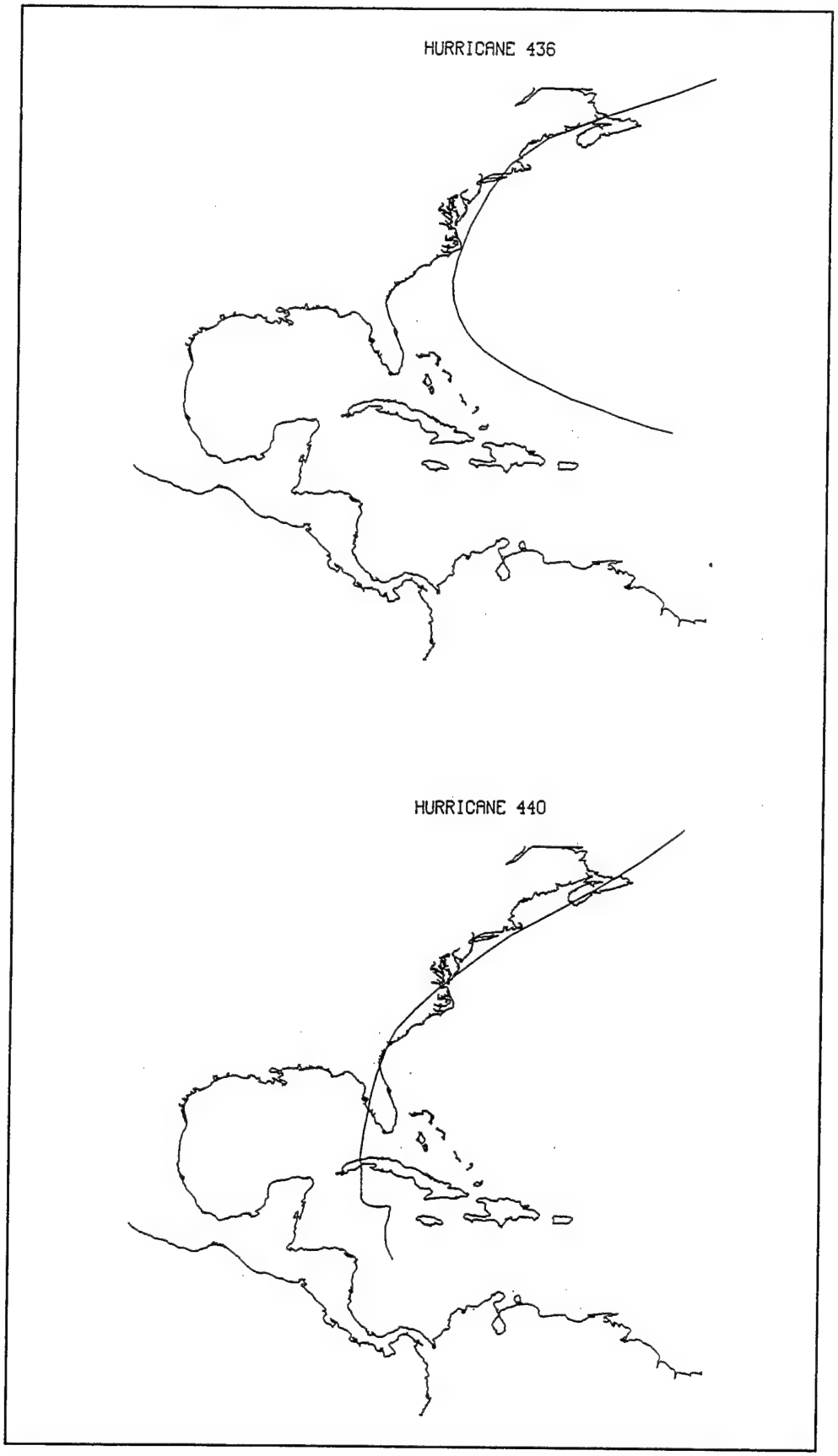
HURRICANE 436
HURRICANE 440

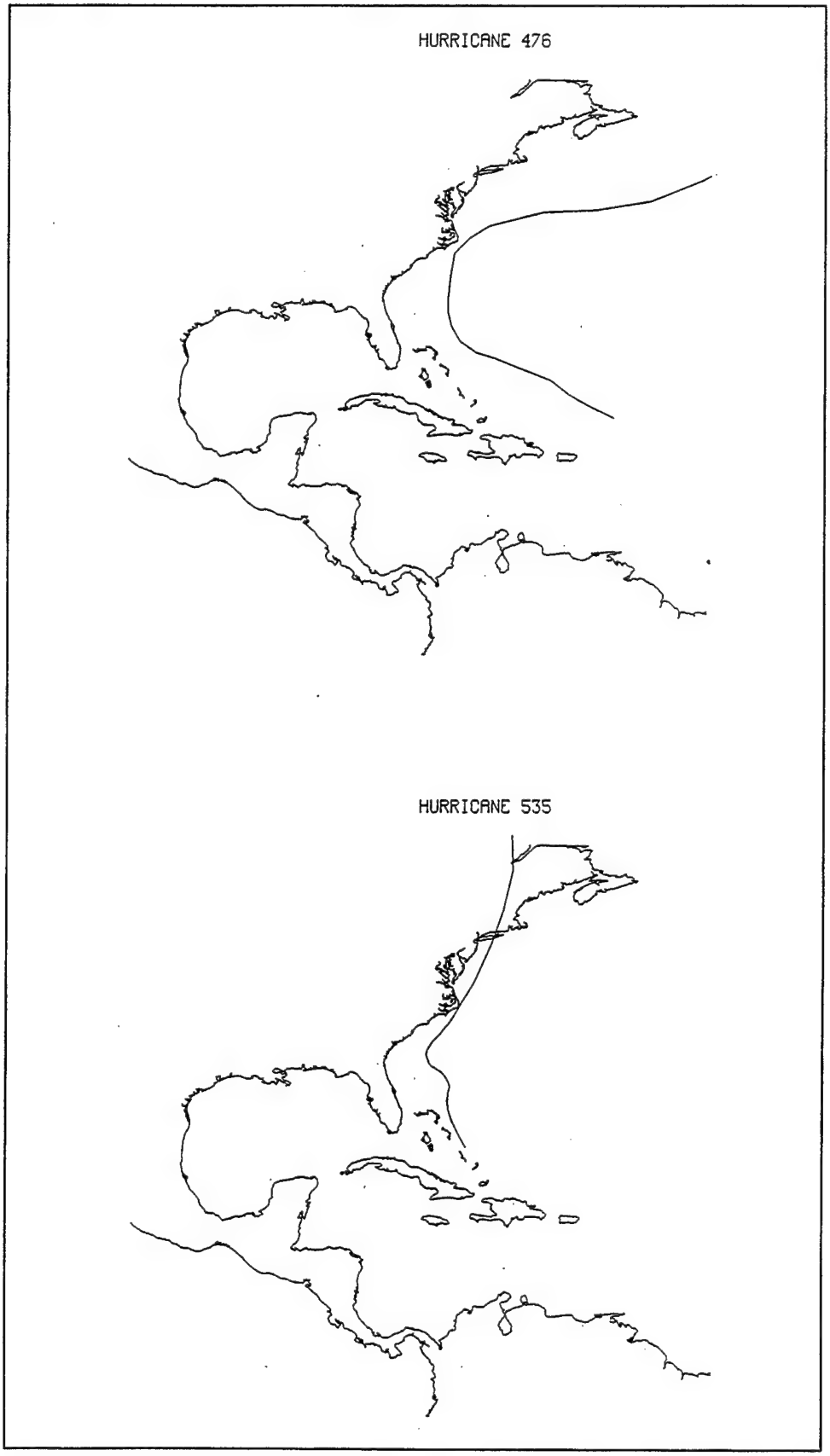
HURRICANE 476
HURRICANE 535

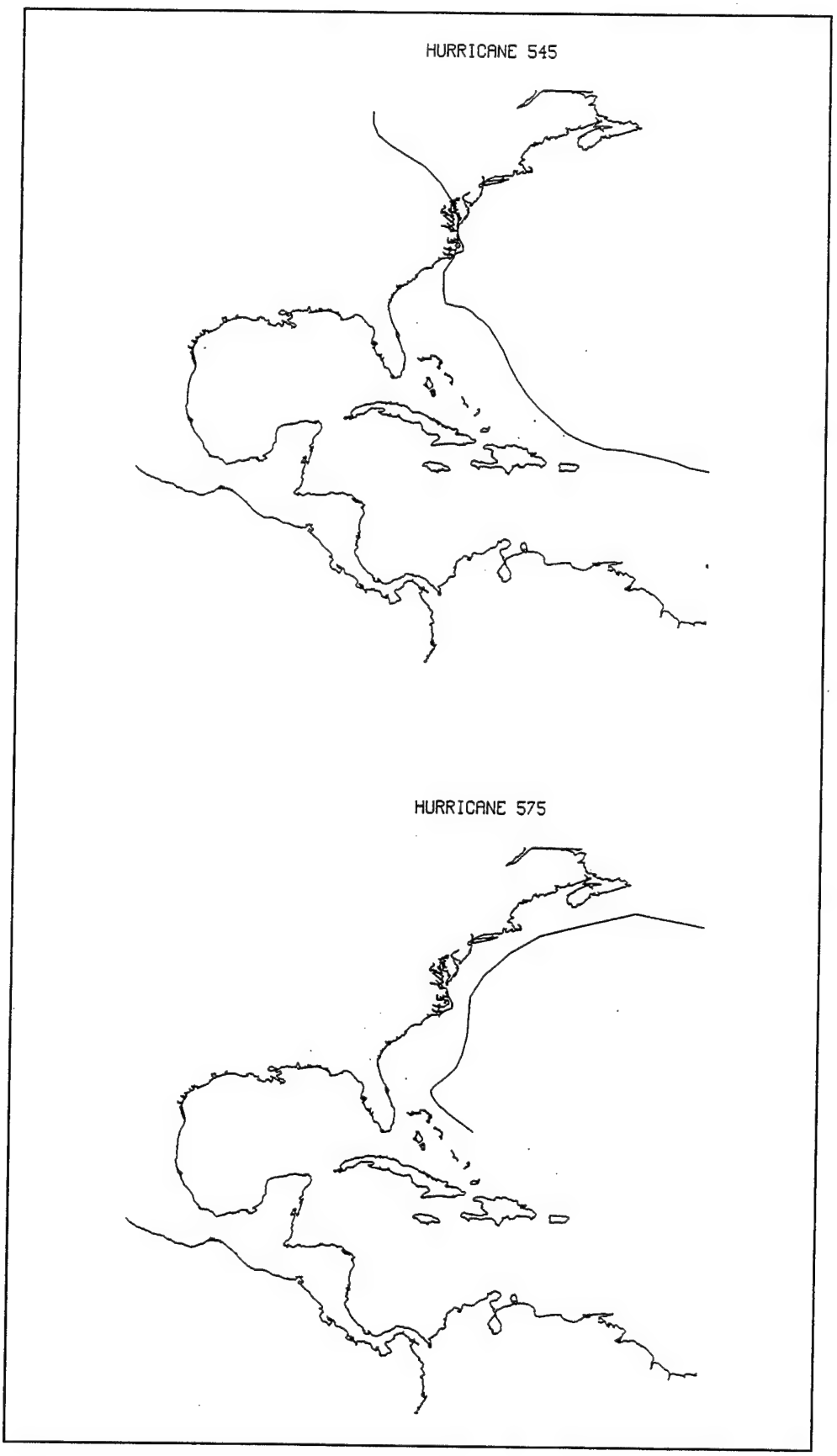
HURRICANE 545
HURRICANE 575

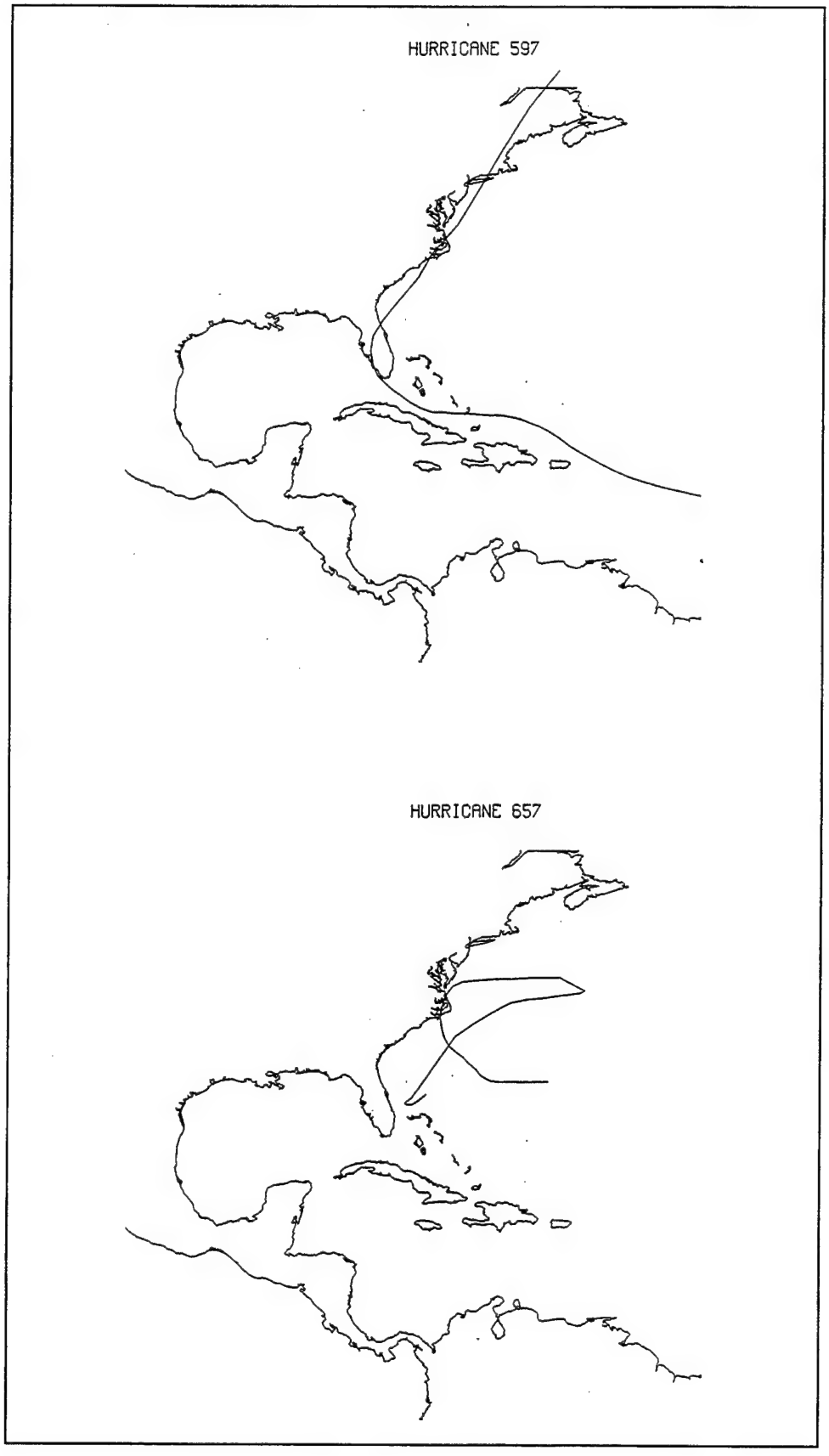
HURRICANE 597
HURRICANE 657

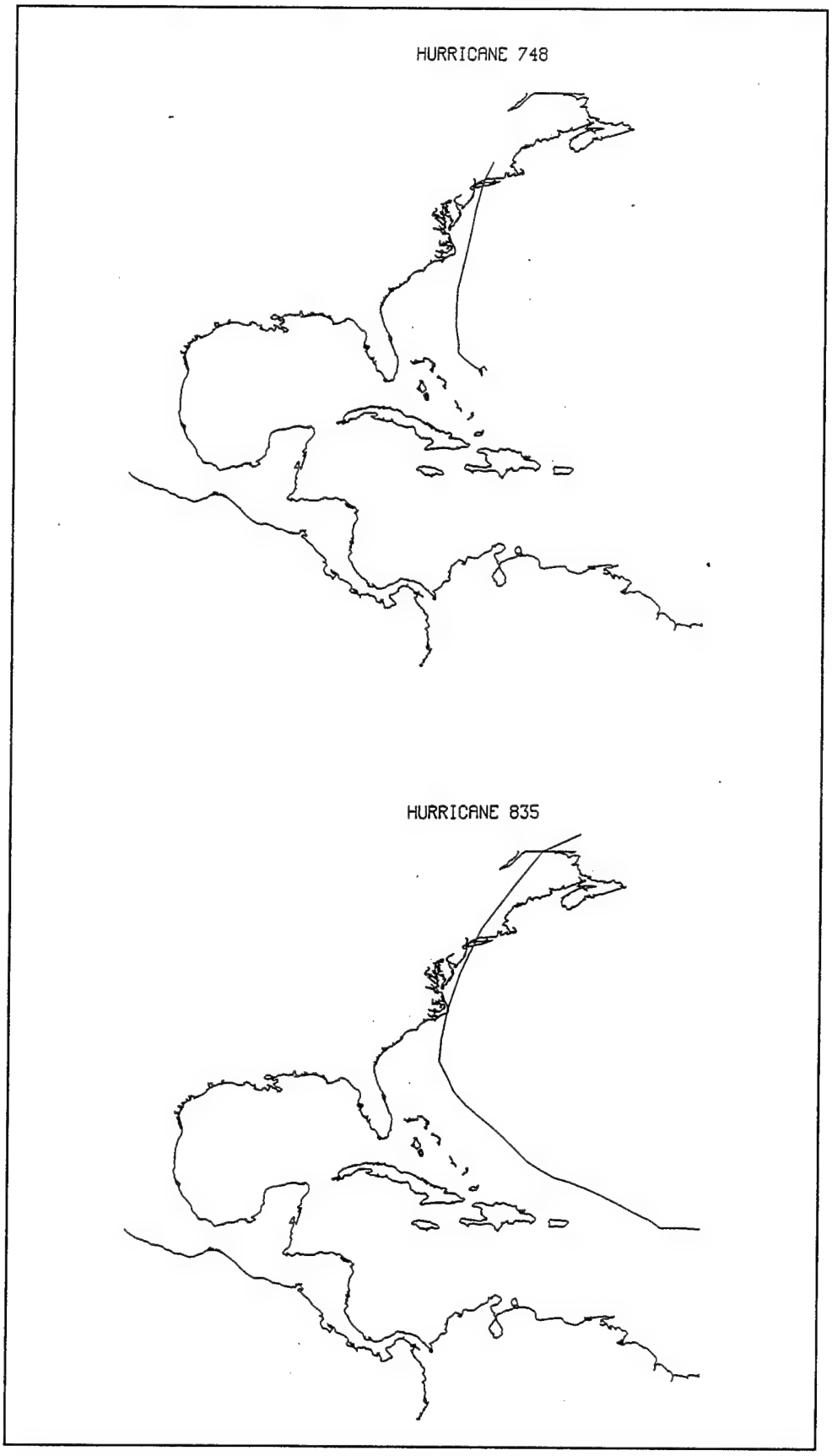
HURRICANE 748
HURRICANE 835

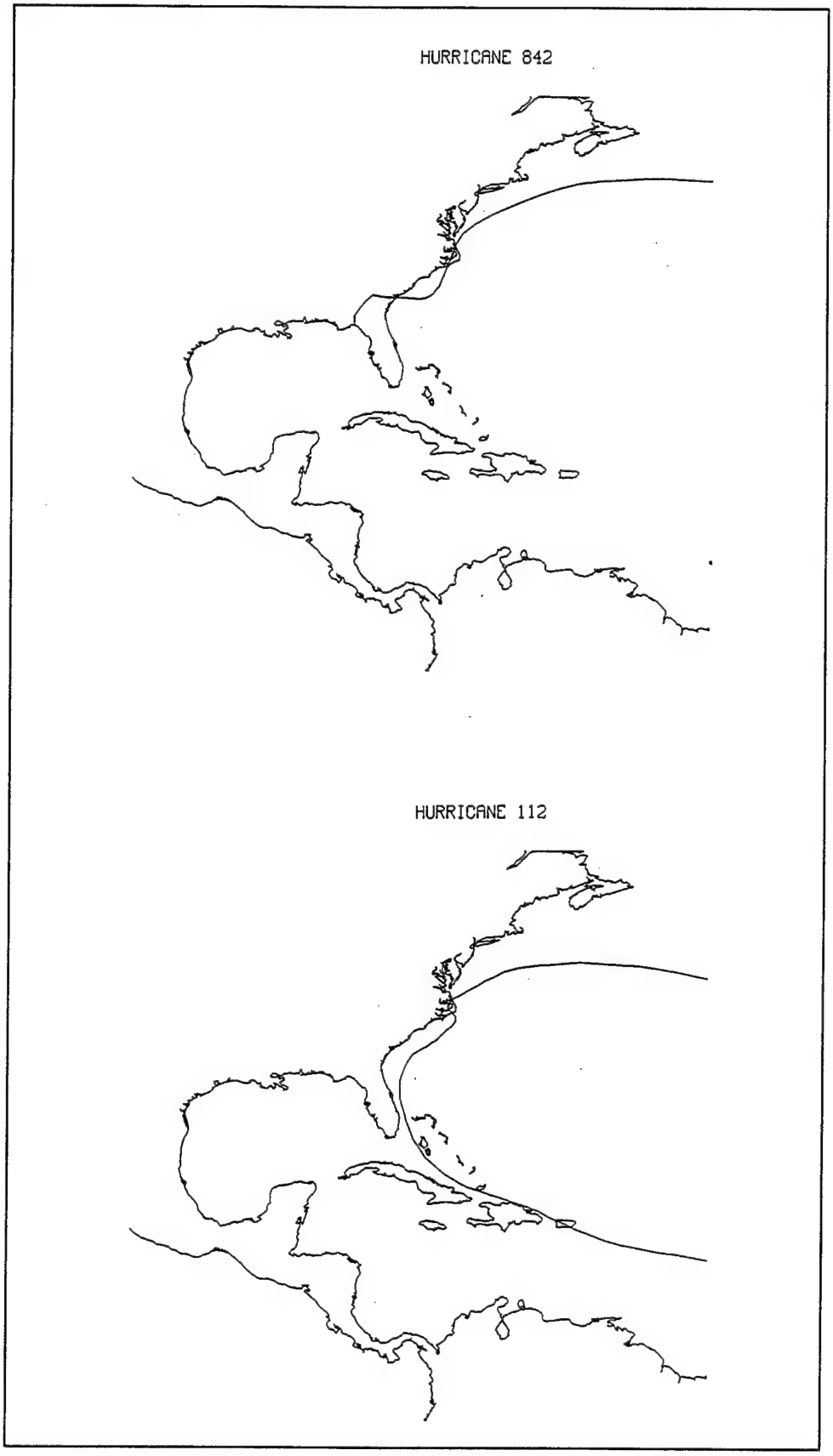
HURRICANE 842
HURRICANE 112

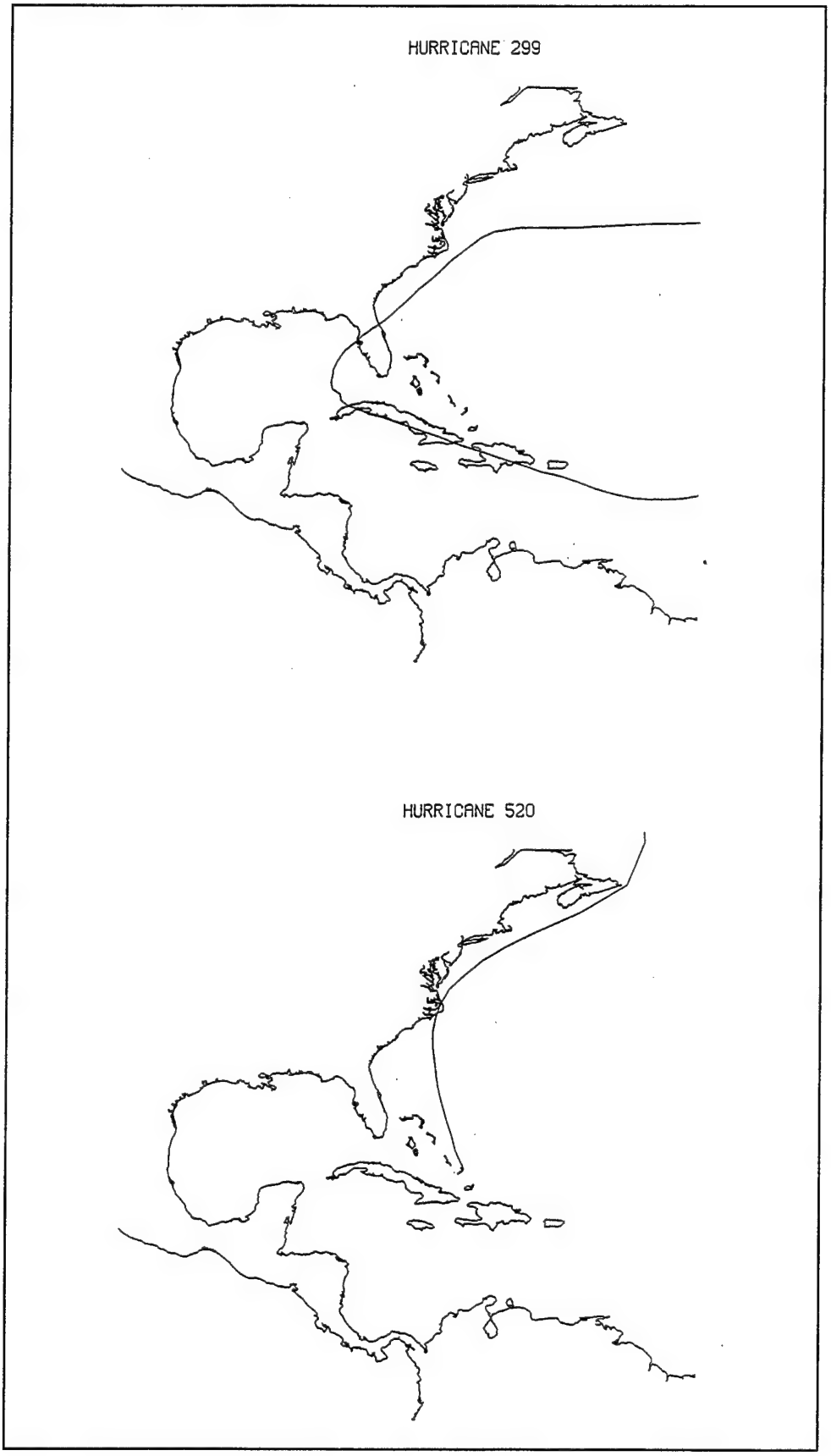
HURRICANE 299
HURRICANE 520

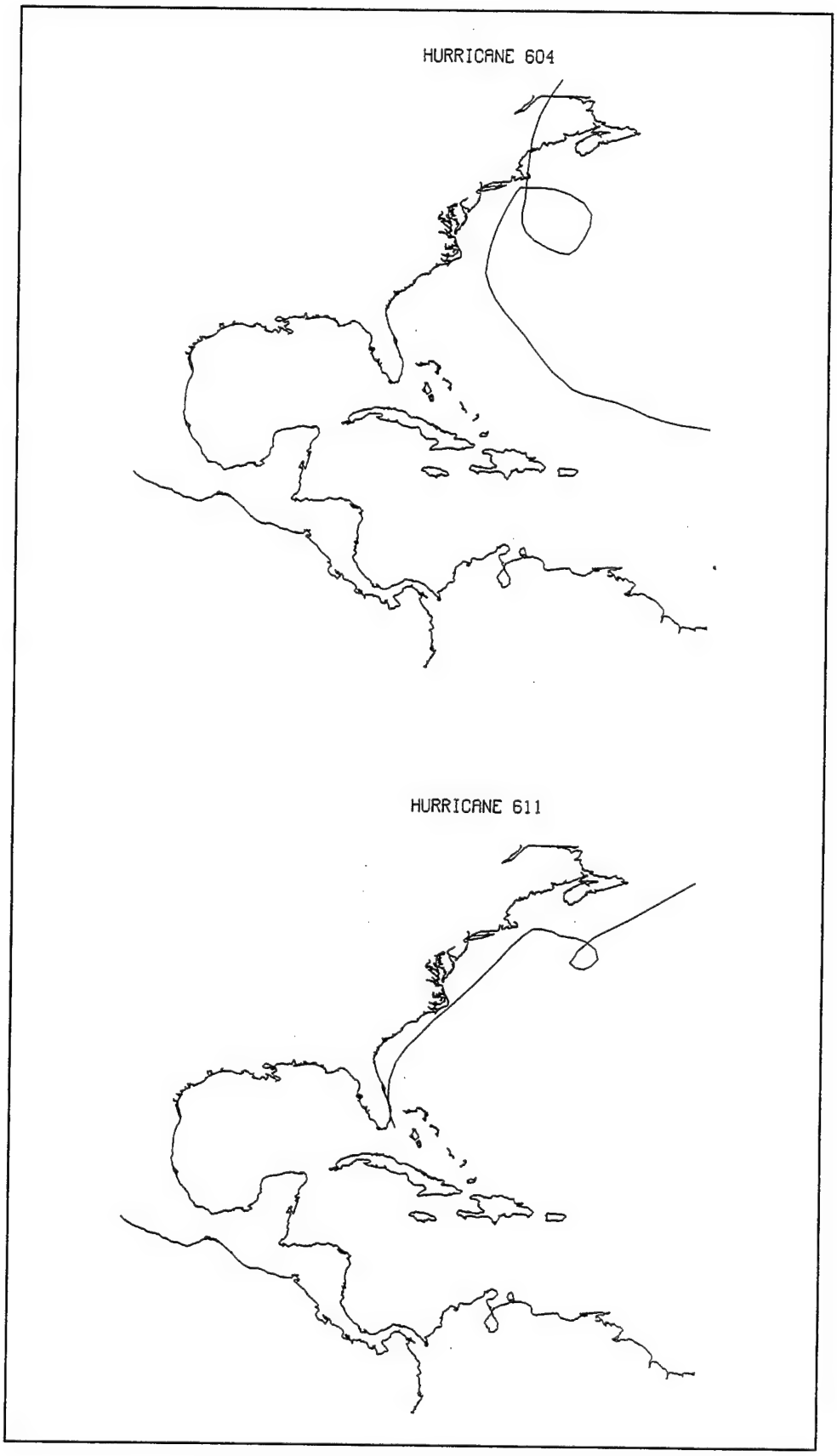
HURRICANE 604
HURRICANE 611

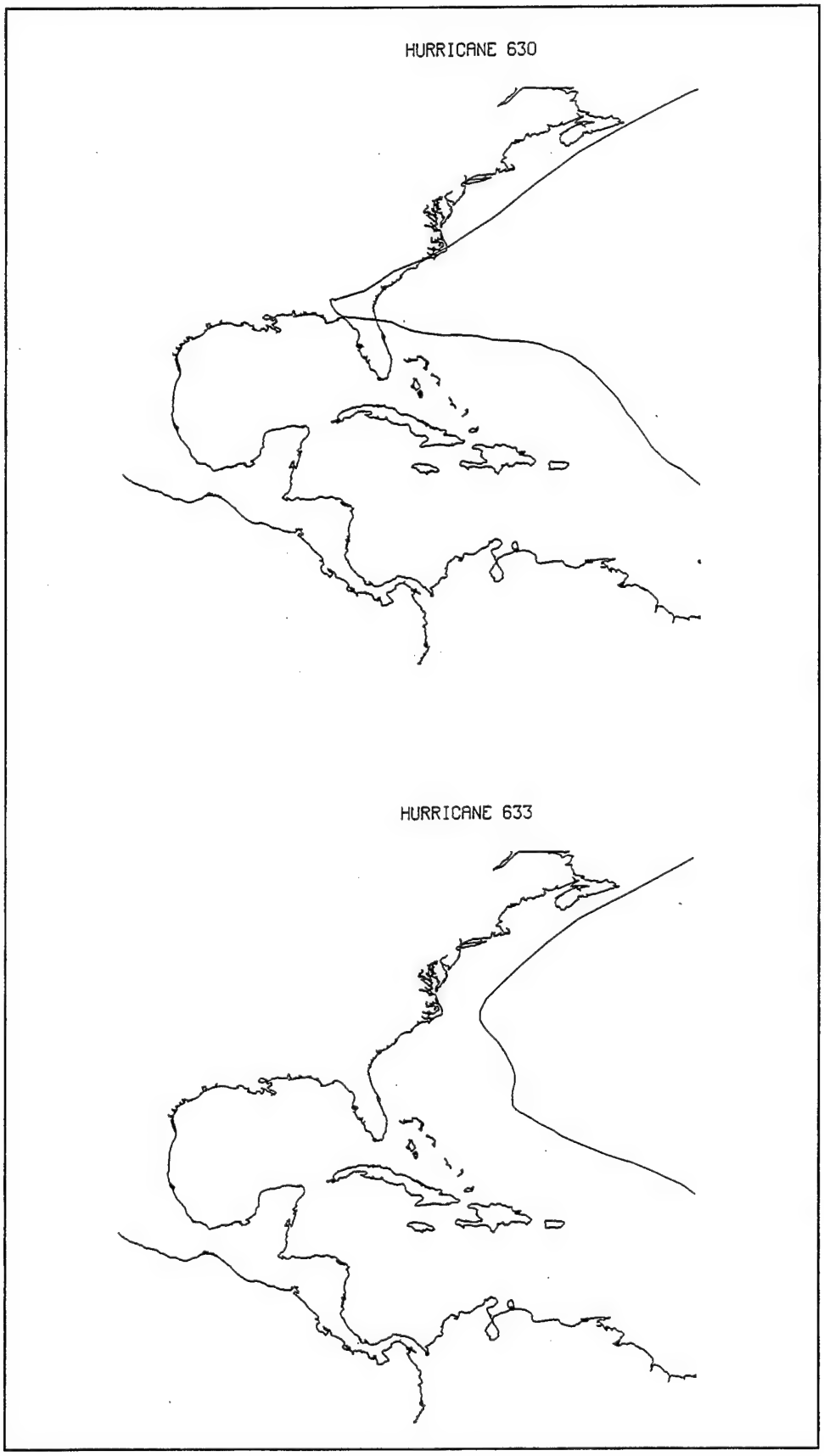
HURRICANE 630
HURRICANE 633

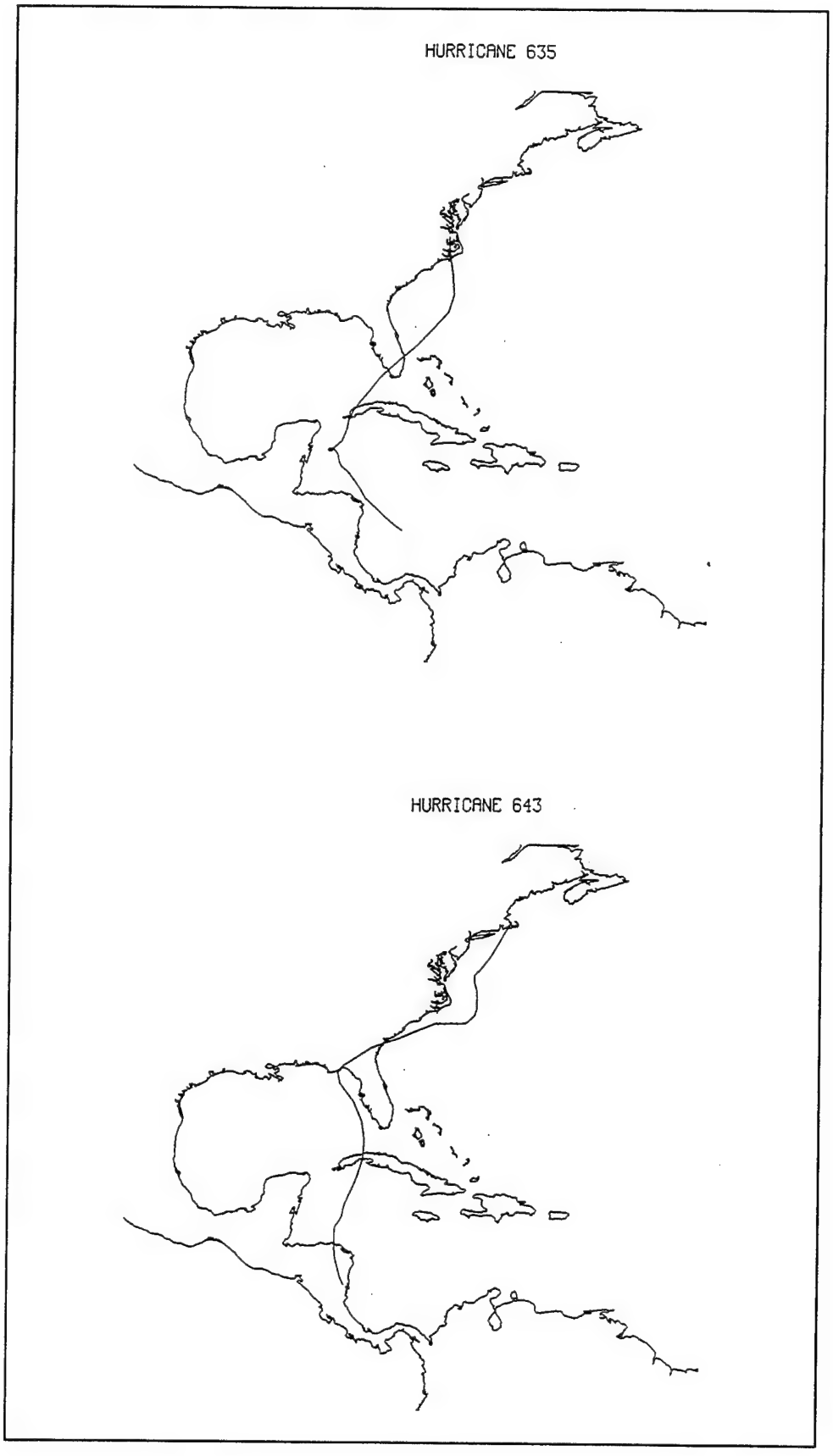
HURRICANE 635
HURRICANE 643

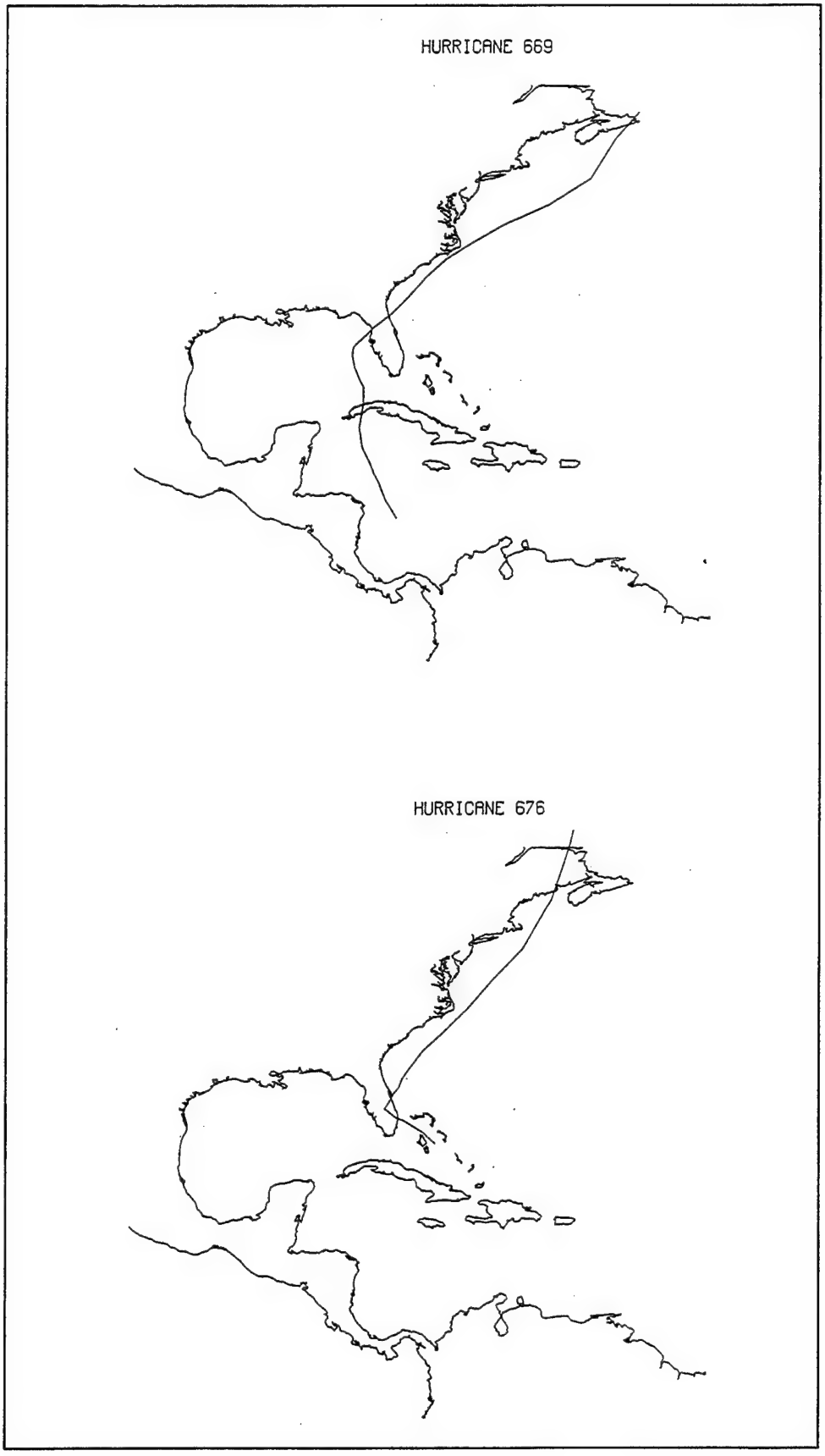
HURRICANE 669
HURRICANE 676

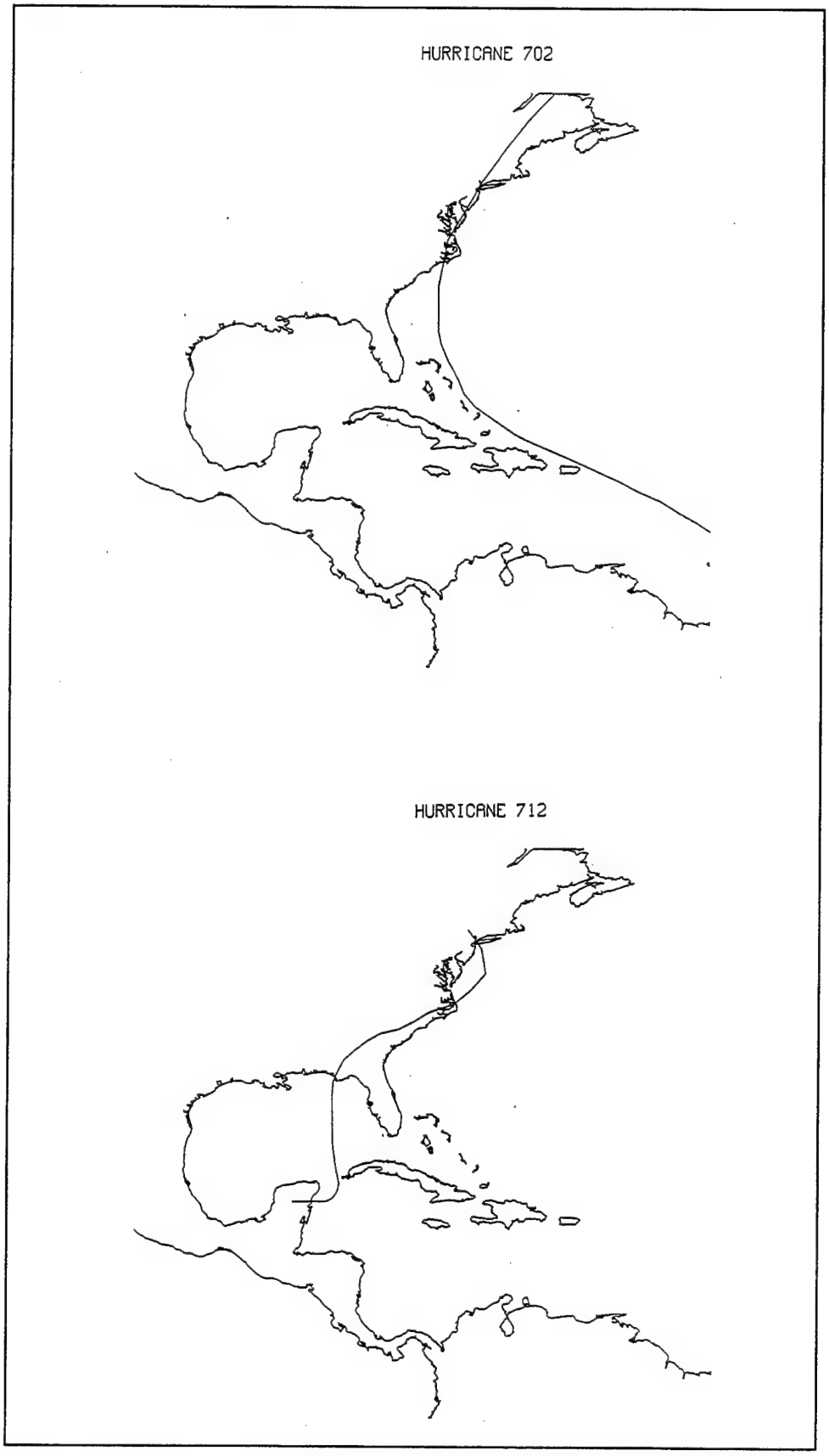
HURRICANE 702
HURRICANE 712

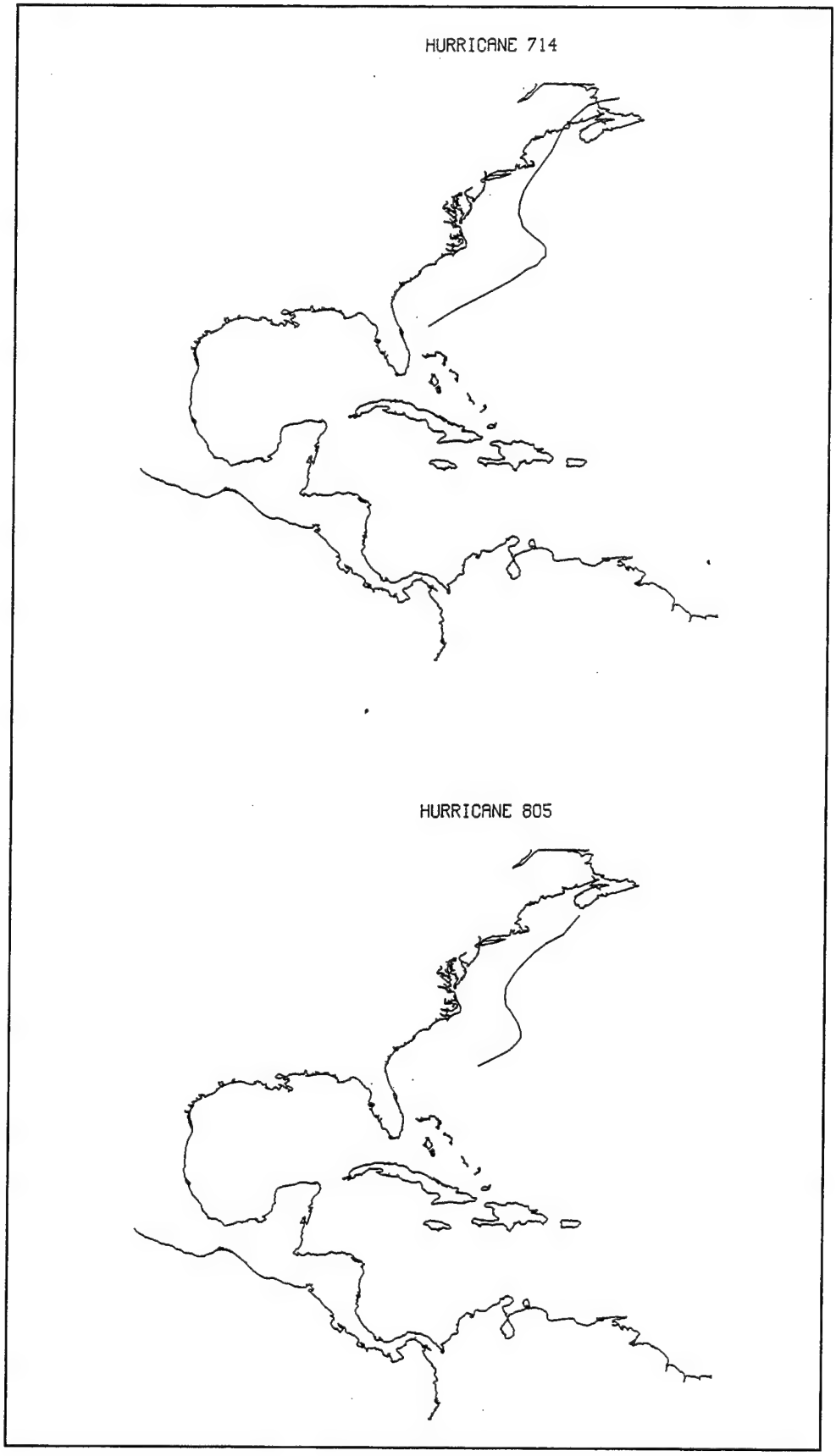
HURRICANE 714
HURRICANE 805

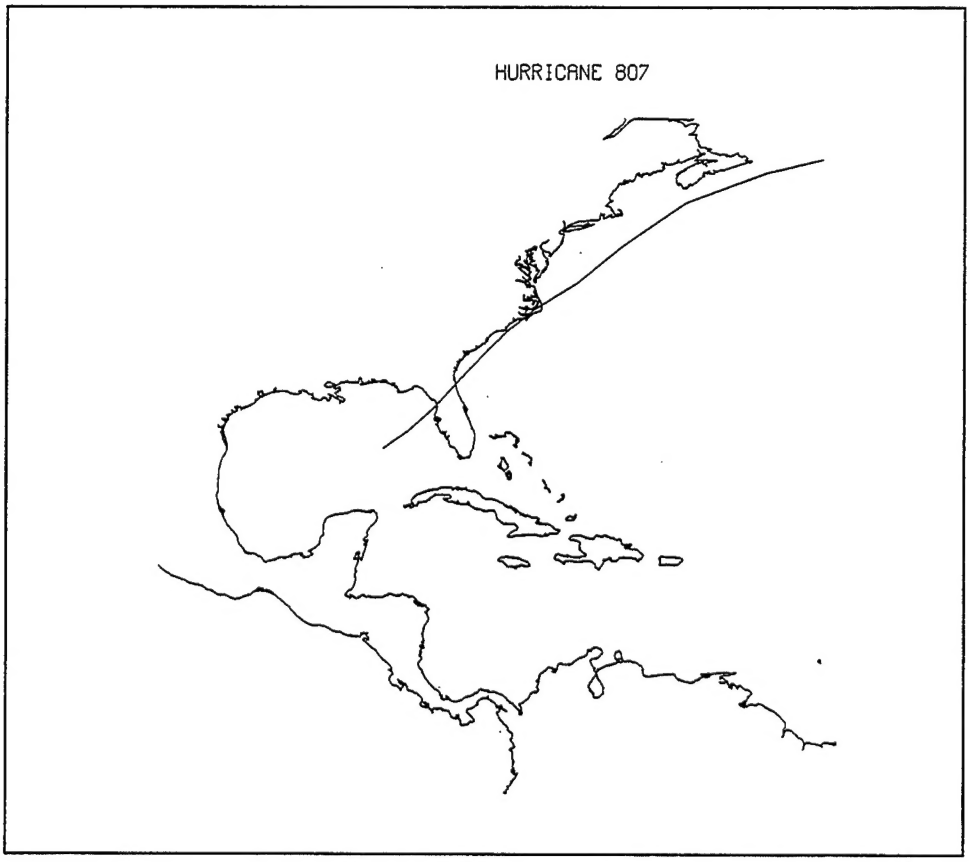
HURRICANE 807

Appendix D
Notation

A_{rms}	rms difference in amplitude
F(n)	Cumulative probability of occurrence for an event with a return period of n years
$F_x(x)$	Cumulative probability density function ranging from 0.0 to 1.0
G	Average gain
I	Number of historical storm events
L_m	Average lag
L_{rms}	rms lag
Pr[]	Probability that the random variable X is less than or equal to some value x
$Pr(s;\lambda)$	Poisson's distribution
$r_1,r_2,r_3,...$	Response vectors
T_c	Time of extrema occurrence in the computed time-series
T_m	Time of extrema occurrence in the measured time-series
v_j^*	"training set" of historical storm events
$v_1,v_2,v_3,...$	Input vectors
$X_1,X_2,X_3,...$	n-independent, identically distributed random vectors

Y_c	Computed extrema value
Y_m	Measured extrema value
λ	Measure of the historically based number of events per year
ν	Number of extrema pairs contained in time-series data
$\Re^{dv}$	d_v-dimensional space

REPORT DOCUMENTATION PAGE

Form Approved
OMB No. 0704-0188

1. AGENCY USE ONLY *(Leave blank)*	2. REPORT DATE	3. REPORT TYPE AND DATES COVERED
	January 1997	Final report

4. TITLE AND SUBTITLE

Coast of Delaware Hurricane Stage-Frequency Analysis

5. FUNDING NUMBERS

6. AUTHOR(S)

David J. Mark, Norman W. Scheffner

7. PERFORMING ORGANIZATION NAME(S) AND ADDRESS(ES)

U.S. Army Engineer Waterways Experiment Station
3909 Halls Ferry Road
Vicksburg, MS 39180-6199

8. PERFORMING ORGANIZATION REPORT NUMBER

Miscellaneous Paper
CHL-97-1

9. SPONSORING/MONITORING AGENCY NAME(S) AND ADDRESS(ES)

U.S. Army Engineer District, Philadelphia
Philadelphia, PA 19106-2991

10. SPONSORING/MONITORING AGENCY REPORT NUMBER

11. SUPPLEMENTARY NOTES

Available from National Technical Information Service, 5285 Port Royal Road, Springfield, VA 22161.

12a. DISTRIBUTION/AVAILABILITY STATEMENT

Approved for public release; distribution is unlimited.

12b. DISTRIBUTION CODE

13. ABSTRACT *(Maximum 200 words)*

This report describes the procedure and results of a hurricane stage-frequency analysis for the open coast of Delaware. This analysis consisted of three interrelated tasks, each employing a numerical model. In the first task, historical hurricanes impacting the study area were analyzed to determine storm statistics and correlations. In the second task, storm surge events developed with the wind model output were simulated using a long-wave, finite-element-based hydrodynamic model to obtain peak storm surge elevations. With the hurricane parameters serving as input to the wind field model, together with the corresponding storm surge elevations predicted by the storm surge model, statistical techniques are used for developing frequency-of-occurrence relationships in the third task.

14. SUBJECT TERMS

Coast of Delaware
Empirical simulation technique
Finite-element-based model
Hurricane stage-frequency analysis
Hurricane tracking
Storm surge

15. NUMBER OF PAGES

112

16. PRICE CODE

17. SECURITY CLASSIFICATION OF REPORT	18. SECURITY CLASSIFICATION OF THIS PAGE	19. SECURITY CLASSIFICATION OF ABSTRACT	20. LIMITATION OF ABSTRACT
UNCLASSIFIED	UNCLASSIFIED		